Multi-Grid Genetic Algorithms For Optimal Radiation Shield Design

by

Stephen T. Asbury

A dissertation submitted in partial fulfillment
of the requirements for the degree of
Doctor of Philosophy
(Nuclear Engineering and Radiation Sciences)
in The University of Michigan
2012

Doctoral Committee:

Professor James Paul Holloway, Chair
Professor Ronald F. Fleming
Professor Alec D. Gallimore
Professor William R. Martin

For My Beloved Wife Cheryl

ACKNOWLEDGEMENTS

I cannot thank my wife Cheryl enough for supporting me when I decided to return graduate school, when I was working late and when I traveled to Michigan to complete this dissertation. Without her support I would never have had the courage to return to school or the energy to finish. After Cheryl, Doctor Holloway deserves my unending appreciation. I know that he was hesitant to take me on a student when I wanted to return to the University after a hiatus, and I know he probably still wonders about that decision. But despite being a less than optimal situation, he has supported, educated, mentored and helped me every step of the way.

There have been four department heads during my time at the University: Dr. Knoll, Dr. Martin, Dr. Lee and Dr. Gilgenbach. I thank all of them for supporting me despite my unusual situation. If not for Peggy Jo Gramer I would probably not have considered returning to Michigan. Her warm welcome when I brought up the idea, as well as Dr. Martin's support, were central to my return. I owe a deep debt of gratitude to my original advisor, Dr. Kammash, for his help when I started graduate school and support in obtaining funding.

Finally I want to thank my friends and family who supported me. Most especially I appreciate everyone backing off from the ”how is the PhD going?” question when I waved my hands in frustration.

This work was supported in part by DTRA grant number HDTRA1-08-1-0043.

TABLE OF CONTENTS

CHAPTER

LIST OF FIGURES

Figure

LIST OF TABLES

Table

LIST OF APPENDICES

Appendix

ABSTRACT

Multi-Grid Genetic Algorithms For Optimal Radiation Shield Design

by

Stephen T. Asbury

Chair: James Paul Holloway

Genetic Algorithms (GA) are a powerful search and optimization technique that can be applied to numerous problems. Unfortunately, GA relies on large numbers of fitness evaluations to determine the relative merits of various solutions to a problem. For problems requiring computationally intensive fitness evaluations this can make GA too expensive to use. We describe a hierarchical technique that we have created called Multi-Grid Genetic Algorithms (MGGA). MGGA leverages the geometry of a problem space to build a hierarchy of increasingly smaller problem spaces. Optimizations over these smaller spaces are used to seed a population of solutions in a larger space. We explore how MGGA can be applied to several radiation shielding problems.

CHAPTER I

Introduction

The first thing most people would think of when asked, "how do you protect someone from radiation," is the single word *lead*. Lead is used to shield us when we go to the dentist for an X-Ray, or at least that is what we think is in that heavy blanket they put on us. Lead is in the travel pouches for high speed film, and many people would think incorrectly that nuclear reactors are surrounded by lead, when in fact they generally use concrete and water to shield against neutron radiation because hydrogen is a good material for shielding neutrons.

Protecting something or someone from radiation is more complex than stacking lead bricks. The real world is a multi-objective function. It isn't usually sufficient to just build a shield. You also have to build a shield that meets numerous criteria. Perhaps the shield must be as light as possible, or as cheap as possible. Maybe the shield needs to be thin or made from specific materials for another reason. As we will see in Chapter IV the type of radiation you are shielding against affects the type of materials that will make a good shield. All of these objectives can play a role in designing a good shield. Knights couldn't carry a castle around with them, so they carried a metal shield to stop their opponent's sword. It wasn't the best way to stop the sword, but it was lighter and more maneuverable than a large stone structure.

Designing a shield can be hard. Moreover, the best solution can sometimes chal-

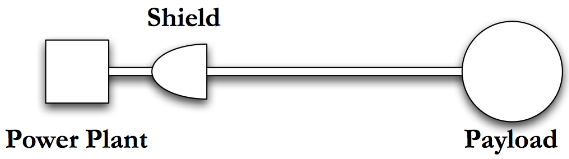

Figure 1.1: Geometry of a simple shadow shield

lenge *common knowledge*. Take a simple shadow shield. It turns out that the best design is not necessarily a solid piece of material, [Alpay & Holloway (2005)]. My goal in this dissertation is to attack several shielding problems using genetic algorithms. Genetic Algorithms, GA, are an automated search strategy that will not be subject to human preferences and expectations. By developing an advanced algorithm on top of GA for shielding problems we hope to find unexpected solutions to interesting problems and to demonstrate better solutions than might be found using standard genetic algorithms.

1.1 The Scenarios

Take, for example, the challenge of building a shield for a space mission powered by a nuclear reactor, like the design in Figure 1.1. The reactor will be generating neutrons that could easily damage sensitive equipment in the payload. The answer to this challenge can't be the layman's idea to "put a bunch of lead in there", nor is the best solution necessarily to put a large container of water between the reactor and the shield. Whatever the shield is made from will have to be launched into space, and the cost of the launch is dependent on mass and can be very expensive. According to SpaceX [Space X (2011)], it costs over $5,000 to launch a single kilogram into geosynchronous orbit, this number is optimistic, and the actual cost can be much higher. On the other hand, the shield can be leaky, in the sense that it doesn't have to surround the reactor. It only needs to protect the payload itself. The solution to this problem must balance shielding quality against mass, cost and other factors.

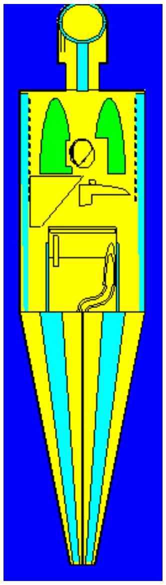

Figure 1.2: Advanced phantom for a radiation worker

In Chapter V, I will discuss how Genetic Algorithms can arrive at an unexpected solution for the space shield problem. This solution will include splitting the shield and leveraging geometric effects.

A completely different shielding problem is the design of a shield for radiation workers, like the one modeled in Figure 1.2. In this application the shield should be *wearable* or at least movable. Moreover, it should focus on shielding against the primary dangers, generally gamma radiation, an x-ray technician, patient or first responder will encounter. Finally, the shield must balance mass against protecting the primary danger zones in the human body. Not all parts of the body are equally susceptible to damage from radiation and an ideal shield might take advantage of this.

In Chapter VI, I will explore the possibility of protecting a person from gamma radiation. While it will prove fruitless to try to beat lead for a high energy gamma shield, the final solution for low energy gamma shielding will represent a more than 50% improvement over a simple lead shield for the same mass.

The final problem I will explore involves the concept of a *bowtie filter*, as in the

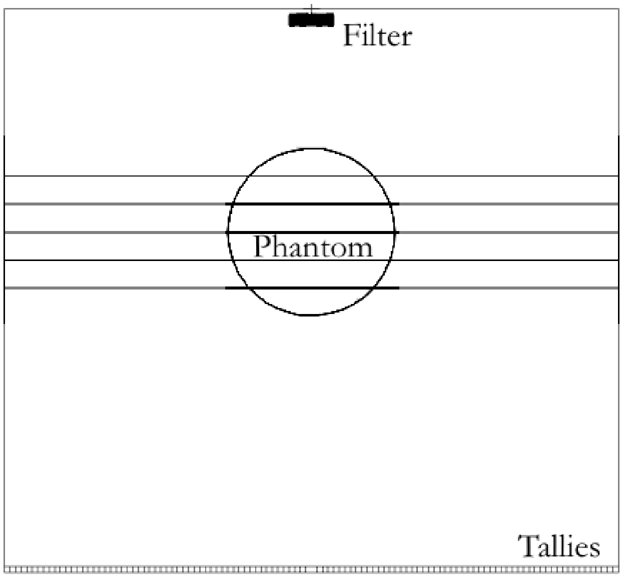

Figure 1.3: A bowtie filter geometry

geometry from Figure 1.3. These filters are used in CT scanners and other devices to control the intensity of radiation incident on the detector plane. This problem doesn't suffer from mass restrictions but does present a different type of challenge. Rather than trying to shield the target from all radiation, we are trying to shape the incident radiation field. In Chapter VII, I will show how Genetic Algorithms can help design a good bowtie filter with very few constraints.

By addressing these different scenarios I will show how our new Genetic Algorithm provides a powerful tool to the shield designers toolbox.

1.2 The Toolbox

The primary tool discussed in this dissertation is a new Genetic Algorithm which we call Multigrid Genetic Algorithms (MGGA). Chapter II discusses Genetic Algorithms in a generic way, and provides a basic idea of how they solve problems. I will introduce GA's configuration parameters in Chapter II and discuss my choices throughout the dissertation. A very important part of GA is the concept of a *fit-*

ness function. This fitness function is used to score possible solutions to a problem. The goal of a Genetic Algorithm is ultimately to find a solution that has the best score from the fitness function. In each chapter I will describe what fitness function we are using, and why. Moreover, I will be discussing how that function captures and balances different objectives for each shielding scenario. For example, the fitness function for the space shield looks for a low mass solution as well as a good shield.

One disadvantage of Genetic Algorithms is that they must evaluate the fitness function numerous times. It is common to design GAs where the fitness function could be run millions of times, although we will generally stay to below one hundred thousand invocations in this dissertation. In the case of radiation shielding, the fitness function will always involve performing a radiation transport simulation with a code like MCNP. These codes can take minutes, hours or even days to run. As a result, the fitness function evaluation becomes a time constraint.

To help address this time constraint I pursued several avenues of research. First, I created a Genetic Algorithm library that would allow me to scavenge time on a computing cluster. Over the course of my research I moved through several cluster implementations, each move altered the optimal design for the Genetic Algorithm code. This evolution is described in Section 2.9.

Second, my GA library implements a number of smart algorithms to minimize work. Caching is used eliminate retesting of individuals where their score is known. An algorithm called *pre-calculation* was tested to see if we could eliminate fitness function evaluations in cases where selection wouldn't pick an individual, independent of their fitness.

Third, we created a new form of Genetic Algorithm called the *Multi-Grid Genetic Algorithm* (MGGA) which leverages geometric considerations to move the algorithm to a good solution more quickly, using fewer calls to the fitness function. MGGA is described in Chapter III and used for each problem I describe in this dissertation. MGGA and its application to radiation shielding design is the most significant contribution of this work.

1.3 Does It Work?

Ultimately the question that must be asked is, “does GA and MGGA help design better shields?” Based on the results in this dissertation I will show that the answer is yes. GA, and specifically MGGA, helps design shields. For the space shield, the MGGA was able to find a non-obvious solution that allowed neutrons to scatter away from the shield while reducing shield mass. MGGA was also able to reduce the total dose on a realistic human phantom by over 50% for 75 kev gammas compared to a lead shield of equal mass.

Perhaps equally as important, in most cases, MGGA is able to produce a better result than GA with the same or fewer computing resources. MGGA is a new way of exploring a problem space that leverages the geometric features of shielding problems to reduce the computing resources required to explore them.

CHAPTER II

Genetic Algorithms

2.1 Introduction

As early as the 1950s scientists were looking at how evolution could be used to optimize solutions in engineering and scientific problems [Mitchel (1998)]. John Holland at the University of Michigan [Holland (1992,1975)] began working and publishing on the idea of Genetic Algorithms in particular over 30 years ago. Genetic Algorithms, GA, are a way to automate the optimization process based on techniques used in biological evolution. GA can be compared to other optimization techniques like hill climbing or simulated annealing, in that these techniques all try to find optimal solutions to problems in a generic enough way that they can be applied to a large range of problem types.

GA is generally implemented using the following high level steps:

1. Determine a way to encode solutions to your problem, the encoding will be used to define the *chromosomes* for your Genetic Algorithm.

2. Determine a way to score your solutions. We will call this scoring mechanism the *fitness function.*

3. Run the Genetic Algorithm using your encoding and scoring to find a "best"

solution. In the next few sections we will see how GA generates new individuals to score.

The individual elements of a chromosome will be called *genes* to match the biological terminology.

2.2 A Sample Problem: The Shortest Path

Let's look at an example of the first two high level steps for applying GA. Imagine the X-Y plane, with the unit square between 0.0 and 1.0 in each direction. Place a point at $(0.0, 0.0)$ and another at $(1.0, 1.0)$. These are the lower-left and upper-right corners. Create a grid of squares by breaking the remaining X and Y space into equal length sections. Our problem is to place points at intersections of the grid, pictured in Figure 2.1, one for each X value, that when connected makes the shortest line. In other words, minimize the distance between a set of points where the first and last point are in a fixed position and the X value of the points is pre-determined. Keep in mind that the possible values for X and Y are discrete based on the grid.

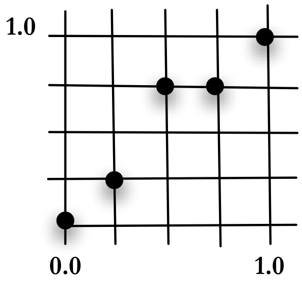

Figure 2.1: The shortest path problem

The answer for this problem can be determined in many ways. The question will be, can GA find the solution. As we explore GA with this problem, it is worth noting that GA may not be the best technique to solve it. This is ideal for a test problem, since it allows us to appreciate how GA is performing compared to other techniques. This problem also offers an interesting framework because changing one point at a time, as hill climbing or a steepest descent technique would try to do, won't necessarily work; moving one point might create a longer section between it and its neighbors. For an algorithm to optimize the solution, it may be necessary for all of the values in the encoding to move toward the best answer at the same time. The solution space is non-trivial.

2.2.0.1 Encoding the Shortest Path Problem

We will encode the shortest path problem onto a discrete grid using a constant called ψ, and the following steps:

1. Break the X-axis and Y-axis from 0 to 1.0 into ψ sections.

2. Store the Y-value at each X point, excluding the two ends, as a single integer from 0 to ψ

The first point is always $(0.0, 0.0)$ and last point is always $(1.0, 1.0)$ and are not stored in the chromosome. For example, the chromosome in Figure 2.2 will translate into the set of points in Figure 2.3.

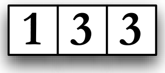

1	3	3

Figure 2.2: A sample chromosome for the shortest path problem with $\psi = 4$

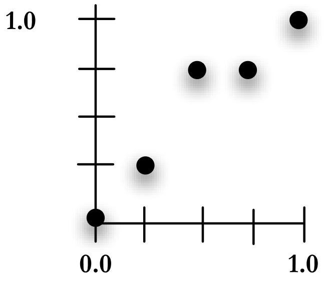

Figure 2.3: An example of the shortest path problem with $\psi = 4$

Because we are going to fix the first and last point to the two corners, we will have a total of $\psi - 1$ integers for each chromosome. This insures that we can scale this problem for MGGA by splitting each X value in half. The value of ψ is also used to split the X and Y axis equally so that scaling during MGGA, discussed in the next section, will be equal in both directions.

This is a pretty simple problem and encoding. But imagine that we use $\psi = 128$ This would result in a problem space with 127 X's, each with 129 possible values, or $129^{127} = 1.1 \times 10^{268}$ possible encodings. That is a huge search space.

2.2.0.2 Scoring the Shortest Path Problem

To score each individual we use a fitness function that performs the following steps:

1. Calculate the X value for each point by dividing the X axis into ψ parts, keeping in mind that the first element of the chromosome is at 0.0 and the last at 1.0. In Figure 2.3 with $\psi = 4$ the X values will be 0, 0.25, 0.5, 0.75 and 1.0.

2. Treat the value for each X location as ψ units that add up to a height of 1.0, so if $\psi = 4$ the Y values will range from 0 to 4, corresponding to values of 0, 0.25, 0.5, 0.75 and 1.0.

3. Calculate the length of the line connecting all of the points by adding up the distance between the points defined by consecutive genes, looping and summing until all of the gene pairs are mapped onto line segments and included.

4. Subtract the result from 1.0 to make 1.0 the best fitness and all others less than 1.0. The value of 1.0 is not achievable, since the distance is always greater than 0. However, I use this convention throughout this dissertation to provide a consistent value for the best possible fitness.

Put simply the fitness for a chromosome is:

$$\begin{aligned} F(x) &= 1 - \text{sum of length of line segments} \\ &= 1 - \sum_{i=0}^{\psi} \sqrt[2]{(x_{i+1} - x_i)^2 + (y_{i+1} - y_i)^2} \end{aligned} \tag{2.1}$$

Given a problem encoding and fitness function, lets look at the Genetic Algorithm itself.

2.3 The Genetic Algorithm

Genetic algorithms are generally run in one of two modes: steady state or generational, [Langon & Poli (2002) page 9]. In steady state GA the program will perform the following steps, pictured in Fig. 2.4.

1. Generate a number of possible solutions to the problem. Encode these solutions using an appropriate format. This group of encoded solutions is called a *population*.

2. Score the individuals in the population using the fitness function.

3. Use some sort of selection mechanism, see Section 2.4, to pull out good individuals, call these individuals *parents*.

4. Build new solutions from the parents using GA operations, see Section 2.5. Call these new individuals *children*, and this process *reproduction*.

5. Insert the children into the population, either by replacing their parents, by growing the population or by replacing some other set of individuals chosen using a selection mechanism.

6. Return to step 2. (In steady state GA, the population remains basically the same, or steady, we just replace or add to it.)

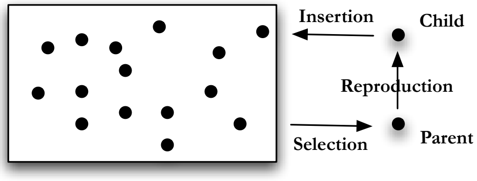

Figure 2.4: Steady state GA

Generational GA changes the last step in this algorithm. In generational GA the algorithm will perform the following steps, pictured in Fig. 2.5.

1. Generate a number of possible solutions to the problem, encode these solutions using an appropriate format. This group of solutions is called a population or generation.

2. Score the individuals in the population using the fitness function.

3. Use some sort of selection mechanism, see Section 2.4, to pull out good individuals, we will use these as parents.

4. Build new solutions from the parents using GA operations, see Section 2.5. Call these new individuals the children and this process reproduction.

5. Insert the children into a new population. (Note - in generational GA we make a new population each time, in steady state GA we reused the same population.)

6. Repeat generating children until the new population is full.

7. Return to step 2, with the new population as the current population.

The genetic algorithm will loop until it meets some termination condition. Termination conditions include: a sufficiently good individual is found, some number of

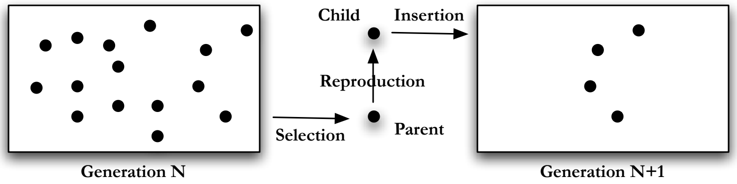

Figure 2.5: Generational GA

individuals have been tested, or a fixed amount of computing time is used. Generational GA includes an additional termination condition of running until a specific number of generations are executed.

For this dissertation I have used generational GA exclusively because it is the most like other optimization techniques. Also, generational GA fit well into a batch processing model that runs on the available clusters at the University of Michigan. This model is described in Section 2.8.1.

2.3.1 Diversity

As in biology, GA has to worry about available genetic material. The concept of available material is called *diversity.* In GA, diversity is a measure of how much of the problem space the current population represents, [Eiben & Smith (2003) page 20]. In our sample problem, if all of the individuals had a zero for the first gene, this would represent less diversity than if some individuals have a one in the first gene. Diversity can be thought of as a measure of the available genetic material. In order to truly search a problem space, we want to have as much viable genetic material as possible.

Perhaps the main implication of good diversity is the ability to avoid local minimum and maximum in a problem space, [Tomassini (2005) page 37]. GA has a number of ways to keep and indeed improve diversity in the population. These will be discussed in the sections below.

2.4 Selection Mechanisms

One of the key steps in the "Genetic Algorithm" is selecting parents for the next generation. Selection is one of the main ways to maintain diversity in a population. The selection process can be handled a number of ways.

2.4.1 Random Selection

Random selection is the process of picking individuals from the population with no concern for their fitness. This selection scheme keeps a lot of diversity, but doesn't help move the algorithm toward a solution. Random selection can suffer from the side effect that it loses good individuals to bad luck, simply because they are not randomly picked.

2.4.2 Top Selection

Top selection takes the fitness for every individual in a population and ranks them. Then the highest scoring individual is used as the parent for every child. Always selecting the top individual makes very little sense in generational GA, but can make some sense in steady state GA. If we use top section for generational GA we would be creating a new population with a single parent. As we will see in the next few sections, the only way to change that parent will be mutation. So with top selection we would essentially be performing an inefficient hill climbing optimization. With steady state GA, we would still be essentially hill climbing, but without completely replacing the population each time.

2.4.3 Truncation Selection

Truncation selection also ranks the individuals by fitness, but instead of always picking the top scoring individual, truncation selection randomly picks individuals from the top $N\%$ of individuals. If N is small, only the very top individuals are picked. If $N = 100\%$, truncation selection becomes random selection.

Truncation selection has a small cost in the ranking process. Depending on population size this can be an issue. But the more important issue with truncation selection is that it removes "bad" individuals from the population. This is a concern because sometimes, the bad individuals are holding useful genetic material. In our shortest path sample problem, a bad individual might be the only one with a one in the first gene. By always killing lower fitness individuals, truncation selection can hurt the long term success of the population.

2.4.4 Roulette, or Fitness Proportional Selection

Roulette selection tries to solve the problem of reduced diversity associated with losing bad individuals by randomly choosing from all individuals, [Banzhal *et al.* (1998) page 130]. However, unlike random selection where every individual has an equal chance to be picked, roulette selection uses the fitness of each individual to give more fit individuals a higher probability of being picked. To achieve this, roulette assigns a selection probability for each individual based on its fitness, as follows:

1. Calculates the sum across all fitness scores.

$$S = \sum_{i=0} f_i, \text{ where } f_i \text{ is the fitness for individual } i \tag{2.2}$$

2. Assign each individual a probability based on its fitness divided by the sum of all fitness scores, see Fig. 2.6.

$$p_i = f_i/S \tag{2.3}$$

3. Spin the wheel to get a number r between 0 and 1.

4. Walk the list of individuals, from the first one in the population to the last,

adding each individuals probability to the running total:

$$s_j = \sum_{i=0}^{r} p_i. \tag{2.4}$$

5. Stop when the value on the wheel falls in an individual's probability zone,

$$s_{j-1} < r \leq s_j, \text{ select individual } j. \tag{2.5}$$

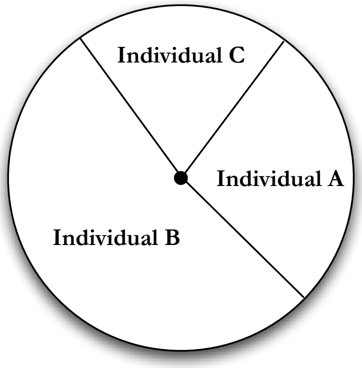

Figure 2.6: An example probability chart for roulette selection

Roulette selection won't necessarily lose "bad" individuals, and has only a small overhead. Roulette selection also puts selective pressure on the Genetic Algorithm by giving good individuals a better chance to be used for reproduction. However, it does suffer from the ability for a very fit individual to drown out a number of worse individuals. For example, given a population of 10 individuals, if one has a fitness of 1.0 and the rest have a fitness of 0.1, the higher scoring individual will be selected about $\frac{1}{2}$ of the time. This, like rank and truncation selection, can hurt diversity in a population.

2.4.5 Rank Selection

There is another version of Roulette selection, sometimes called Rank Selection, that uses the individual's rank, rather than its raw fitness to assign a probability.

This selection method removes the chance for a single individual, or small group of individuals, to dominate the fitness wheel, [Eiben & Smith (2003) page 60]. Rank selection reduces the chance of keeping a "bad" individual with "good" genes.

2.4.6 Tournament Selection

Tournament selection [Eiben & Smith (2003) page 63] tries to solve the problem of choosing good individuals at the cost of diversity in a novel way. In tournament selection we chose a tournament size, call it TS. In its simple form, each time an individual needs to be selected for reproduction, a small tournament is run by:

1. Randomly pick TS individuals
2. Take the highest scoring individual from this group

This algorithm uses random selection to get the members of the tournament, so good and bad scoring individuals are equally likely to make it into a tournament. Unfortunately, in this simple form, tournament selection will leave zero chance for the worst individual to be used for reproduction, since it can't win a tournament. This leads to a modified algorithm:

1. Pick a percentage of times we want the worst individual to win the tournament. This value, PW, can be tuned. A low value of PW will keep bad individuals out, while a high value can increase diversity by allowing more bad individuals in.
2. Pick TS individuals
3. Randomly pick a number between 0 and 100.
4. If the number is greater than PW take the highest scoring individual from this group, otherwise take the lowest scoring individual in the group

A useful feature of tournament selection for GA users is that it has two tuning mechanisms, the size of the tournament and the chance that bad individuals win. Tournament selection is good for diversity, since it allows bad individuals to win in a controllable way. By changing tournament size it is possible to make tournament selection more like random selection, using a small tournament, or more like truncation selection, by using a large tournament.

Because of these nice features, all of the GA done in later chapters will use tournament selection. The tournament sizes will be 4 or 5 individuals. Based on experiments these values allow close to 98% of each population to participate in at least one tournament. The PW for my runs will generally be 25%. The value of 25% was based on an initial desire to allow lower scoring individuals to win tournaments without overwhelming good individuals. In places where my runs suffer from diversity issues, a possible direction for future work will be to try different values for this tuning parameter.

2.4.7 Selection and Fitness Function Requirements

The choice of fitness function and selection mechanism are connected. Suppose that you have the choice of two fitness functions. Both rank properly, in that the better individuals have higher fitnesses. But one is smooth and the other is discontinuous or lumpy. What I mean by lumpy is that the fitness function likes to group individuals around certain scores, and if individuals improve they might jump to another group of scores.

Given these two choices of fitness function, which is best? To answer that really depends on the selection algorithm. If you use roulette selection, then lumpy or discontinuous fitness functions could be bad because they would give larger probabilities to an individual that is near a discontinuity in the fitness function, even if the difference between that individual and one on the other side of the discontinuity is ultimately minimal. On the other hand, rank selection or tournament selection won't have this problem because they use the ordering of fitness scores rather than the raw fitness scores to make decisions.

For the tournament selection used throughout this dissertation, our goal is to make sure that two individuals raking by score is correct, regardless of their absolute difference in score. In other words, if A has a higher fitness than B then A is better than B. But it doesn't matter if there are gaps in the possible fitness values. Put simply, it doesn't matter how much better A scores than B.

2.5 GA Operations

Once individuals are selected for reproduction the children are created using *operations*. There are three operations in particular that have come to define GA: mutation, crossover and copy. Other operations can be created for specific problems. GA is normally implemented to chose a single operation, from a fixed set of choices, to generate each child. The available operations and the chance for each operation to be chosen will effect the performance of the GA for a specific problem, [Eiben & Smith (2003); Jong (2006); Mitchel (1998)]. I will discuss these choices more with regards to each operation in the sections below.

2.5.1 Mutation

Mutation is the process of changing an individual in a random way, Fig. 2.7. For the shortest path problem, all of the genes are an integer between 0 and ψ, so mutation might change a randomly selected Y-value, or gene, from 3 to 2 or vice-versa. As implemented for this dissertation, mutation works on a single gene, picked randomly, and changes it to another appropriate random value. Mutation is a powerful operator because it can add diversity into a population. This can allow GA to move a population away from a local minimum in search of a global one.

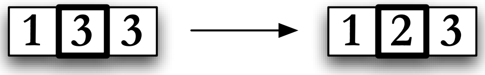

Figure 2.7: Mutation of a chromosome at a single gene

If mutation is used too heavily the user will move from the genetic algorithm to a random search, on the other hand, using mutation too sparingly can allow a population to stagnate. For most of the runs discussed in this dissertation, mutation will be the chosen operation 20% of the time. This value is common in the literature, and showed reasonable diversity growth for GA in all of my simulations.

2.5.2 Crossover

In crossover, two parents are chosen to create a new child by combining their genetic material, [Eiben & Smith (2003)]. Often crossover treats the two parents differently, like a vector cross product crossing parent A with parent B may be different than crossing parent B with parent A. Many implementations will actually do crossover twice, creating two children instead of one, allowing each of the two parents to be parent A for one of the offspring.

When diversity is high, crossover can work like mutation to keep the population from stagnating. However, as a population loses diversity, crossover can start to become a process of combining very similar individuals. In this case, crossover can't always add back diversity, while mutation can.

Several crossover operations are defined in the following subsections. Most of the GA runs described in this dissertation use uniform crossover as the reproduction operator 70% of the time. Unless noted, all of the runs produce two children from each crossover.

2.5.2.1 Single Point Crossover

The simplest form of crossover is single point crossover. Think of the encoded individual as a chromosome of length L. Pick a random number between 0 and L, call it X. Take all of the encoded information to the left of X from one parent, and to the right of X, inclusive, from the other parent. Concatenate these together to get a new child. This is single point crossover as pictured in Fig. 2.8.

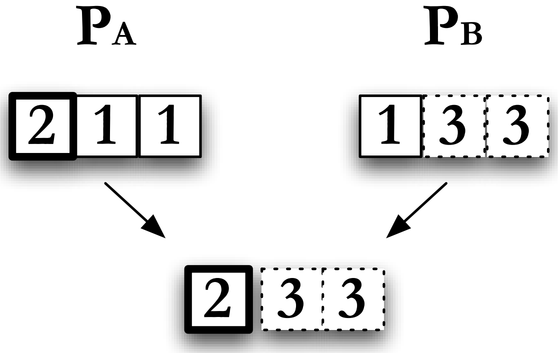

Figure 2.8: Single point crossover with $X = 1$

Single point crossover can be restricted by the encoding scheme. For example, if individuals can only be a fixed size, single point cross over has to use the same value for X for both parents. However, if children can have a longer encoding than their parents we can choose different values of X for each parent. If the encoding requires specific groupings of genes, the crossover scheme can be customized to respect these groupings when picking X.

2.5.2.2 Multipoint Crossover

Multi-point crossover, pictured in Fig. 2.9, is similar to single point crossover, except that more than one crossover point X is selected. Like single-point crossover, there are variations that allow the genes to grow or shrink. The number of points used for crossover can range from 1, which is just single point crossover, to the total number of elements in an individual. This limit is called uniform crossover.

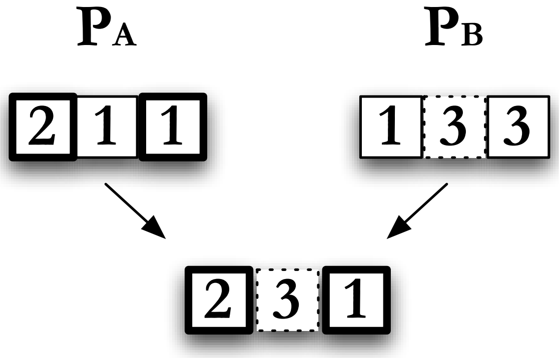

Figure 2.9: Multipoint crossover, with 2 points at 1 and 3

2.5.2.3 Uniform Crossover

In uniform crossover, each gene of the child is selected from one parent or the other by coin-flip, at the same gene location. So, for example, if a child has 5 genes, numbered 1 to 5, for the first gene you randomly pick parent A or parent B and take their value for gene 1. Then you continue this process for the other 4 genes. This is the same as doing multipoint crossover with a crossover point at every gene.

Uniform crossover may appear random at first glance. But as individuals approach an optimized solution, and become more alike, the random choice between parents becomes uneventful and will produce the same gene in either case.

Many of the projects performed for this dissertation attempt to optimize geometric solutions where material is moved around in a two and three dimensional space. Uniform crossover was chosen as the main crossover type because it allows a nice random mixing of parents to create new children, see Section 5.6. Each gene for our shielding problems will represent shield material at a specific location. Uniform crossover will simply mix two shields, location by location.

Uniform crossover easily produces two children, by using parent A for the first child's and parent B for the second child's gene for each slot. I will use it this way throughout the dissertation.

2.5.3 Copy

The simplest operation in GA is copying. A parent is copied, or cloned, to create a child. Copying is especially valuable in generational GA since it allows good individuals, or bad individuals with some good genetic material, to stick around unchanged between generations. Keep in mind that this idea of keeping good genetic material is abstract, the GA itself has no concept of good versus bad material, only fitness scores to judge individuals on. Most of the optimizations discussed in this dissertation have a 10% chance of copy forward as the reproductive operator. This results in a standard break down for this dissertation of 10% copy forward, 70% crossover and 20% mutation when an operation is required.

2.6 Results for the Shortest Path Problem

Now that we have a basic understanding of what a genetic algorithm is and the standard operations, let's take a look at how GA performs on the sample problem from Section 2.2. We will look at the problem with two values of ψ to see how GA deals with increasing the size of the search space.

2.6.1 The Shortest Path Problem with $\psi = 8$

To start, I will set $\psi = 8$. This means there will be 7 elements in the chromosome, and each element can be an integer from 0 to 8. This results in a problem space of size $9^7 = 4.78 \times 10^6$, or about 5 million possible individuals.

The GA will use tournament selection with a tournament size of 5. There will be a 25% chance of the worst individual being selected in a tournament. Each new individual will be created using the following operational breakdown:

- 70% chance of single point crossover on reproduction
- 20% chance of mutation on reproduction

- 10% chance of copy on reproduction

GA will run for 40 generations with 2,500 individuals per generation. As a result, the GA will test a total of 100,000 individuals. These individuals will not necessarily be unique, so this is an upper bound. The GA will test less than 2% of the possible solutions that use this encoding.

I did three runs of GA using these settings. The best possible score with $\psi = 8$ is -0.414 which is equal to one minus the length of a straight line from the origin to $(1, 1)$; all three runs produced an individual that matched this score. Graphically, these three best results look like the data in Figure 2.10.

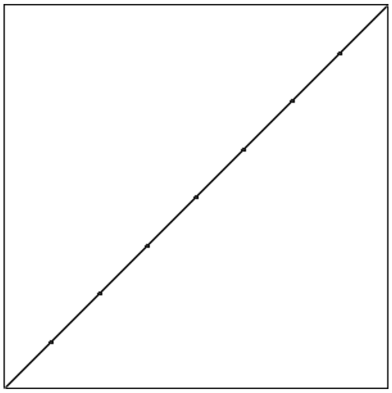

Figure 2.10: The best solution from GA for $\psi = 8$ on the shortest path problem

To really see how well GA did, we need to look at the best fitness for each generation in one of these three runs. Graphing the fitness for the best individual in each generation versus the generation count gives the plot in Figure 2.11.

GA is finding the best solution in generation 11. This means that GA only needed $27,500$ individuals to find the best solution, which is well under 1% of the total possible solutions.

So what is GA doing after generation 11? For the most part it is improving the suboptimal individuals. We can see this by looking at the average fitness by generation, pictured in Figure 2.12. The average fitness is going up with each generation

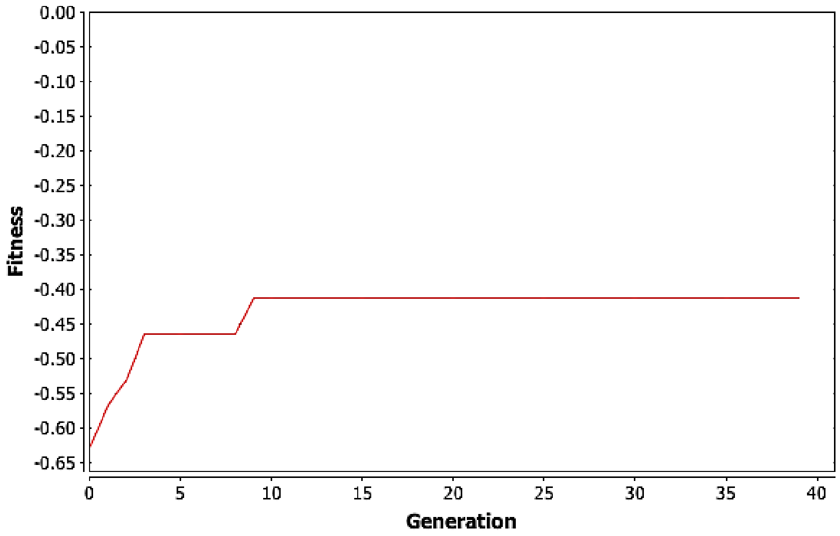

Figure 2.11: A plot of maximum fitness vs. generation for a run of GA with $\psi = 8$ on the shortest path problem

as the good genetic material is spread around the population. Then at around 30 generations, GA is reaching a plateau where the average fitness is basically trapped.

Having the average fitness get trapped is not unexpected. As the population becomes more homogeneous, the only operator that really moves individuals around the solution space is mutation. Consider the simple example of a population where no individuals contain a 0 in their first gene. Mutation is the only way to get a 0 into that gene. But mutation can both hurt and help and individuals score. As the population gets closer to the best solution, or a local maximum, mutation can move it away from that maxima, and it can take numerous tries for an individual with a needed gene to participate in reproduction. In the worst case, mutation could cause the best individual in a population to score lower on the fitness function.

2.6.2 The Shortest Path Problem with $\psi = 16$

GA was able to handle a search space with five million individuals pretty easily. Let's look at how it will do with a bigger search space. In this case, we will look at our shortest path problem with $\psi = 16$. This is a problem space with $17^{15} = 2.86 \times 10^{18}$ or

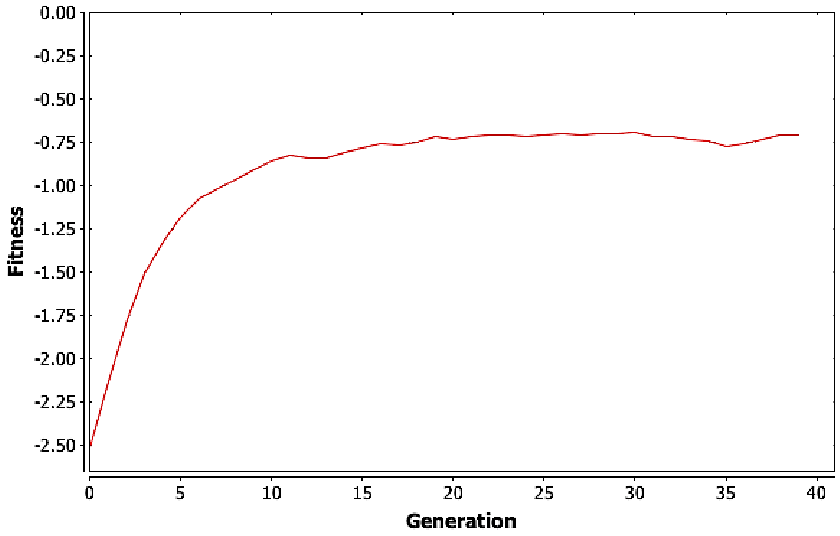

Figure 2.12: Average fitness vs. generation for a run of GA with $\psi = 8$ on the shortest path problem

2.86 quintillion individuals. We will keep our GA parameters the same. The $100,000$ individuals tested will represent only 2.86×10^{-11} percent of the possible solutions.

I did three runs of this problem, and all three resulted in a best fitness of -0.4396 compared to the best possible fitness of -0.414. While the runs all had the same best fitness score, they did not result in the same solutions. Solutions with the best fitness from each run are pictured in Figure 2.13.

Each of these solutions is partially on the optimal line, and partially off the line by one unit, creating a bump. It is important to note that while these three individuals had the best score for their run, they are not the only individuals in that run to achieve that score.

The fitness for one of these runs, pictured in Figure 2.14, shows that the GA is stagnating. It hasn't had time to find a solution that can move the bump onto the line.

Consider the montage of 25 individuals from the last generation of Run 3, Figure 2.15, we can see that the population does have the genetic material needed to find the best solution. It just hasn't found that solution yet. A few of the solutions

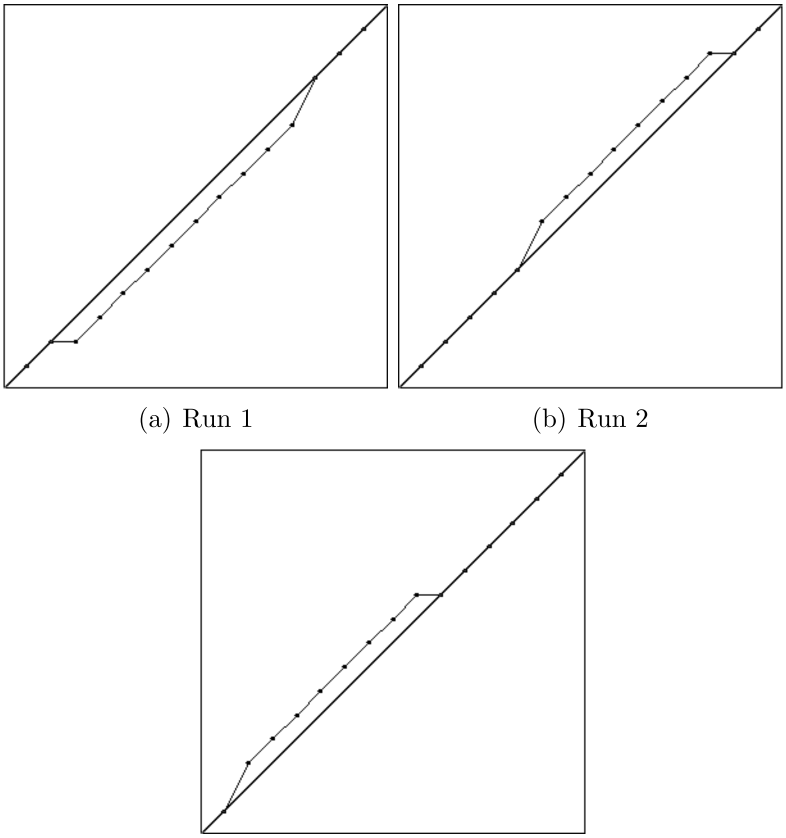

(a) Run 1

(b) Run 2

(c) Run 3

Figure 2.13: The best results from 3 runs of GA with $\psi = 16$ on the shortest path problem

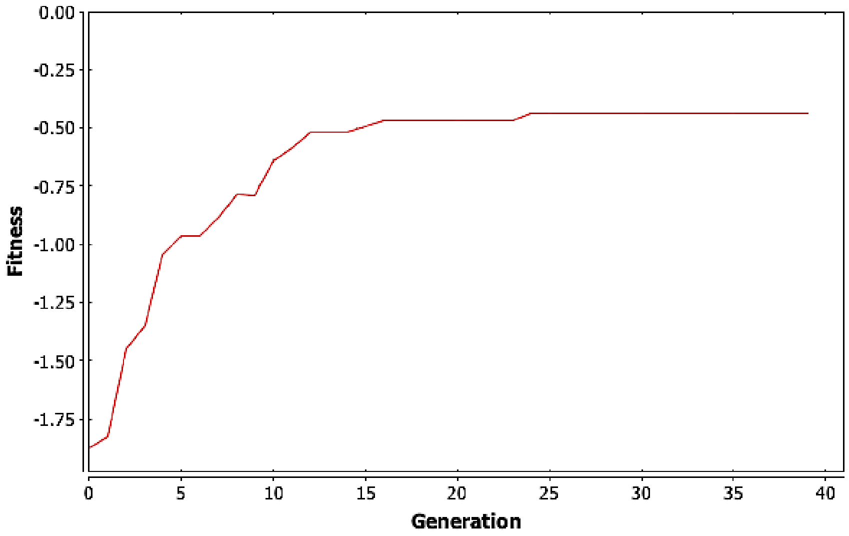

Figure 2.14: The maximum fitness vs. generation for a single run of GA with $\psi = 16$ on the shortest path problem

in the montage are on the line except at the ends, while others have trouble in the middle.

One way to try to help GA is to give it more resources in the form of larger populations or more generations. Trying this on the $\psi = 16$ problem, I did three more runs, but this time I used a population size of 4000 and a maximum generation count of 50. This effectively doubled the number of individuals tested.

Using these new resources, two of the runs were able to find the best possible solution, as pictured in Figure 2.16. Only one run failed to find the best solution.

The run that failed to find the best solution actually ended up with a worse solution than the runs with fewer resources. This variance demonstrates the problematic randomness of GA, while the improvement of the other two runs shows how more resources can help GA move toward a better answer. Keep in mind that while we did double the number of individuals, the number of individuals tried versus the total number of possible individuals is still miniscule.

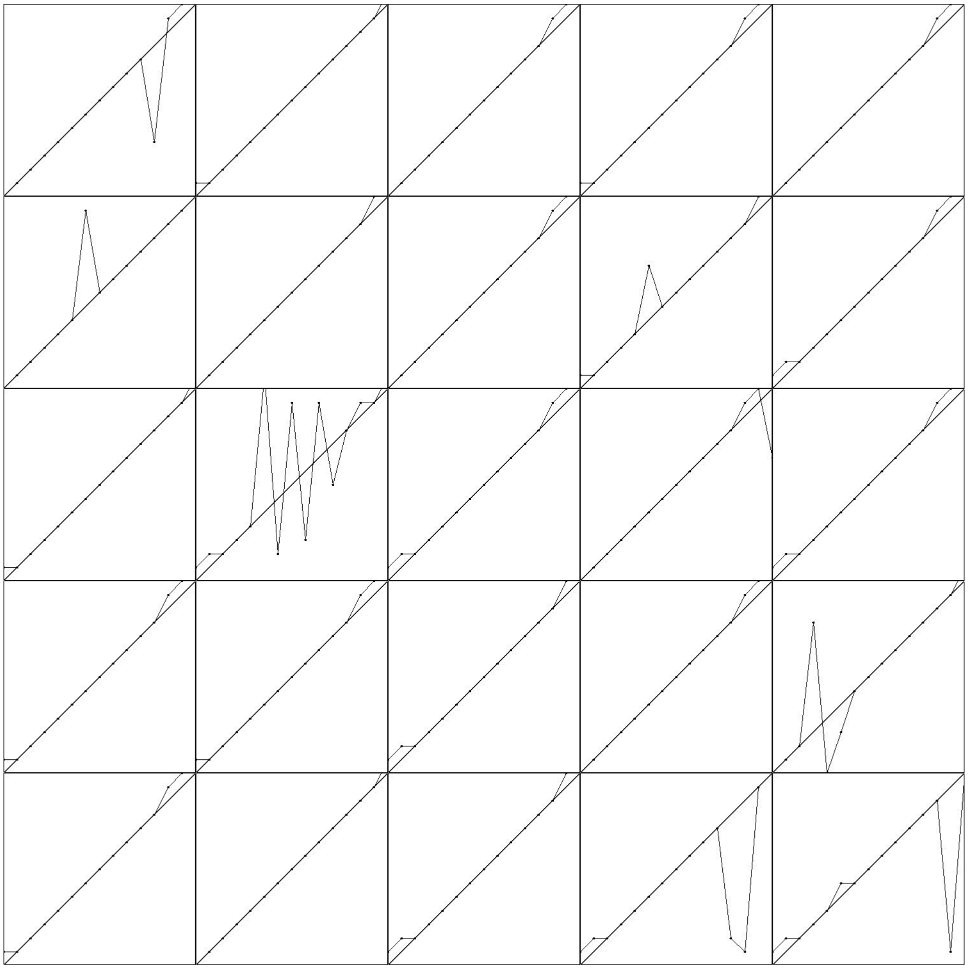

Figure 2.15: 25 random solutions from the final generation of GA Run 3 on the shortest path problem with $\psi = 16$

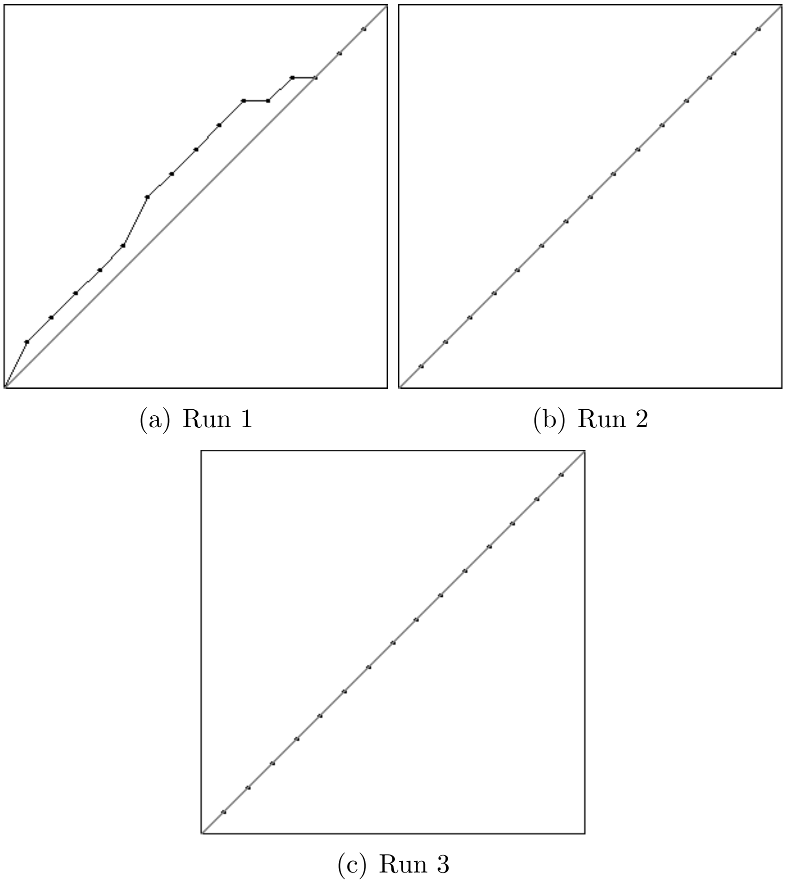

(a) Run 1

(b) Run 2

(c) Run 3

Figure 2.16: The best results from 3 runs of GA with $\psi = 16$ on the shortest path problem with more resources

2.7 Population Sizing and the Number of Generations

The test problem has lead us to an interesting question. How big should a population be for a given problem?

At the lower end, GA needs a population that is big enough to have sufficient diversity. For example, if we use $\psi = 4$ and a population of 2 there will not be enough diversity to try to solve the problem. In order to formalize this idea of sufficient information, researchers have decomposed the Genetic Algorithm into a set of requirements. One decomposition that has been proposed, [Goldberg (1989)] , and used extensively relies on the concept of building blocks. Building blocks, [Goldberg *et al.* (1991)], are the elements that can be used to make solutions. In our sample problem the building blocks would simply be the individual points, or possibly chains of values that fall on the line that makes the best solution. Building blocks are a very abstract idea that tries to provide a concept for the useful information chunks encoded in a chromosome. In biology a building block might be the set of genes that create the heart or lungs.

The building block decomposition works like this:

1. Know what the GA is processing: building blocks
2. Ensure an adequate supply of building blocks, either initially or temporarily
3. Ensure the growth of necessary building blocks
4. Ensure the mixing of necessary building blocks
5. Encode problems that are building block tractable or can be recoded so that they are
6. Decide well among competing building blocks

The population size question address the second item of this decomposition: ensuring an adequate supply. The genetic operators like crossover and mutation ensure the growth of necessary blocks. Selection, along with the operators, ensures proper mixing. The chromosome encoding and fitness function address the last two pieces of this decomposition. We could re-write this decomposition using the terms we have been using to say:

1. Encode problems in a way that works well with mutation and crossover
2. Ensure an adequate and diverse population
3. Ensure that mutation and crossover can reach all of the genes
4. Define a good fitness function

If we consider that the initial population for GA is usually generated randomly, it is easy to see that a very small population size could prevent GA from having all of the necessary building blocks in the initial population. If this were the case, GA would have to try to use mutation to create these building blocks, which could be quite inefficient. As a result, we can theorize that given limited resources there is a population size that is too small for GA to build a solution in a reasonable amount of time.

Population sizing is bounded from above based on computing resources. While there are no papers saying that an infinite population is bad, it would require infinite resources. So as GA is applied to a problem, researchers want to find the smallest population that will still allow GA to work. Moreover, because a small population provides more opportunity for two specific individuals to crossover, small populations have the potential to evolve faster during the initial generations. Large populations, on the other hand, will have a harder time putting two specific individuals together, which can result in slower evolution.

One attack on the population sizing problem is given by Harik [Harik *et al.* (1997)]. In this paper the building blocks that represent parts of a good solution are treated as individuals that might be removed from the population via standard operators and selection, a form of gambler's ruin. Using this concept Harik et.al. show that problems that require more building blocks are more susceptible to noise and thus more susceptible to failure. They were also able to show that while this semi-obvious connection exists it is not a scary one. The required population size for a problem is shown to grow with the square root of the size of the problem, as defined as the number of building blocks in a chromosome.

Another look at the sizing problem was done by [Goldberg *et al.* (1991)]. Goldberg et.al. used an analysis of noise in the GA to show that the required population size is $O(l)$ where l is the length of a chromosome, or encoding. The multiplier for this equation can depend on χ, the number of possible values for each element in the chromosome, which is a fixed value for the problem.

These two analysis used different techniques to arrive at a scaling, and resulted in different values. Harik's analysis says that the required population goes with the square root of the number of building blocks, while Goldberg's analysis says that it increases linearly. While both analysis rely on assumptions that make them inexact, we can at least see that GA does not appear to require a population size that grows exponentially or with some power of the problem size.

On the other side of the table is the question of how many generations we should run. [Goldberg & Deb (1991)] have analyzed this problem as well to show that using standard selection mechanisms GA should converge in $O(\log(n))$ or $O(n \log(n))$ generations, where n is the population size. While this equation doesn't give us an exact value for the number of generations to use, it does tell us that adding generations is not going to give us exponential improvement. It also explains the shape of the fitness graphs in Figures 2.11 and 2.14, where we could see the slope of the fitness improvements going down with each generation.

In all of the experiments presented in this dissertation, the population sizes and generation counts have been arrived at primarily through resources constraints. I have tried to find a compromise between computing resources and reasonable results from the GA.

2.8 GA For Hard Problems

As we saw in Section 2.6, even a simple problem description can result in a huge problem space. As the problem spaces get bigger, the problems get harder to solve. Hard problems can also be defined by the amount of resources they require to calculate a fitness function. In this dissertation I will be discussing problems that require radiation transport simulations to calculate a fitness score. These problems can run for minutes or hours, as opposed to the microsecond test times of the shortest path problem. As people have tried to apply GA to harder problems, they have reached a point where a single computer cannot provide sufficient resources for their problem. When this happens, the Genetic Algorithm has to be distributed to multiple computers.

Luckily, GA has an inherent parallelism. The most expensive part of GA is generally the scoring step and the process of scoring individuals can be distributed quite easily. In this section I will discuss a number of the techniques used to distribute GA onto multiple processors and machines.

Hard problems can also introduce other issues into standard GA. Sometimes diversity becomes an issue in a very large problem space. Populations can converge too quickly, or not quickly enough due to resource constraints. Some of the following techniques have been created to help change the diversity from the standard algorithm or distribute on a network, or both. These techniques are important to understand so that they can be contrasted with our new approach, MGGA.

2.8.1 Simple Distributed Genetic Algorithms

Perhaps the simplest way to distribute GA is to distribute the scoring phase using some form of messaging passing technology like MPI. Distributing GA using messaging passing involves running numerous agents. Most of the agents score individuals in the genetic run. A central, or master, agent performs the initial population creation, hands out scoring work, coalesces scoring results and performs reproduction. By scaling the number of agents, the scoring work can be scaled to any number of machines.

Distributed GA relies on data sharing to pass scores from the scoring workers to the scaling worker. Some form of synchronization must be provided to keep each agent doing work at the right time, and waiting while new work is created. Simple GA codes will generally use memory to hold populations, but by leveraging a shared file system, database or distributed cache, these techniques can support gigantic problems [SQLite (2011)].

Ironically, the biggest drawback of these distributed GA is that it doesn't change the underlying algorithm. If diversity is a problem for a specific application, distributing it won't increase the diversity. Distribution simply adds processing power. The next few sections discuss techniques that have been used to alter the fundamental algorithm. These can be combined with simple distributed Genetic Algorithms, or be distributed themselves.

2.8.2 Island Model Genetic Algorithms

The island model of GA, [Eby *et al.* (1999); Tomassini (2005)], breaks a single Genetic Algorithm run into a set of runs. Each run uses the standard iterative approach discussed in 2.3. What makes the island model different than running a bunch of separate GAs, is that individuals from each population, or island, are traded with other islands. So individuals from one run will migrate to, or be injected into, another run. This immigration model allows the sharing of genetic material and can add diversity by adding variety to a stagnating population.

The island model is the basis for most of the distributed algorithms used for GA by other researchers. It can be altered to allow things like different fitness functions for each island, or different GA parameters for each island. In Chapter III we will see how MGGA is similar to the island model, except that we will not be performing immigration every generation or two, rather we will be using a hierarchy of populations, that could be thought of as islands.

2.8.3 Pyramidal Genetic Algorithms

In pyramidal GA, [Aickelin (2002)], a number of islands or agents are used to perform separate Genetic Algorithms. Each agent uses a different fitness function to score individuals. These individuals are then combined, or injected into a different agent that uses a higher order fitness function. For example, one agent might score a shield on mass, while another scores it on shielding quality. The final population is generated from shields that are good for mass, combined with those that are good for shielding, and GA is performed on this combination population. The final agent would use a fitness that scales for both mass and shielding.

2.8.4 Multiscale Genetic Algorithms

Multi-scale GA, [M Babbar (2002)], is a version of the island model where the fitness functions for each island leverage some sort of scaling in the fitness function. For example, one island might use a coarse grid, while another uses a fine grid, to score individuals, [Babbar & Minsker (2003)]. This technique is one of the motivators for MGGA. Multi-scale GA allows some of the islands to perform quick fitness tests using low resolution models, while other islands use higher resolution models to determine higher quality fitness values.

2.8.5 Hierarchical Genetic Algorithms

Hierarchical GA, [De Jong (2011)], is a term used for a version of the island model that is similar to Multiscale GA and Pyramidal GA. Essentially the islands form a hierarchy, where each looks for individuals based on a subset of the total criteria, and those individuals are used to feed islands looking at more criteria. Hierarchical GA has primarily been implemented as part of Genetic Programming to protect functions or other modules that have been found in the lower level islands.

2.8.6 Messy Genetic Algorithms

Another technique used to apply GA to hard problems is called Messy Genetic Algorithms, [Goldberg *et al.* (1993)]. Messy Genetic Algorithms use genes to encode name-value pairs so they can change size without breaking the standard operator semantics. The MessyGA uses a series of phases, [Merkle *et al.* (1998)], just like generational GA, but the phases are slightly different. First, there is an *initialization* phase. This phase is used to create all of the fundamental building blocks, but not all of the possible individuals. In our sample problem this would mean making sure that at least one individual had each of the appropriate points, but not necessarily all of the appropriate points. In a shielding problem, this might mean making sure that we have at least one individual with each part of the shield geometry included. For very large problem spaces, this rule can be reduced to simply try to create as many as the resources support.

After initialization, MessyGA uses a *primordial* phase composed of alternating tournament selection and building block filtering (BBF). The tournament selection finds fit individuals, and BBF deletes genes. Individuals that can have genes deleted and are still highly fit are passed into the next phase. The next phase is called *juxtaposition.* In this phase, individuals are recombined to build better individuals. These phases are often distributed across multiple machines.

Messy GA focuses on the building block concept by trying to ensure that all of the good building blocks are available and that these building blocks are highlighted and combined into highly fit individuals. Messy GA has been written in a highly parallel fashion to support hard problems and its building block nature helps it focus on preserving good building blocks even in limited populations.

2.9 Genetic Algorithms on an Off-The-Shelf Cluster Scheduler

The problems discussed later in this dissertation are "hard problems." They have large solution spaces, and they require a lot of computing resources to score. Luckily a large cluster is available at the University of Michigan. This section discusses why I developed a genetic algorithm library to execute GA on the U of M cluster.

The U of M cluster uses the Portable Batch System (PBS) scheduler, see [pbs (2011)]. This is a very standard, open source, cluster job scheduler. In order to put GA onto the Michigan cluster and scheduler I had to stay within a set of restrictions.

1. All jobs for a genetic run must be scheduled in advance.

2. Jobs must be assigned an estimated time.

3. Jobs are only given their estimated time to complete, plus a margin for error.

4. Jobs that run over their time, plus the margin, are treated as failed and killed.

5. The longer the estimated time for a job, the lower priority it has.

6. Jobs can depend on one or more other jobs, in a flexible manner.

7. There is a line length associated with listing dependencies.

8. My jobs running on another user's nodes can be interrupted.

9. Jobs have access to a shared file system.

Estimating time, dealing with errors for fault tolerance and working around line length limits are the main issues with leveraging the existing cluster. Moreover, in order to scavenge the most resources, my code had to be resilient to interruptions. The PBS scheduler doesn't like to schedule many long running jobs for a single user on shared computers. Having long running jobs reduced our resource usage by reducing our priority. Finally, the cluster administrators didn't want my jobs to schedule other jobs to solve this problem.

Considering these restrictions I decided to leverage the PBS scheduler as the master node and use the job running nodes as the scoring slaves in a distributed GA. In order meet the restrictions I also replaced the message passing design with a batch design. Instead of agents running all of the time, a series of jobs is scheduled for each phase in the GA process. For example, a job builds the initial population, a set of jobs score the population, a job processes the scores, a job performs reproduction, etc.. As with the message passing design, batch distributed GA can be scaled to fill available computing resources. Unfortunately, there are no GA libraries, that I could find, that support the concept of the batch-oriented distributed GA on this type of job scheduler, with my resource restrictions. As a result, I implemented batch distributed GA in a custom library called *Genetik*, discussed in Appendix A.

I was unable to find any reference to this style of distributed GA in the literature and as a result, this implementation of batch GA in the context of a job scheduler appears to be a new technique.

2.9.1 Generational GA As Jobs

Genetik uses the following basic job types to do the actual work:

Build Build a population, either randomly or from a previous one.

Score Score a sub-set of a population.

Collect And Scale Join the scored sub-sets and perform any fitness score scaling we want to do.

The input file for Genetik includes how many individuals should be included in each generation and how many generations to increment over. Genetik uses this information to schedule one build job for each generation and one collect and scale job for each generation. The input file also contains the size of the scoring populations. Genetik uses this information to schedule enough scoring jobs to cover the population.

The build job uses a cache of all previously scored individuals to ensure that no individual is scored in two different generations. It is possible that the same individual is scored by 2 scoring jobs, but it will not be scored again in a later generation.

The genetik input file also contains time estimates for each job type. These are included in the PBS job description files.

2.9.2 Dealing with Dependency Limits

PBS has a line length limit for describing dependencies. This restriction is at odds with our desire to scavenge as many computing resources as possible. In order to scavenge all possible resources we want to run a lot of short running jobs, rather than a few long running jobs. Having a lot of scoring jobs for each generation places a long dependency list on the Collect and Scale job that follows them. In order to coalesce these dependencies into reasonable line lengths, I use no-op jobs called Joins. These jobs do nothing, but do have dependencies. Using a 5-to-1 scaling I can quickly reduce a large number of scoring jobs into a small number of Join jobs that can be depended on by the Collect job.

2.9.3 Dealing with Errors

Scoring jobs can fail; the easiest way this can happen is if we underestimate the time it takes to score an individual. I have built in some resilience against scoring jobs failing. This resilience comes in the form of a repair step in the collection process. Repairs simply replace an individual that couldn't be scored with a random, scored, individual.[1]

2.9.4 Processing

The final step in my implementation of GA on the PBS scheduler was to add pre-processing and post-processing jobs. These jobs allow different runs to initialize data sets, and to build reports. Also, the standard post processing step cleans up the PBS job descriptions.

These two new jobs, along with the others I have described result in the following mapping of GA onto the PBS scheduler.

Pre-Process Perform any initialization.

Build Build a population, either randomly or from a previous one.

Score Score a sub-set of a population by running a radiation transport code multiple times.

Join Join scoring jobs, treated as dependency lists, into 4 or fewer dependencies.

Collect And Scale Make sure that the scoring jobs worked, and if not replace individuals that didn't get scored with random copies from their parent generation. Join the scored sub-sets and perform any scaling we want to do.

Post-Process Build a report of the results and clean up unneeded files.

[1] I only take scored individuals for repairs, to insure that failed scoring jobs aren't propagated to the next generation.

To iterate over generations, I unroll the loops associated with generational GA. This design has been tested with numerous runs on the Michigan cluster called NYX and provides good cluster usage, some runs used over 40 machines across several hundred jobs.

2.9.5 Genetik On A Proprietary Cluster

For parts of this dissertation, funded by a grant, I was able to reserve time on the U of M cluster. This allowed me to move to a single job that ran GA and used an MPI version of MNCP to leverage the clusters computing resources. This single job model is not unique and is very powerful, but was only available after I obtained reserved computing resources, so that my single jobs could run for days. This type of long running job would not work when I was scavenging resources. The single large job with MPI-based MCNP performed similarly to the batch model, but was easier for the cluster administrators to support.

2.9.6 Optimizing GA

The Genetik library included two mechanisms to try to reduce fitness function executions, caching and pre-calculating. These two methods optimize the time spent on the cluster.

Caching involves remembering or at least checking the scores of individuals against the fitness functions that have already been run before executing their fitness function. On a very fast problem, like the shortest path, this is not very useful. But for the problems discussed in this dissertation where a fitness evaluation can take more than ten minutes, the time spent building and checking a cache becomes a very good investment. Genetik builds a cache from previous generations before scoring the next generation. This cache maps the chromosome for an individual to a score. By caching in this way, GA can save scoring time even if an individual disappears from the population and reappears in a later generation.

When Genetik was being written I had a novel idea that we could pre-determine all of the work we would have to do before we start running. Using this information, we could eliminate fitness function executions by finding individuals that never reproduce and not scoring them. I implemented this concept, called *pre-calculation*, by building a plan for each generation that included which individuals would be chosen with selection, which were mutated, which were copied and which participated in crossover to create the next generation. By finding which individuals were never chosen I was able to avoid scoring them. This method does not actually know which individuals will exist, it depends on indices into the population. So the plan might say, perform a tournament on 1,5,20,54 and 100 and create a child by mutating the winner. We don't know which will win, but we do know that we need to score the individuals at those five indices in the population to run the tournament.

The first version of Genetik implemented pre-calculation, but it turned out that very few individuals were skipped. This is a good thing. Tournament selection does a very good job of allowing almost every individual to participate in tournaments. So almost every individual at least has a chance to reproduce. While pre-calculation appears to be a novel idea, and I was unable to find it in any prior work, it doesn't appear to be an incredibly useful idea, so I removed it from the second version of Genetik, greatly simplifying the code.

2.10 Summary

Genetic Algorithms are a very powerful technique for finding solutions to hard problems. Using a few standard operators, GA is able to find solutions in huge search spaces without examining the entire space. Solutions are assigned a value using a fitness function. Execution of the fitness functions can be distributed allowing GA to work in parallel, making it even more powerful. Using the cluster at the University of Michigan I was able to build an implementation of GA that would run in a batch mode and take advantage of free computing resources.

In the next chapter I will discuss a novel technique for dealing with a hard problems that allowed me to find solutions to three hard radiation shielding design problems despite their complexity and the large run time of their fitness tests. This new technique, called MGGA, is a powerful tool for driving GA to good solutions quickly.

CHAPTER III

Multi-Grid Genetic Algorithms

3.1 Introduction

Radiation transport problems are often modeled using Monte Carlo simulations, [Fishman (2006)]. These simulations can take a very long time to run, often on the order of hours. If we put these simulations in the context of Genetic Algorithms a problem emerges. The generation and population sizes required by GA go up with the problem complexity. As a result, GA wants to do thousands or even millions of fitness function computations for a large problem space. If we are running Monte Carlo, say MCNP [Monte Carlo Codes Group - Los Alamos National Laboratory (2011)], for each fitness function and that MCNP run takes 10 minutes to complete, we are talking about hundreds of thousands of minutes, or potentially tens of thousands of computing hours to complete a simple GA run. Had I been working at a national lab, this type of computing time may have been easy to acquire. But as a graduate student I was faced with a conundrum. How can I use GA on expensive problems?

There are a number of existing models of parallel GA, [Cant-paz (1998)]. My first thought was to use some kind of island model, [Skolicki (2005)]. This model generally relies on at least one job per island executing for the duration of the run. Other master-slave models I looked at including [Berntsson & Tang (2005)] and [Sullivan *et al.* (2008)] also rely on a master node. This master node is a single long running process to manage the GA work. In all of the architectures I found at least one job was expected to run for a long time. Moreover, this job was often responsible for scheduling work. The best computing resources available to me were in the form of a cluster that used an existing scheduler, discussed in Section 2.9. In this context, it would be hard for me to execute numerous GA runs if it meant many long running jobs.

Luckily, from constraints grows creative solutions, [Heath & Heath (2007)], and from limited computing resources with a desire to look at GA for radiation shielding applications comes Multi-Grid Genetic Algorithms and a library for running them on an existing scheduler.

Multi-Grid Genetic Algorithms are a new class of GA in which we leverage geometric features in a problem space to build a hierarchy of problem spaces and reduce the number of fitness function evaluations required to reach a good solution. Normally GA starts with a random population. This can create a lot of diversity, which is good. It also requires GA to work through a lot of potentially bad genetic material, which is bad. The question is, can we create a better starting population without losing good diversity. MGGA is a mechanism for exploring this question.

In MGGA we start with a complex problem space. Take the example from Section 2.2 where each element of the chromosome is an integer from 0 to ψ. If we start with $\psi = 32$, there are 31 integers per chromosome, with each integer ranging from 0 to 32. This is equivalent to a search space with 33^{31} individuals. However, if we start with $\psi = 4$, we have a search space with only 5^3 individuals. By running GA on the $\psi = 4$ problem space, we can get some reasonable solutions for that space. Then we can tranlate these solutions to a $\psi = 8$ version of the problem space, run GA again and get new solutions that are closer to what we want in the final $\psi = 32$ problem space.

We will call the different executions of GA for our MGGA *phases*. So in this example, phase one is a GA with $\psi = 4$, phase two is a GA with $\psi = 8$ and phase three is a GA with $\psi = 32$. The individuals in the final generation of phase one are used to generate the initial population for phase two. The individuals in the final generation of phase two are used to generate the initial population for phase three. The process of moving individuals between phases is called *translation*.

MGGA works in problems where the solutions can be mapped between phases. For example, the solutions in the $\psi = 4$ space can be mapped to the final $\psi = 32$ problem space by adding points, as will be described in Section 3.2 below. This means that the fitness function can be written in such a way that the fitness of this individual remains the same in both the lower resolution space and the higher resolution space. Unlike hierarchical GA, [De Jong (2011)], pyramidal GA, [Aickelin (2002)], or multiscale GA, [Babbar & Minsker (2003)], which build on different fitness functions to lead to a final result, MGGA uses a single fitness function across a range of problem spaces. In essence, the early phases of the MGGA are constraining the possible solutions to try.

MGGA works by creating good building blocks over a restricted, coarsened, version of the search space. Then MGGA uses these building blocks to seed the initial population on a finer version of the search space. This process is applied recursively so that a fine search space can be explored rapidly at successively coarser levels. In order for MGGA to work, there must be a reasonable hierarchy in the search space. Moreover, as we will see in the next section, the problem must have building blocks that make sense across the hierarchy. When this precondition is met, MGGA is able to create larger building blocks more quickly than GA because it does so in the coarser, restricted, search space while GA has to build all of its building blocks in the finest space where there are more non-optimal solutions to weed out.

3.2 Translation

MGGA is run as a set of Genetic Algorithms performed in serial. These phases each perform a complete generational Genetic Algorithm run. Between phases a translator is used to move the encoding for each individual from one problem space to the next. As a result of this translation phase, MGGA introduces a number of new parameters to Genetic Algorithms, including the method for translation and the method for picking individuals to translate when moving between phases.

3.2.1 Translation and Population Size

Each phase in an MGGA can use a completely different set of the standard GA parameters. This means that you could use a different type of crossover in each phase, or a different percentage of crossover, versus mutation. For the experiments performed for this dissertation, I have tried to minimize the changes from one phase to the next. The only real change is in the size of the populations and the number of generations tested for each phase. By using a small number of generations and a small population for earlier stages, we can scale the total resources used, and also focus them on the more complex problem spaces in later phases.

In order to move between a smaller population and a larger one I use the standard selection mechanisms, see Section 2.4. In particular, I use tournament selection throughout this dissertation. By using selection to get individuals from one phase to the next we can think of the translation process as just another, albeit special, genetic operation like the ones discussed in Section 2.5.

3.2.2 Translation between Encodings

The translation operation is basically a recoding of the genome. Each individual from one phase is mapped to the equivalent individual for the next phase. For geometric problems we can make this mapping exact if we use an appropriate scale.

For this dissertation, we have accomplished this by doubling the scale of the problem space at each step.

3.3 GA for the Shortest Path Problem with $\psi = 128$

Perhaps the easiest way to see how MGGA works is to first show an example where plain GA does poorly. Let's take the shortest path problem from Section 2.2. Moreover, let's blow the problem up to a very large size by setting $\psi = 128$. This results in a search space that has $129^{127} = 1.1 \times 10^{268}$ individuals. This is a gargantuan search space.

The best possible score on this problem is approximately -0.414, which represents 1 minus the length of the line from $(0, 0)$ to $(1, 1)$.

Using the fitness function described in Section 2.2 I ran a GA using tournament selection with a tournament size of 5. There will be a 25% chance of the worst individual being selected in a tournament. Each new individual will be created using the following operational breakdown:

- 70% chance of single point crossover on reproduction
- 20% chance of mutation on reproduction
- 10% chance of copy on reproduction

GA ran for 40 generations with 2,500 individuals per generation. As a result, the GA will test a total of 100,000 out of 1.1×10^{268} possible individuals. These individuals will not necessarily be unique, so this is an upper bound. In Section 2.6.2 we saw that GA had trouble with $\psi = 16$ for these settings, so we should expect it to have even more trouble with this much bigger search space.

I performed five runs to minimize the chance of a statistical anomaly throwing off the results. These runs produced a best individual with the fitness value shown in Table 3.1.

Run	Best Fitness
Run 1	-10.34
Run 2	-10.96
Run 3	-9.97
Run 4	-10.62
Run 5	-9.3

Table 3.1: Results of GA for $\psi = 128$ on the shortest path problem

The best of these runs resulted in a fitness around -9.3. This individual is pictured in Figure 3.1 and it is clearly having trouble getting all of the 127 points to converge. GA did accomplish some improvement on a very complex problem space. If we compare this best individual to the best individual in the first generation, which was randomly generated, Figure 3.2, we can see that GA reduced the noise by a great deal with only $100,000$ total individuals tested, and raised the fitness from -33.3 to -9.3.

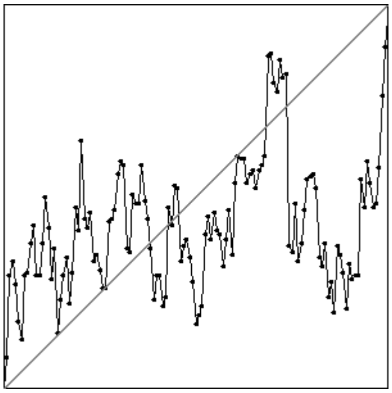

Figure 3.1: The best individual from five GA runs with $\psi = 128$ on the shortest path problem

One way to observe how well GA is converging is to look at a plot of the best fitness versus generation. This plot for run 5 is pictured in Figure 3.3, it clearly shows how GA is continuously improving the fitness of the best individual. In the runs from Chapter II, with a lower value of ψ, the GA was stagnating because it had found the best solution, or close to it. Figure 3.3, on the other hand, shows that the GA isn't stagnating in the 40 generations run.

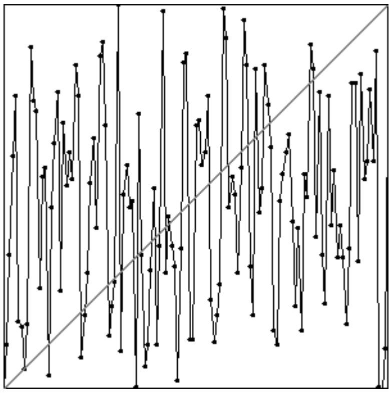

Figure 3.2: The best individual from the first generation of GA run 2 on the shortest path problem with $\psi = 128$

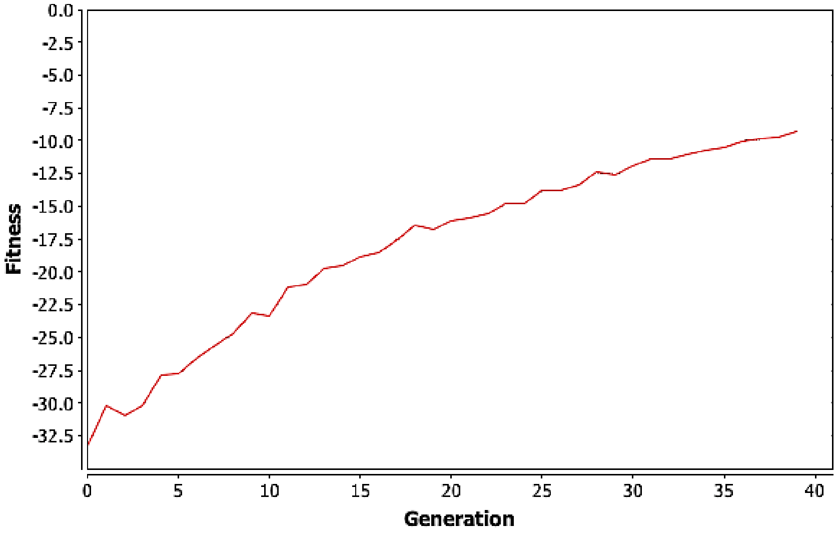

Figure 3.3: A plot of the best fitness versus the generation for run 5 on the shortest path problem with $\psi = 128$

Run	Population Size	Generation Count	Best Fitness
Small	1250	20	-18.42
Small Gen	2500	20	-17.31
Small Pop	1250	40	-10.75
Standard	2500	40	-9.3
Big Gen	2500	80	-7.3
Big Pop	5000	40	-9.5
Big	5000	80	-4.84

Table 3.2: Results of GA for $\psi = 128$ on the shortest path problem with different resources

Before we look at MGGA for this problem, let's take a moment to look at how GA performs with difference resources. In particular, I performed the same GA runs with different values for the population size and generation count. These runs, and the resulting best fitness are listed in Table 3.2.

Plotting these values, see Figure 3.4, we observe that adding resources is helping GA, although not in a guaranteed fashion. Based on the results from Section 2.6.2 this is a reasonable expectation, since adding resources to the $\psi = 16$ problem both found a better solution in two runs and a worse solution in one run.

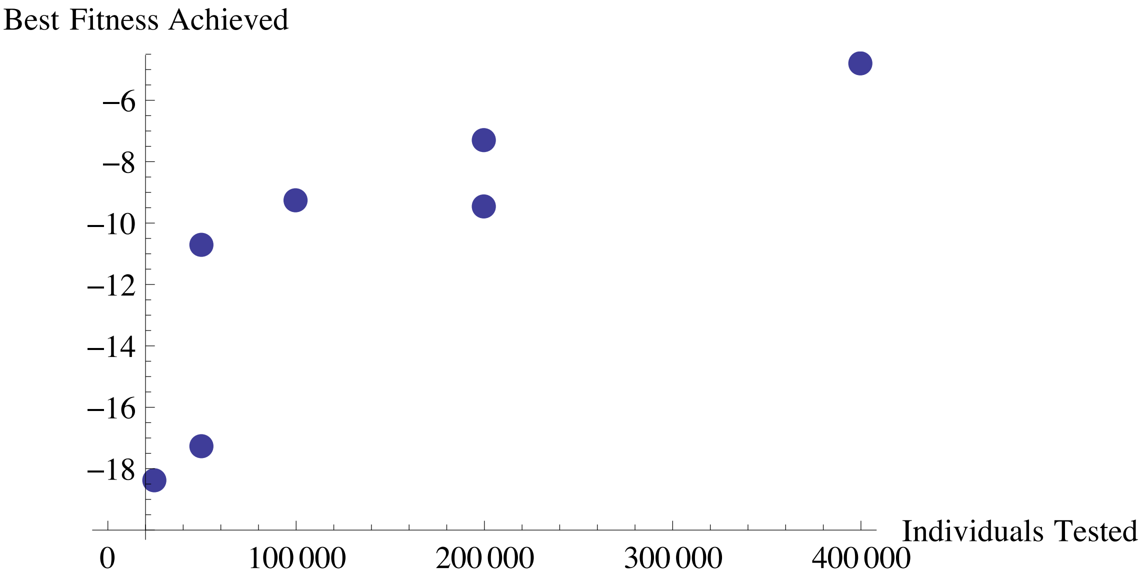

Figure 3.4: A comparison of the best fitness vs total possible individuals for different resources runs of GA with $\psi = 128$

3.4 MGGA for the Shortest Path Problem with $\psi = 128$

In order to run MGGA on this problem we need to define our translation operator. The translation operator for the shortest path problem will do two things. First it will double the number of possible Y values. Second it will change the number of genes to be $\psi - 1$ for the new phase by inserting values between the existing ones. The Y values that match X values from the previous phase will just be double the value in the previous phase. So a Y value of 1 in the first phase, becomes 2 in the second phase. The Y value for new X values is interpolated from the points on each side of them using a simple linear interpolation.

Consider the translation from $\psi = 4$ to $\psi = 8$, pictured in Figure 3.5. The initial phase will have 3 genes and two fixed endpoints. For example, a chromosome might look like 012. To calculate the chromosome for the next phase we start by adding four new genes to get a total of seven; 012 becomes $x0x1x2x$. Next we double the known genes; $x0x2x4x$. Finally we calculate the new genes using linear interpolation, limited to the grid; resulting in 0012346.

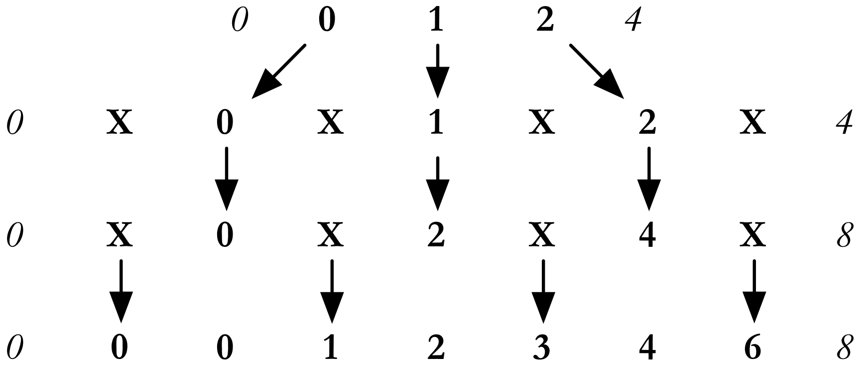

Figure 3.5: Translating from $\psi = 4$ to $\psi = 8$

Each MGGA phase used the same parameters as the GA discussed previously. Tournament selection is used to choose the individuals that move between phases. The following phases were run:

Run	Phase 1	Phase 2	Phase 3	Phase 4	Phase 5
Run 1	-0.52	-0.44	-0.48	-0.48	-0.49
Run 2	-0.53	-0.53	-0.56	-0.62	-0.65
Run 3	-0.57	-0.71	-0.86	-0.95	-1.00
Run 4	-0.46	-0.50	-0.59	-0.67	-0.72
Run 5	-0.41	-0.44	-0.50	-0.53	-0.58

Table 3.3: Results of MGGA for $\psi = 128$ on the shortest path problem

- $\psi = 8$, 100 individuals per generation and 10 generations
- $\psi = 16$, 300 individuals per generation and 10 generations
- $\psi = 32$, 600 individuals per generation and 10 generations
- $\psi = 64$, 1000 individuals per generation and 20 generations
- $\psi = 128$, 1000 individuals per generation and 20 generations

While the GA tested a total of $100,000$ individuals, the MGGA only tests $50,000$ individuals. This is a reduction of over 50% in fitness calculations performed. As with the GA I did five runs on MGGA on this problem. The results for the best fitness for each phase are listed in Table 3.3.

The random nature of selecting individuals that translate between phases allowed some backslide during the start of each phase, for example, Run 1 had the best fitness go from -0.44 to -0.48 between phases two and three. Despite this backslide effect, all of the MGGA runs resulted in individuals that beat the best individuals from the GA runs, even though MGGA tested less than half of the total individuals that GA tested. This is an great result. Despite using fewer resources, MGGA is beating GA on this type of problem. Moreover, MGGA is testing an extremely small part of the fitness space to accomplish this. Focusing on the first MGGA run, that had the best final fitness, lets look at why this happened.

Figure 3.4 shows the best individual from the final generation of each phase of the first MGGA run. These individuals are much less noisy than the results from the GA.

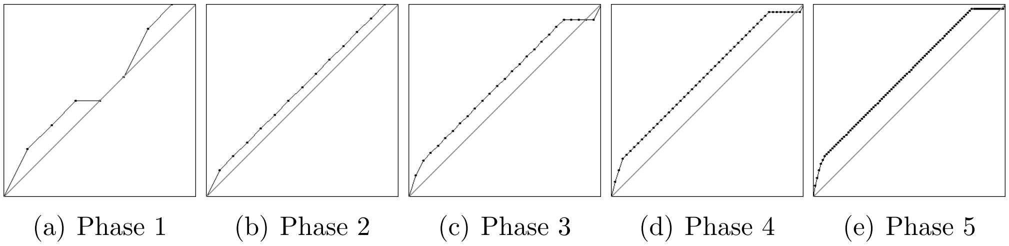

Figure 3.6: The best results from each phase of MGGA in run 1 on the shortest path problem with $\psi = 128$

The improvement of MGGA over GA occurs because the good individuals from the first phase are ultimately feeding into the very large problem space for phase 5. By feeding good individuals into the final phase we produce a better set of initial building blocks and therefore can produce better results. In the shortest path problem it is even possible for MGGA to find the best solution, a straight line, in phase 1 that remains the best solution until the final phase. While this didn't happen, it would have been specific to the problem space. The shield designs in later sections will generally require the finer problem spaces of later phases to find the best solutions.

The problem MGGA appears to be having is that it is stagnating on a sub-optimal solution. Because the problem space we are investigating doesn't favor mutation very well, it is hard for the GA to move to a better solution once it finds a good line of points. Moving the points off the line usually lowers the fitness score. While crossover also allows GA to explore new regions of the search space, the present example is using single point crossover, which really only allows splicing two line segments together. This is not a powerful enough operator to move away from a local maximum.

Our first step in trying to improve MGGA's results is to add resources. As with GA I did a few runs of MGGA with different population and generation parameters. The values for the each phase of the new runs were scaled the same way I did for the GA results in Table 3.2. For example, the smallest run used half the population and half of the generations for each phase, when compared to the base run described

Run	Population Size	Generation Size	Best Fitness
Small	50/150/300/500/500	5/5/5/10/10	-0.8
Small Gen	100/200/600/1000/1000	5/5/5/10/10	-0.48
Small Pop	50/150/300/500/500	10/10/10/20/20	-0.92
Standard	100/200/600/1000/1000	10/10/10/20/20	-0.49
Big Gen	100/200/600/1000/1000	20/20/20/40/40	-0.71
Big Pop	200/600/1200/2000/2000	10/10/10/20/20	-0.49
Big	200/600/1200/2000/2000	20/20/20/40/40	-0.48
Very Big	400/1200/2400/4000/4000	40/40/40/80/80	-0.53

Table 3.4: Results of MGGA for $\psi = 128$ on the shortest path problem with different resources

above. These runs, and the resulting best fitness are listed in Table 3.4, where the values in the population size and generation count columns are multipliers, indicating the amount changed from the initial runs. The fitness listed is the best fitness from the final phase.

These results are interesting in that adding resources did help in some cases, but not in others. One thing the data shows is how shrinking the population size seems to be worse than shrinking the generation count. Based on the discussion in Section 2.7 this could be because the smallest population is just too small to provide the necessary building blocks for our GA to work efficiently. Another possible issue is that even the "very big" run may have had insufficient resources. Also, we may simply be suffering from the problem that mutation has a hard time improving fitness.

Having tried quadrupling the generations and populations for each phase without finding the optimal solution I decided to try other techniques for improving MGGA. One such technique was to change the operators I was using. Up until now I have been using single point crossover. This allows GA to combine two lines, but doesn't provide a way to pull sections of one line into another line. Basically the crossover point for single point crossover has the same problem that mutation does; if a line of points gets broken, it can reduce fitness. Uniform crossover could break more lines, but it can also move line segments together across the entire individual in a single

Run	Best Fitness
Run 1	-10.66
Run 2	-10.56
Run 3	-10.26

Table 3.5: Results of GA for $\psi = 128$ on the shortest path problem with uniform crossover

Run	Best Fitness
Run 1	-0.418
Run 2	-0.795
Run 3	-0.485

Table 3.6: Results of MGGA for $\psi = 128$ on the shortest path problem with uniform crossover

step. Ultimately uniform crossover provides a very strong way to change individuals, and will help if these major changes result in better populations as a whole.

3.5 Uniform Crossover for the Shortest Path Problem

To see if changing the GA operations would help GA and MGGA solve the shortest path problem I did three runs of each with uniform crossover, getting the results listed in Table 3.5. These results, for GA, are no better than the results with single point crossover. This is not too surprising since both sets of runs are incredibly resource starved when we consider the size of the search space.

Running MGGA with uniform crossover had a very different effect. The runs listed in Table 3.6 produced an individual that is only a few points away from the perfect solution, which would score -0.414. The best individual, pictured in Figure 3.7, is the result of MGGA with only $50,000$ total individuals tried from a search space of 1.1×10^{268} individuals and is a wonderful result.

MGGA is able to take advantage of uniform crossover in the early phases, where there are fewer possible values on the grid. Later, these better solutions work together through uniform crossover, to create even better results. Because uniform crossover touches more of the genes, it is helping avoid the artificial plateaus that MGGA

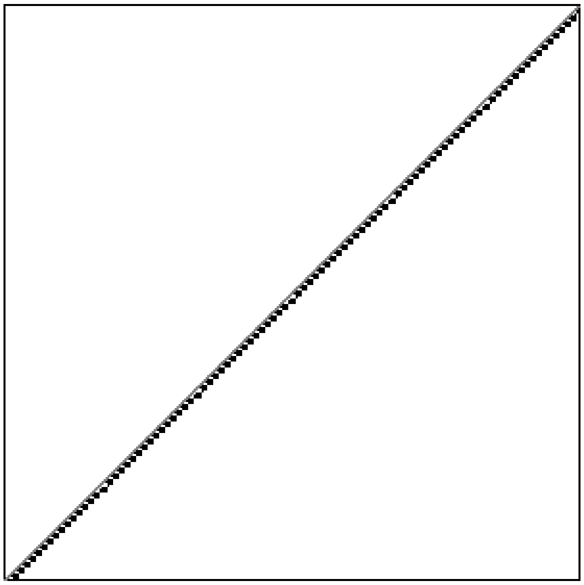

Figure 3.7: The best result from MGGA with uniform crossover and $\psi = 128$ - Fitness $= -0.418$

encountered when using single point crossover.

Given these results on the test problem, we can see that MGGA does a great job of removing noise from a complex search space and honing in on good solutions with very few resources.

3.6 Miscellaneous Thoughts On MGGA

So why does MGGA work? MGGA can be thought of in a number of ways. One way is to think of MGGA as simply partitioning the problem space. The beauty of MGGA is that this partitioning doesn't have to change the problem space. An example of this is pictured in Figure 3.8. Where the individuals are expressed as areas of space that are turned on. The individual on the left is from phase 1 and the individual on the right is from phase 2. We can completely express all of the individuals from phase 1 in phase 2, with no differences in geometry. If the fitness function works at a high resolution, it can still score the lower resolution individuals.

It is very important to note that although this mapping from phase 1 to phase 2 is exact, there is not an equivalent reverse mapping. While you can map from phase 2 to phase 1, you will potentially be adding material to a shield, or area to a geometry problem.

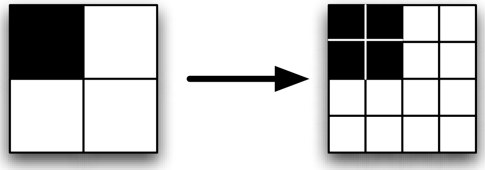

Figure 3.8: An example of an MGGA translation with exact mapping

In problem spaces where an exact mapping from one phase to the next is possible we can think of MGGA another way. MGGA is treating a group of individuals as having the same fitness in the early phases, while they may have a different fitness in the higher phases. Using the concept of building blocks, MGGA is saying that a set of building blocks from the final problem may be equivalent in earlier phases.

In Figure 3.9 we see three individuals. All three of these are impossible to map onto the 2×2 grid exactly. If we say that moving from 4×4 to 2×2 involves looking at the material in the finer grid and if any material would appear in the coarser grid, fill in the coarser grid. So in this example, we would fill in the upper-left square for all three individuals. In other words, those three individuals are the same in one phase and different in another phase.

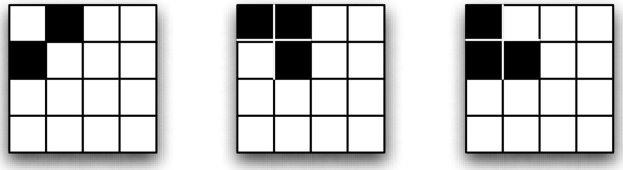

Figure 3.9: An example of individuals being grouped to one fitness

As long as the exact mapping holds between phases, we can extend this thinking. At the highest level MGGA on the early phases is just creating a grouping of fitness scores for individuals in the later phases.

Based on these ideas, we can conclude that MGGA uses early phases to identify the best groups of building blocks to use in later phases by filtering out groups that don't work well in the earlier phases. In our shortest path sample, MGGA is using early phases to remove groups of points that aren't near the line, then using later phases to refine those groups to ones that are actually on the line.

One of my concerns with MGGA is what happens if we start with a very small problem space in the first few phases? If the early GA creates a homogeneous population then the later phases may be hindered by a lack of diversity. There are two obvious ways to battle this problem. First we can simply start at a phase where the GA doesn't produce a homogenous population. I studied this technique with the shadow shield and have discussed the results in section 5.8.2. The second option is to try to force some diversity into the population during the translation phase. An easy way to do this is to perform some mutations on each individual going through translation. An investigation of this technique is discussed in Section 5.8.3.

A final question about MGGA is whether or not it limits the possible solutions found? The answer to this is, unfortunately, it depends. Given limited resources, early phases of MGGA could block out good solutions from later phases. However, the last phase of MGGA is just a normal GA, with non-random inputs. The last phase should be able to find anything that GA can find. Therefore, given unlimited resources there is no reason to think that MGGA can't find all possible solutions. But this does mean that tuning the parameters for early phases of MGGA is important to insure that later phases are not locked out of important parts of the problem space.

3.7 Conclusions

The shortest path problem shows that MGGA is able to beat GA with fewer resources for at least one very large problem space. The question is, can MGGA help reduce resource usage for more real-world problems. The remainder of this dissertation is focused on answering that question. I will look at three real world problems, a shadow shield, a wearable shield and a bow tie filter. The shadow shield problem will be fairly simplified, while the wearable shield and bow tie filter will use more realistic physics. The goal of these three problems is to see how MGGA holds up as the problem space grows in complexity and the actual cost of the fitness calculation increases.

CHAPTER IV

A Short Introduction to Radiation Shielding

4.1 Introduction

Before diving in to my first application of MGGA, let's take a step back and look at the larger context of the applications we will be looking at. Each of the three applications of MGGA presented in this dissertation are related to radiation shielding. At the highest level, each application looks at designing a shield or filter to alter the effects of a radiation source on a target area. Before we talk about how MGGA can help, let's look at what the MGGA will try to do.

4.2 Radiation Basics

Radiation is particles traveling through space, or interacting with other materials. There are several categories of radiation based on the particles involved:

Alpha

Alpha radiation is associated with the travel of alpha particles. Alpha particles are essentially helium ions, with 2 neutrons and 2 protons. There are no electrons in an alpha particle.

Beta

Beta radiation is transmitted via electrons, or beta particles. In some cases

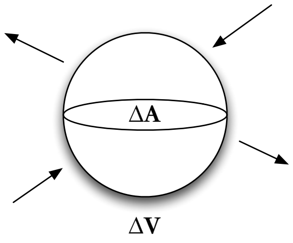

Figure 4.1: A sphere with volume ΔV used to define fluence

materials may emit positrons, which carry the opposite charge of an electron but otherwise behave similarly.

Gamma

Gamma radiation is in the form of photons. Photons are sometimes referred to as x-rays or gamma-rays depending on their energy and source. This is a reasonable distinction, but ultimately the same particle is in flight.

Neutrons

Neutrons are often emitted during nuclear reactions and can travel as a single particle.

When describing radiation, one of the easiest ways to think about it is to consider the number of particles hitting something. Because large numbers of very small particles are involved, this quantity has been abstracted into the idea of *fluence*. Fluence is defined in terms of two values. ΔN_p, a number of particles, and ΔA a cross section that defines the hypothetical sphere, pictured in Figure 4.1, that those particles cross during some period of time. The fluence, Φ, is defined by taking the limit as ΔA goes to zero,

$$\Phi \equiv \lim_{\Delta A \to 0} \left[\frac{\Delta N_p}{\Delta A} \right]. \tag{4.1}$$

Formally, according to [International Commission on Radiation Units and Measurements (2011)], we can write the fluence as:

$$\Phi = \frac{dN}{dA} \tag{4.2}$$

where N is the number of particles and A is the cross section of the sphere. In many of our simulations we will rely on MCNP to calculate the value of fluence. This is usually done by using the equivalent definition in 4.3 where we use the length of the tracks, dl, crossing the sphere of volume dV, and

$$\Phi = \frac{dl}{dV}. \tag{4.3}$$

Another way to think about radiation is to think in terms of time. Fluence rate is the change of fluence over time. This quantity is sometimes called the particle flux density, or flux,

$$\dot{\Phi} = \frac{d\Phi}{dt}. \tag{4.4}$$

4.3 Interaction Quantities

When particles encounter matter there is a possibility that they interact. The chance of an interaction occurring depends on the type of particle coming in, the type of material it is encountering, the energy of the particle, the energy of the material, and the possible interactions. The concept of a *linear attenuation coefficient*, μ, is used to capture this chance of interaction into a single measurable quantity, [International Commission on Radiation Units and Measurements (2011)]. μ is defined as:

$$\mu = \frac{1}{dl}\frac{dN}{N} \tag{4.5}$$

where dN/N is the fraction of particles that have an interaction with the material in a distance dl.

Because μ depends on the density of the target material, this definition can be written in terms of the mass attenuation coefficient μ/ρ:

$$\frac{\mu}{\rho} = \frac{1}{\rho dl}\frac{dN}{N} \tag{4.6}$$

By writing the mass coefficient in this way, we can also get to another quantity called the *microscopic cross section*, σ. The units for the microscopic cross section is m^{-2}, which are sometimes written using *barns*, where one barn is $10^{-24}cm^2$. The mass coefficient is linked to the cross section by replacing the density by Avagadro's number, N_A, times the molar mass of the target material, A.

$$\frac{\mu}{\rho} = \frac{N_A}{A}\sigma \tag{4.7}$$

The intensity, I, of a beam of radiation at depth t is described by

$$\frac{I}{I_0} = e^{-\sigma N t} \tag{4.8}$$

where N is the number of atoms per cm^3 and I_0 is the initial intensity of the beam. So the intensity goes down by a factor of e when the thickness is $\frac{1}{\mu}$. This is also the average distance that a particle moves from the point of its birth to its first interaction and is called the *mean free path.*

In the case where there are multiple mutually exclusive interactions the cross section is often thought of as:

$$\sigma = \sum_j \sigma_j \tag{4.9}$$

where σ_j is the cross section for a particular interaction. Also, for homogeneous mixtures or compounds we can think of the total value for μ as a sum:

$$\mu = \sum_j \mu_j = \sum_j N_j \sigma_j \tag{4.10}$$

where N_j is the atomic density of the j-th element.

The cross section is also energy dependent, which will have an important effect on our ability to shield various particles.

4.4 Shielding Basics and Radiation Interactions with Matter

Shielding at its most basic is the process of stopping radiation from hitting something. The basic question is how much of something is needed and what is the best something to put in the way.

Because alpha particles are charged they are relatively easy to shield against and can be stopped by even a thin sheet of material. A Po-210 nucleus can produce alphas with an energy of 5.3 MeV, but these will only travel $4cm$ in air at 1 atmosphere, and less than a few millimeters in human skin or aluminum. However, their charge also allows them to transfer a great deal of energy and if allowed to hit sensitive materials alpha particles can be devastating. Alphas had a small burst of fame in the mid-2000s when Polonium was used to kill an ex-K.G.B. spy. But in this case, the material had to be ingested to do real damage [Cowall (2006)].

Beta particles are charged so they interact with the electrons and nuclei of materials, making them relatively easy to shield against. For example an incoming beam of 4 MeV beta particles only needs a centimeter or so of aluminum to stop it [Cember & Johnson (2009)].

Gamma particles will interact with the electron clouds around atoms, allowing them to be shielded against. However, unlike alpha and beta particles, gammas should not be thought of as stoppable, and are better treated as something you attenuate with a shield or filter. This process is described in 4.4.1.

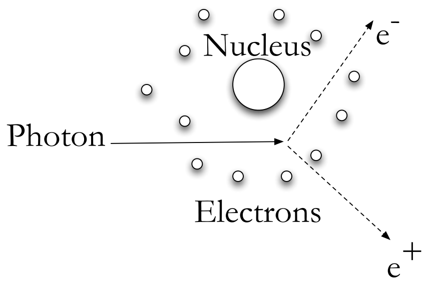

Figure 4.2: Pair production

Neutrons have mass and no charge. This allows neutrons to carry a great deal of energy, but makes them hard to shield against since they do not interact with the charge of a target. Neutrons transfer energy and momentum via a short range nuclear force, potentially causing a cascade of nuclear reactions.

4.4.1 Interactions in Gamma Shields

Gamma particles, photons, can interact with materials in a number of ways, including pair-production, Compton scattering, photo-electric absorption and photo-nuclear effects.

Photons above an energy of 1.02 MeV have a chance of performing a quantum mechanically beautiful reaction called *pair production*, [Cember & Johnson (2009)]. Pair production occurs when a photon, with sufficient energy, travels near the nucleus of an atom and spontaneously turns into a pair of particles. One particle will be an electron, e^-, the other a positron, e^+. Each of the particles will have half of the mass-energy of the photon. The photon has to have enough energy to provide the mass for the two particles, thus the lower limit on its energy. This reaction only happens near another particle so that conservation of momentum can be ensured with any extra energy.

The probability of pair-production goes up with higher Z materials, and ultimately results in the positron being annihilated with another electron. As a result, pair

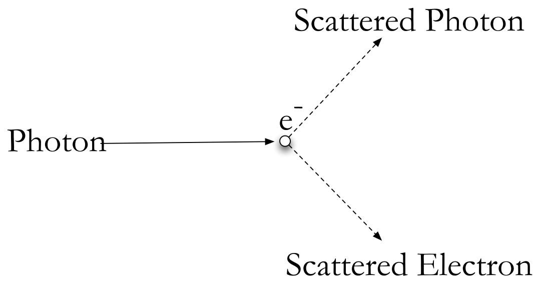

Figure 4.3: Compton scattering

production generally deposits energy into a shield and also generates lower energy photons that continue to pose a hazard.

Compton scattering occurs when a photon collides with an electron in an atom that is bound to the atom with a binding energy lower than the photon energy. When a Compton scatter occurs, the electron is knocked free of the atom. This electron will have some new velocity, and will ultimately be absorbed as a beta particle. The photon, unable to transfer all of its energy to a single electron, will continue on with a reduced energy. Because Compton scattering is related to electrons, more electrons will increase the chance of it occurring.

When a photon collides with an electron that is bound tightly to the atom, it is possible to have *photoelectric absorption*. In this case, the electron, called a photoelectron is kicked out of the atom with most of the photon's energy and the photon is absorbed. The probability for the photoelectric effect is related to the binding energy of electron shells, and will play a key role in shielding lower energy gamma particles.

At very high energies it is possible for a photon to kick a neutron or proton out of the nucleus. This is called *photodisintegration*. One example of photodisintegration is in Be-9, which can interact with a 1.666 MeV photon to produce a neutron.

The collective μ/ρ values measured for lead are pictured in Figure 4.4. These values tell an important story. First, at low energy, where the photo-electric effect takes precedence, we can see that there are sharp peaks and valleys. These *edges*

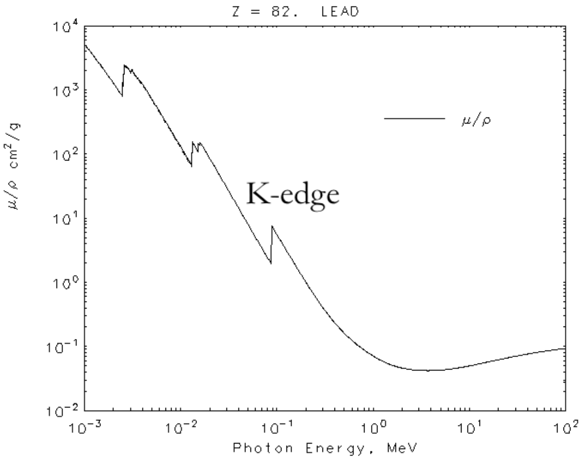

Figure 4.4: The γ cross-section for lead, [National Institute of Standards and Technology (2011)]

correspond to the electron shells. The highest energy edge corresponds to the inner most shell, which requires the most energy to eject an electron. This inner most shell is called the *K-shell* so this edge is called the *K-edge*.

The edges in an element's cross section will play a role in the design of low energy gamma shields discussed in Chapter VI. Consider, for example, a shield made out of a combination of Lead and Antimony. Figure 4.5 shows the cross sections for these two elements on the same plot. Notice that the edges aren't at the same energy. Moreover, there are places where the edges for lead causes it to have a lower cross section than antimony, a lower atomic number element. We will leverage this physical feature when trying to construct layered gamma shields.

4.4.2 Interactions in Neutron Shields

Neutrons are grouped into two categories: fast and slow. Fast neutrons, generally with energies over 0.1 MeV interact with the atomic nuclei in shields via inelastic and elastic collisions. The value for cross sections is very energy dependent, and the effect of the collisions is very dependent on the mass of the nucleus being collided with.

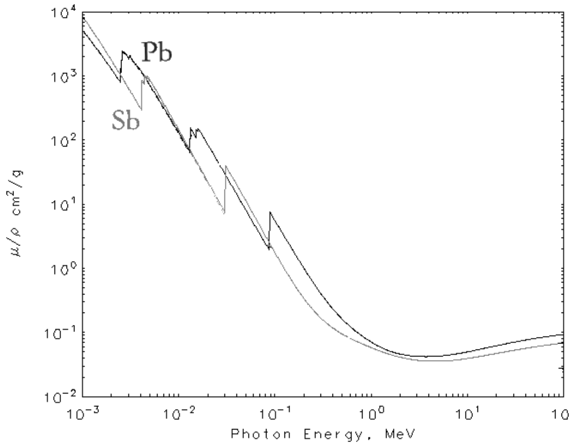

Figure 4.5: The γ cross-sections for lead and antimony, National Institute of Standards and Technology (2011)

When a head-on elastic collision occurs, the energy of the neutron after the collision is given by simple mechanics as

$$E = E_0 \left[\frac{M - m}{M + m} \right]^2 \tag{4.11}$$

where m is the mass of the neutron and M is the mass of the nucleus. Thus, for hydrogen it is possible to have a collision that takes all of the neutron's energy. While collisions slow the neutrons, they can also damage the shielding material and can generate γ-ray emissions.

Slow neutrons interact with a shield via elastic scattering, inelastic scattering and absorption. This can cause nuclear reactions in the material resulting in secondary radiation that may be emitted even over very long time periods. The chance of absorption, or capture, goes up as the energy of the neutron goes down. Stopping neutrons is therefore achieved by slowing them with collisions until they are absorbable.

4.5 Health Physics Basics

Interactions in the body follow the same physics as interactions in a shield. The trick with radiation in people is figuring out the biological effects of the radiation. With a shield, we might worry about cracking or long-term radioactivity, but with a person we have to worry about numerous biological effects ranging from cell mutations to death. Quantifying radiation on the body is therefore harder than in a single material. We will use the quantity called *absorbed dose* to measure radiation in a body. Absorbed dose is defined as

$$D = \frac{d\epsilon}{dm} \tag{4.12}$$

where $d\epsilon$ is the mean energy deposited to the infinitesimal volume with mass dm. The unit for absorbed does is the Gray, which is equivalent to J/kg, or $m^2 s^{-2}$.

When we deal with a person, we are dealing with a very complex set of interactions between radiation and a number of materials. The human body contains different organs that perform different biological functions. Often the health physicist will be concerned with the *whole body dose*, or the dose to the entire body. There are also concerns for specific organs, and in this case it is not enough to say how much radiation hit that organ. We will also have to take into account a weighting that indicates how sensitive that organ is to radiation. These weights can be used to calculate something called the *effective dose*, defined as:

$$\varepsilon = \sum_T w_T H_T = \sum_T w_T \sum_R w_R D_{T,R} \tag{4.13}$$

where H_T is the equivalent dose in organ or tissue T, $D_{T,R}$ is the mean absorbed dose in the organ or tissue T, w_R is a radiation weighting factor for radiation R and w_T is a tissue weight factor. w_R is independent of the tissue or organ and can range from 1 for gamma radiation to 20 for some energies of neutrons. w_T is independent of the radiation, and can range from 0.01 for skin to 0.2 for the gonads.

4.6 Summary

Radiation is categorized into four main forms. Alpha radiation, made up of 2 neutrons and 2 protons, is easily shielded against. Beta radiation, generally electrons but also positrons, can be shielded against with rather thin layers because it interacts easily with atoms. Gamma radiation is composed of photons and interacts with matter through the electrons circling the nucleus. Gamma radiation can interact in a number of ways based on energy and provides a more challenging shielding problem. Neutrons are perhaps the hardest type of radiation to shield against. Neutrons don't interact with the electron shells around an atom. Rather they interact with the nucleus. At high energies neutrons are basically billiard balls, slamming into nuclei and often weakening shielding materials. At low energies neutrons can be absorbed causing potentially long term radiological effects.

Chapter V discusses how MGGA can be used to build a neutron shield, and will focus on scattering interactions. Chapter VI discusses building a shield for gamma radiation and Chapter VII discusses using MGGA to design a filter for gamma radiation. The two chapters will focus more on Compton scattering and the photo-electric effect. Chapter VI is focused on shielding a human and will rely on the some of the health physics concepts discussed here, especially the weighting factors for each organ.

CHAPTER V

Designing a Shadow Shield

5.1 Introduction

Minimization of mass is critical for space applications and naturally raises the question of what is the optimal shield shape for a space reactor shield? In the vacuum of space a shadow shield is sufficient; it need cover only a small solid-angle while allowing radiation to stream away from the spacecraft payload in other directions. The obvious shield shape is therefore a frustum of a cone, but this obvious solution has been shown to be a suboptimal design, [Alpay & Holloway (2005)]. Splitting a frustum into two parts can open up radial streaming paths that can reduce the payload dose for a fixed shield mass. There is no reason to believe that the split design in [Alpay & Holloway (2005)] is the best. Moreover that result required a large number of MCNP runs to find a good strategy for splitting the shield. The combination of flexible geometry and mass constraints makes the problem of designing a shield for space applications a complex and interesting one, dominated by a large search space, a perfect testing ground for MGGA.

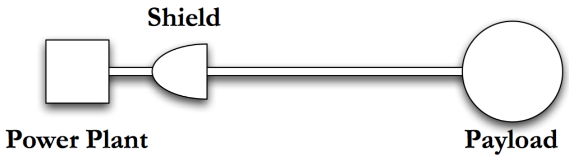

Figure 5.1: The geometry of a simple shadow shield

5.2 The Shadow Shield Problem

In this chapter I will discuss MGGA in the context of a single test problem: a space shield based on the design pictured in Fig. 5.1. In this problem I am designing a shield that needs to protect a payload from a particle source. I will use a geometry pictured in Fig. 5.2 that is a very simple model of the problem pictured in Fig. 5.1 where I have removed the intervening space and placed the source and detectors next to the shield itself. This simplification is reasonable for comparing shields, but a more accurate geometry would be required to estimate the actual flux on a payload through one of the shields discussed here. The source emits evenly from a disk of radius 90 cm at the origin of the z-axis. This disk is represented by the rectangle on the left of Fig. 5.2.

The shield is cylindrical. GA's task is to place annular rings of material into the vacuum along the z-axis between 10 and 160 cm from the source, with the largest ring extending radially to 300 cm.

5.2.1 Modeling the Shield

There are two key aspects in modeling this shield for GA. First, we need to model the shield's geometry and second we need to model the materials that make up the shield. For most of my work, I will model the shield's geometry as annular rings of equal mass (hence having larger radial extent near the axis). Two shields with the same number of filled rings will weigh the same amount, regardless of where the rings are. In Section 5.7 I will discuss several simulations that use non-equal mass rings.

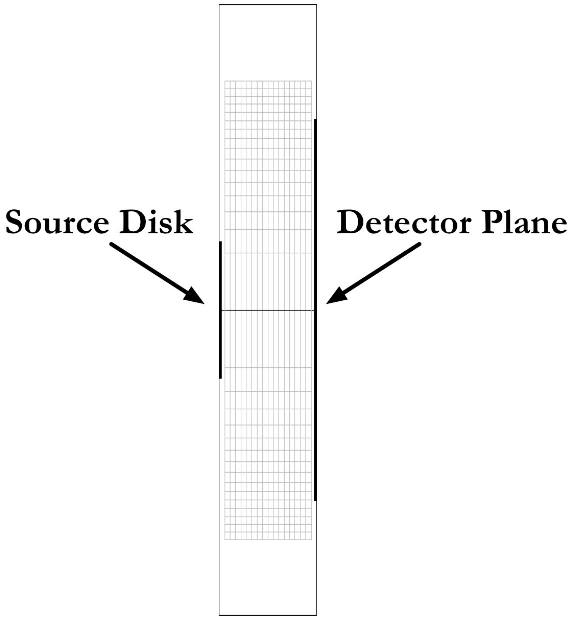

Figure 5.2: The geometry for the shadow shield problem. The r-z plane with a disk source to the left and a detector plane to the right. The goal is to place material in the intervening vacuum to reduce the flux at the detector plane.

In that case, the rings will have an equal radial delta, and the outside rings will be much heavier than the inside rings.

The rings are separated along the z axis into disks. In all simulations these disks have an equal size. Figure 5.2 pictures a shield with 16 rings and 16 disks all with equal mass.

I chose equal mass rings for the majority of these simulations in an attempt to reduce preferential treatment of each ring. If the inside rings are lighter than the outside rings, then they will be preferred on the basis of mass. While physically this may be appropriate for reducing radiation at the ship, I would rather have the GA figure that out, than build a preference into the initial model.

The material for the shield is modeled as a binary value. A value of 0 represents no shield material and a value of 1 represents shield material. Given the simplified physics used, this material is not real, but is loosely based on Lithium-Hydride. I picked Lithium-Hydride for several reasons. In a real-world space shield scenario the shield material is going to have to meet a number of criteria including:

- Reduce the flux of high energy neutrons
- Reduce the flux of low energy neutrons
- Reduce the flux of gamma rays
- Be as light as possible
- Be manufacturable
- Last the life of the mission

For simplification I am focusing my design on high energy neutron shielding, so my first goal is to scatter neutrons. The best way to do this is with hydrogen, [Chilton *et al.* (1984)], which will reduce the energy of the neutrons by an average of 50% in each scatter. Hydrogen also has a high scatter cross section. Unfortunately hydrogen doesn't do a good job of absorbing the thermal neutrons, so in a real shield we would want to put it in some kind of compound, [R.K. *et al.* (2001)]. The question is, what compound to use.

As far back as the 1970s engineers have been looking into shielding for space applications, [Radiobiological Advisory Panel (1970)]. These investigations have focused on the entire set of criteria, including gamma rays and low energy neutrons. The results of the early work was to use LiH [Lee (1987)]. LiH has a low density, so it is lightweight. It contains a lot of hydrogen, so it slows down high energy neutrons quickly. The LiH helps capture thermal neutrons and does so without generating a lot of gamma rays, [Pheil (2006); Bell *et al.* (2010)].

Despite having significant production and durability issues, including hydrogen disassociation and thermal swelling, LiH has historically been considered a prime shielding candidate. Various packaging ideas have been proposed to deal with LiH's issues including storing it in containers. Other designs, [Lee (1987)], have suggested layering LiH with something like tungsten to reduce gamma rays as well. We will only be looking at high energy neutrons for this simulation and will ignore the potential use of tungsten. I ignore the infrastructure of the shield in this problem, focusing instead on designing a shadow shield that has a good material for scattering high energy neutrons.

5.2.2 The Theoretical Shield Material

I model radiation transport for the shadow shield as a one-speed problem, using a purely scattering material with total cross section of 0.275 per cm. This is characteristic of neutron interactions in LiH at 2 MeV, with isotropic scattering, except that LiH scatters somewhat forward. To calculate this simplified cross section I started with the total cross-section for Li at 2 MeV, [Los Alamos National Lab (2011)], which is 1.725 barns. For hydrogen the total cross section at this energy is 2.914 barns. Next I determined the number of Li and H atoms in a cubic centimeter. The molar mass of LiH is 7.95 and its density is 0.78 gm cm^{-3}, [webelements.com (2011)]. This results in an N of 5.9×10^{22}. So to determine the macroscopic total cross section of LiH I used Equation 4.10 to calculate:

$$\Sigma_T = 5.9 \times 10^{22} \times (1.72 + 2.91) \times 10^{-24} \tag{5.1}$$

or 0.275 cm^{-1}. The equivalent calculation for the radiation capture cross section at this energy results in

$$\Sigma_A = 5.9 \times 10^{22} \times (5 \times 10^{-6} + 3.42 \times 10^{-5}) \times 10^{-24} \approx 2.313 \times 10^{-6} cm^{-1} \tag{5.2}$$

a negligible value, indicating that LiH will primarily scatter neutrons at this energy, as we would expect. Note that this is a natural Li, not enriched in Li-6

So, everywhere there is shield material, or a 1 in a shield's chromosome, the fitness test will use this 0.275 cm^{-1} cross section for scattering our neutrons.

5.2.3 Simulating Radiation to Score the Shield

PARTISN is used to model neutron transport through the shield. PARTISN uses two grids to perform calculations, a coarse grid models the problem space, while a fine grid is used for discretizing space for physics calculations. I match the PARTISN coarse grid to the available ring locations as pictured in Fig. 5.2, with the exception that the grid extends to the edges of the system. I set the fine grid to half the size of the coarse grid in the highest resolution case, resulting in a 32×32 fine grid when the finest coarse grid is 16×16. The fine grid's size is kept constant regardless of the size of the coarse grid. Angles are defined using the Rectangular Chebychev-Legendre built-in set, with an ISN value of 24. The flux at each fine grid point located on the detector plane at $z = 170$ cm from the source is used in the fitness functions described below. This detector disk is the dark box on the right side of Fig. 5.2.

Of course I am ignoring much of the structure that would arise in a space reactor application, but our goal is to explore the concept of MGGA, rather than to design the final shield.

5.2.4 Designing a Fitness Function for the Shadow Shield

The ultimate goal of the space shield design problem is to create a shield that reduces radiation on the ship while being as light as possible. Weight represents cost for space applications, so we may be willing to trade shielding for weight above some acceptable shielding value. However, if the shield doesn't protect the ship sufficiently, then the mission will fail. Our fitness function needs to take this balance between weight and shielding into account.

The first task is to decide how much of a reduction in radiation is sufficient. I compare candidate shields against the heaviest shield that the chromosome can encode. This heaviest shield would place material in every grid location in Figure 5.2. We know, based on [Alpay & Holloway (2005)], that the heaviest shield isn't the best shield. But it is a reasonable comparison for an automated search algorithm. Running PARTISN with the heaviest shield will get a set of fluxes on the detector plane. I compare these to each individual in the shield population, and score the candidate shields by how well it does against the heaviest, or *full*, shield. Ideally, the MGGA will either duplicate the split shield idea, or create something better.

Using the heaviest shield, called S, as a comparison for flux, I created two different fitness functions. The first compares the flux at all places on the detector plane to the "worst" flux for the heaviest shield. If the heaviest shield had a neutron flux ranging from 1 to 100, we would only compare our candidate shields to the value of 100, since that is the worst job that the heaviest shield does. Even without running a simulation we can guess that the worst flux value will be on the z axis due to geometry, but we won't require that. Let's call this fitness function, that compares to the worst flux from the heaviest shield, the *MaxFlux* fitness function. We also need to factor mass into the fitness function. We will do this by comparing the mass of a shield to the mass of the heaviest shield.

To compute the MaxFlux fitness of a shield, s, I run PARTISN to get scalar flux values $\phi_i(s)$ at the detector plane for shield s at each of the detector cells i. Let $m(s)$ denote the mass of shield s. The fitness of shield s is

$$F(s) = \begin{cases} \min_i \left(1 - \frac{\phi_i}{\phi_i(S)}\right) & \text{if } \max_k(\phi_k(S)) < \phi_i(s) \text{ for any } i \\ 1 - \frac{m(s)}{m(S)} & \text{otherwise.} \end{cases} \tag{5.3}$$

This fitness function essentially looks for shields that better the full shield's flux at its worst, and then tries to find the lightest shields that meet this goal. The function is defined in such a way that the following two facts are true: First, any shield that doesn't beat the heaviest shield's "worst" flux, i.e. pass the flux criteria, will have a negative fitness. Second, any shield that does pass the flux criteria will have a fitness between zero and one where the best fitness a shield could aspire to is a value of one.

The second way to compare to the heaviest shield's flux, is to try and beat it at every detector. This means that at every grid location on the detector plan a candidate shields flux has to be lower than the heaviest shield's flux at that same detector. Let's call this fitness function the *ByLocation* fitness function. To compute the ByLocation fitness of a shield, s, I run PARTISN to get scalar flux values $\phi_i(s)$ at the detector plane for shield s at each of the detector cells i. Let $m(s)$ denote the mass of shield s. The fitness of shield s is

$$F(s) = \begin{cases} \min_i \left(1 - \frac{\phi_i}{\phi_i(S)}\right) & \text{if } \phi_i(S) < \phi_i(s) \text{ for any } i \\ 1 - \frac{m(s)}{m(S)} & \text{otherwise.} \end{cases} \tag{5.4}$$

This fitness function essentially looks for shields that better the full shield's flux at each detector, and then tries to find the lightest shields that meet this goal. Like the MaxFlux function, the ByLocation function will result in a negative value for shields that fail the flux criteria, and will result in a value from zero to one for shields being graded on mass.

5.2.5 Applying MGGA to the Space Shield Problem

In order to test the concept of MGGA I did several types of runs for the shield problem. Unless otherwise noted, these runs all used the same underlying Genetic Algorithm and MGGA settings. For most of these runs, the finest grid we will look at is a 16×16 r-z grid. This maps onto a binary chromosome with 256 elements indicating if an individual ring is filled with material or is empty. The first type of run uses a standard GA to search the resulting space of 2^{256} possible solutions. This run was performed using a population of 531 individuals, and was run for 20 generations, resulting in a total of 10,620 possible shield candidates. The GA used for these runs is fairly standard [Haupt & Haupt (1998); Mitchel (1998)]; it uses tournament selection with a tournament size of 4, uniform crossover with a chance of 70%, random mutation with a chance of 20% and copy forward with a chance of 10%.

The MGGA runs consisted of the following set of 4 phases:

- 2×2 grid with 10 individuals for 20 generations (200 candidates)
- 4×4 grid with 200 individuals for 20 generations (4000 candidates)
- 8×8 grid with 200 individuals for 20 generations (4000 candidates)
- 16×16 grid with 120 individuals for 20 generations (2400 candidates)

This is a total of $10,600$ shield candidates, just 20 candidates shy of the GA run.

The translation phase for MGGA on the shadow shield is similar to the one used to translation the shortest path problem described in Section 3.4. The grid sizes were chosen so that each phase uses a grid that cuts the other grid in half in both directions. This effectively quarters the size of a grid element at each phase step. Translations from one phase to the next simply look at a grid element in the early phase and if they have shield material, the translation operator turns on the corresponding grid elements in the later phase, see Figure 5.3. As long as the grid halves in size in both directions this mapping is exact and the shield should maintain its flux and mass score across translations.

I performed both GA and MGGA runs with the MaxFlux and ByLocation fitness functions and have performed multiple runs of each type where possible to develop statistics and check the results for random errors or successes.

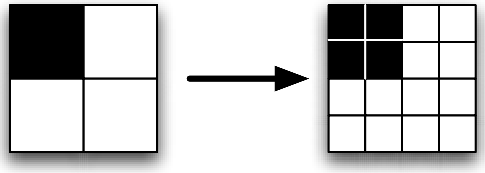

Figure 5.3: The shadow shield translation operator

5.3 Results with a 16×16 Grid Using the MaxFlux Fitness Function

The MaxFlux fitness function from Equation 5.3 compares the flux at all of the detectors for a shield candidate against the worst flux for the heaviest possible shield. I ran ten instances of the simulation described in Section 5.2.5 to see how MGGA compares with GA. The results of these runs are described in Tables 5.1, 5.2, 5.3 and 5.4. The most important result from these runs is that both MGGA and GA beat the heaviest shield on flux. The best shield from each run did a better job of stopping flux at the ship than the heaviest shield. This means two things. First, GA is designing a better shield than the easiest guess. Second, all of the best shields are measured on mass, rather than on flux.

While the shields we are finding with GA beat the heaviest shield, it is possible that at the higher radius values they have a higher flux than the heaviest shield. This is a result of the fitness function. In Section 5.5 we will see how GA can beat the heaviest shield at all locations.

Over the ten runs, MGGA resulted in an average fitness of 0.9449, while GA resulted in an average fitness of 0.7266. This difference doesn't appear very large until we consider the difference in mass this represents. Because the shields are all ranked on mass, and because we are using equal mass rings, we can compare the quality of a shield by the number of rings. The number of rings and the fitness are functionally equivalent for the shields that beat the flux criteria of the fitness function.

Run	2×2	4×4	8×8	16×16
Run 1	0.5	0.875	0.9219	0.9336
Run 2	0.5	0.875	0.9375	0.9492
Run 3	0.5	0.875	0.9375	0.9492
Run 4	0.5	0.875	0.9375	0.9453
Run 5	0.5	0.875	0.9219	0.9414
Run 6	0.5	0.75	0.875	0.9141
Run 7	0.5	0.875	0.9375	0.9532
Run 8	0.5	0.875	0.9375	0.96099
Run 9	0.5	0.875	0.9375	0.9492
Run 10	0.5	0.875	0.9375	0.9532

Table 5.1: The best fitness by phase for MGGA using the MaxFlux fitness function (Note - results for runs 9 and 10 are taken from a longer MGGA run with a 32×32 phase)

Run	Rings
Run 1	17
Run 2	13
Run 3	13
Run 4	14
Run 5	15
Run 6	22
Run 7	12
Run 8	10
Run 9	13
Run 10	12

Table 5.2: Rings of material for MGGA results using the MaxFlux fitness function

Looking at rings, MGGA resulted in an average of 14.1 rings of material while GA resulted in an average of 70 rings of material. GA used over four times the amount of material of that MGGA used to create its best shield.

These results are quite exciting. MGGA is designing shields, and is beating GA in the process. In order to understand why MGGA beats GA let's take a look at the best shield from all of the MGGA runs and the best shield from all of the GA runs.

Run	Fitness
Run 1	0.7383
Run 2	0.6797
Run 3	0.7344
Run 4	0.7383
Run 5	0.707
Run 6	0.7344
Run 7	0.7461
Run 8	0.7109
Run 9	0.7266
Run 10	0.7499

Table 5.3: Best fitness for GA using the MaxFlux fitness function

Run	Rings
Run 1	67
Run 2	82
Run 3	68
Run 4	67
Run 5	75
Run 6	68
Run 7	65
Run 8	74
Run 9	70
Run 10	64

Table 5.4: Rings of material for GA results using the MaxFlux fitness function

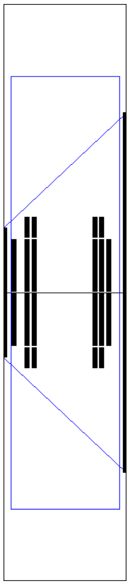

Figure 5.4: The best MGGA shadow shield on a 16 × 16 grid - Fitness = 0.96

5.3.1 The Best of GA Versus MGGA

The best fitness score, 0.96, for MGGA was achieved in run 8. This shield is pictured in Fig. 5.4. The best fitness score, 0.75, from our GA runs was in run 10. This shield is pictured in Fig. 5.5. The most obvious difference between these two shields is that MGGA results in many fewer rings being used. Of course, we knew this from the fitness scores. But the issue isn't just the number of rings, it is their position.

Given the amount of time we ran it, GA wasn't able to clean out rings that are clearly extra material. These rings lay outside of the cone of interest, pictured as diagonal lines on both figures. This cone of interest represents the direct line between the source and detector planes. The shield shouldn't need to have any material outside this cone, but the GA does. Perhaps, given time or human intervention, GA would get rid of this material. Certainly the fitness function should push the shields in that direction. MGGA on the other hand resulted in a shield that had no material outside the cone of interest. This simple fact improved it's fitness over the GA shield. GA is

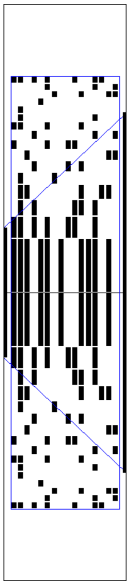

Figure 5.5: The best GA shadow shield on a 16 × 16 grid - Fitness = 0.75

working at the problem. Figure 5.6 shows the average fitness per generation of the GA run. It is clear that the fitness is improving with minor setbacks from random variations but does stagnate eventually.

Both the GA and MGGA shields are split. This is the result we hoped GA would be able to reproduce. Moreover, it is a split frustum of a cone in the case of MGGA, since all of the material is in the cone of interest.

One of the interesting effects of the MaxFlux fitness function is that it lowers expectations at the edges of the detector plan. Simple geometry reduces the flux at larger values of r. Since we compare only to the maximum flux measured for the heaviest shield, we can theorize that the MGGA runs are able to trim away much of the cone and still beat the worst value which is in the middle for the heaviest shield. To test this theory, look at the flux values of the shield produced by the MGGA with the heaviest shield. This comparison is pictured in Fig. 5.7 (This figure also includes an equal mass cone shield that we will discuss in the next section, 5.3.2.)

In this figure we can see that the MGGA shield is losing to the heaviest shield at the edges. But it is maintaining a flux lower than the worst value from the heaviest

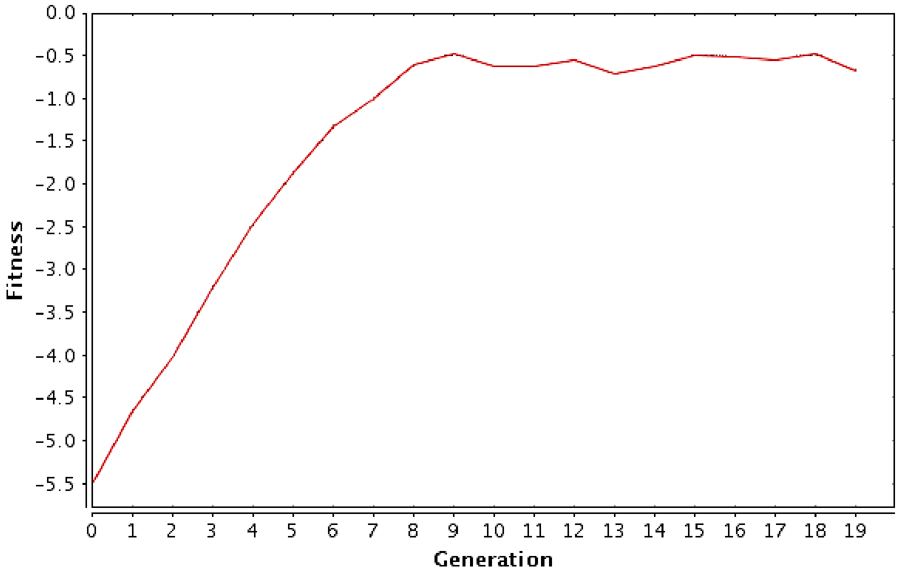

Figure 5.6: Average fitness -vs- generation for GA run with the MaxFlux fitness function

shield, around 0.0042 on the Y-axis. The fitness function is allowing GA and MGGA to trade mass for this flux.

Figure 5.8 shows the same comparison for the best shield from the GA runs, note that the scales for the MGGA and GA graphs are not the same. In this case, all of the extra material is helping the GA shield protect the higher r values. But because our fitness function doesn't require this protection it is really wasted mass.

So, MGGA is designing a split shield. Let's look at how the resulting shield would compare with a simple cone?

5.3.2 GA Versus Manually Designed Shields

If our automated design doesn't build a better shield than a cone, then we really aren't doing much. The question is, how do we compare our best shields to a cone? To make this comparison I stipulate that the cone should have equal mass to the shield we are comparing it to. So if the test shield has 10 rings of material, the cone can have 10 rings of material. Using this stipulation, and building a cone by filling in rings within the cone of interest, from the front to the back, we get the two shields

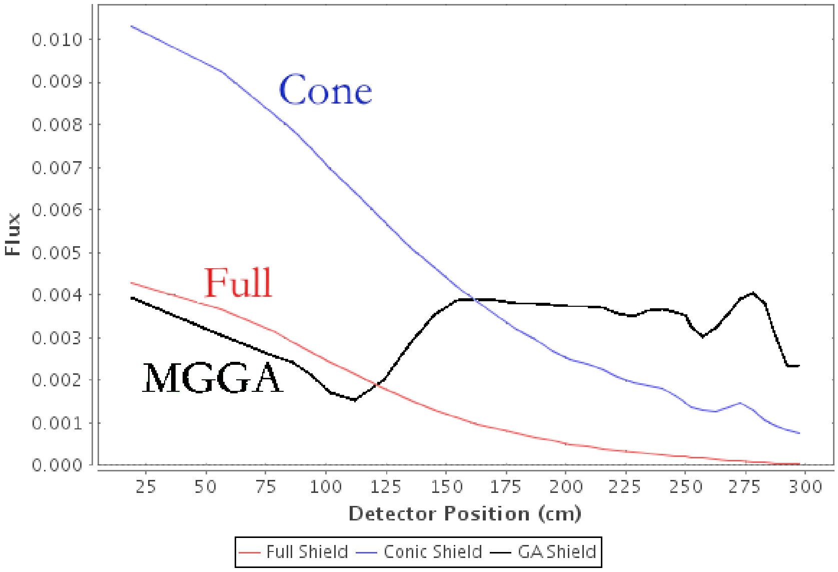

Figure 5.7: Flux vs. Radius - For the best MGGA shield, the full shield, and a cone with mass equal to the MGGA solution for the MaxFlux shadow shield problem

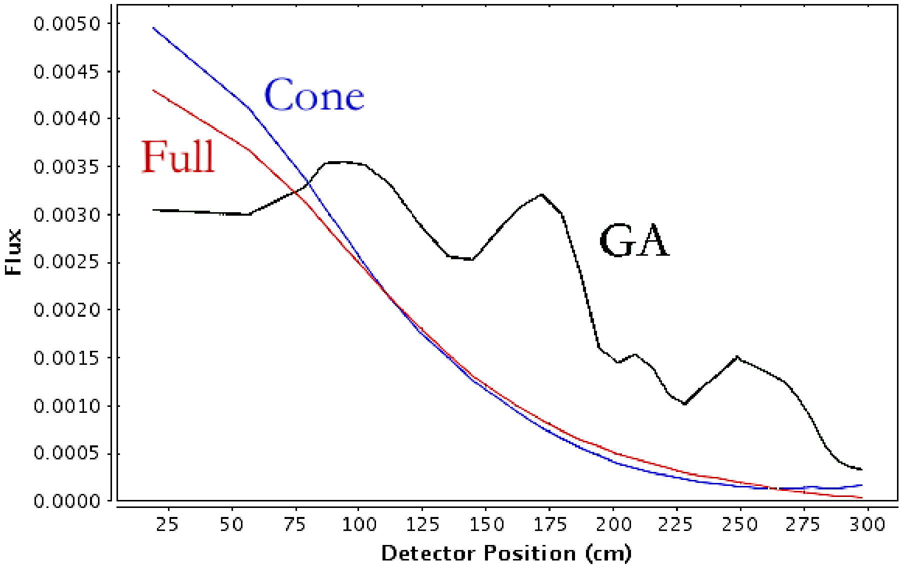

Figure 5.8: Flux vs. Radius - For the best GA shield, the full shield, and a cone with mass equal to the GA solution for the MaxFlux shadow shield problem

pictured in Fig. 5.9 and Fig. 5.10.

The algorithm used to make the cone shields uses the starting radius to determine if a ring is inside of the cone of interest. In the pictures you may see a ring that appears to go outside of the cone of interest. This is because the outer radius goes beyond the cone, while the inner radius, at some value of z, is inside of the cone.

The first thing that really jumps out of these graphics is the difference in mass between the MGGA version and the GA version. The GA version is a massive cone and fills most of the cone of interest with material. These extra rings are coming from the "noise" that was outside of the cone of interest in the generated shield. Even more interesting, the cone version of the GA shield actually fails the flux criteria of the fitness test and ends up with a fitness of -3.54. We can see this failure on the flux graph in Fig. 5.8 where the center of the cone's flux is higher than the heaviest shield. Most likely this failure is due to scattering particles that stay in the shield and come back to the detector plane rather than escaping as they might from a split shield.

The cone version of the MGGA shield appears small compared to its GA counterpart. As we might expect, this conic shield also fails the flux criteria and only scores a fitness of -19.038. Looking at the flux graph in Fig. 5.7 we can see that this cone doesn't even come close to matching the heaviest shield at low values of r.

Another important question about the shields coming from GA is, how would they perform if all of the noise was removed? In the case of the best MGGA shield, there is no noise. But for the best GA shield there is a lot of noise. I cleaned up this noise by removing any rings that lie completely outside of the cone of interest, which represents the line of sight between the source and detector planes. This cleaned shield is pictured in Fig. 5.11. By removing the extra material, this shield's fitness jumped from 0.75 to 0.875, but still doesn't beat the MGGA result.

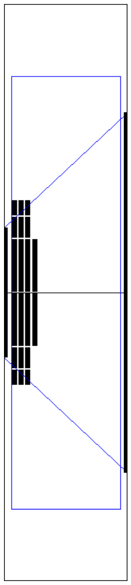

Figure 5.9: An equal mass cone for the best MGGA shadow shield - Fitness = −19.038

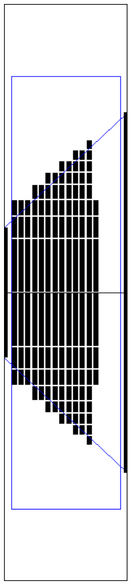

Figure 5.10: An equal mass cone for the best GA shadow shield - Fitness = −3.54

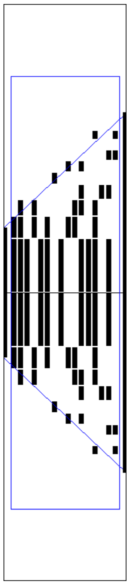

Figure 5.11: An clean version of the best GA shadow shield - Fitness = 0.875

5.3.3 Conclusions from the MaxFlux Fitness Function

Based on the results from the MaxFlux fitness function, it looks like MGGA is doing a great job of optimizing the shield design. The ability for MGGA to take solutions from a smaller problem space into the large one is keeping noise out of the system. Overall MGGA is beating GA consistently, partially because GA is not able to deal with the extra material outside of the cone of interest within the resource constraints provided to it. More importantly it does not have a good set of initial building blocks within the cone, while MGGA has these from the coarser phases.

5.4 Results with a 32×32 Grid using the MaxFlux Fitness Function

After looking at the results for MGGA versus GA on the 16×16 grid, I was curious how MGGA would perform on an even larger search space. To test this, I did several runs with a maximum size of 32×32. This is a huge search space with 2^{1024} individuals. The rings for this grid are still equal mass, I simply chopped them

Run	Fitness	Rings
Run 1	0.955	46
Run 2	0.951	50
Run 3	0.95	51
Run 4	0.948	53
Run 5	0.967	33

Table 5.5: Results with a 32×32 grid for MGGA using the MaxFlux fitness function

Run	Fitness	Rings
Run 1	0.485	527
Run 2	0.495	517
Run 3	0.487	525
Run 4	0.493	519
Run 5	0.477	535

Table 5.6: Results with a 32×32 grid for GA using the MaxFlux fitness function

in half again. All of these runs use the MaxFlux fitness test defined in Equation 5.3.

The results from five runs of MGGA on the 32×32 grid are listed in Table 5.5. The results for GA on the same grid are listed in Table 5.6. While GA does an impressive job of finding shields that beat the full shield with less mass, the MGGA result is wonderful. MGGA is able to find a shield that uses only 33 of the available 1024 rings and passes the flux test, while GA uses 517 rings in its best result.

Looking at the two best solutions from each of these five runs, pictured in Figure 5.12 and Figure 5.13, we can see that MGGA not only passes the flux test, it was able to clean out all of the material outside the shadow cone. GA is still fighting to clean out this material.

An interesting comparison is between the best shield from the 16×16 runs and the 32×32 run, pictured together in Figure 5.14. The best shield from MGGA on the coarser grid used 10 rings to create a shield with fitness of 0.96. MGGA on the finer grid generated a shield with 33 rings, and a fitness of 0.967. A single ring of the 16×16 represents 4 rings on the 32×32 grid. This means that MGGA was able to remove more than an entire rings worth of material from the best result coming out

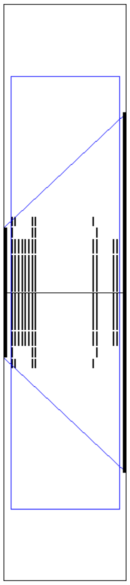

Figure 5.12: The best MGGA shadow shield for a 32 × 32 grid - Fitness = 0.967

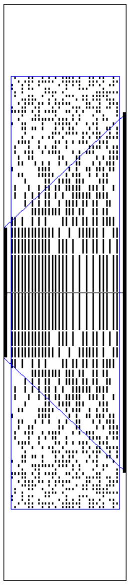

Figure 5.13: The best GA shadow shield for a 32 × 32 grid - Fitness = 0.495

of the 16×16 phase of the MGGA. Visually, both shields are split at about the same place, and both focus material in the center of the detector plane and place material close to the detectors.

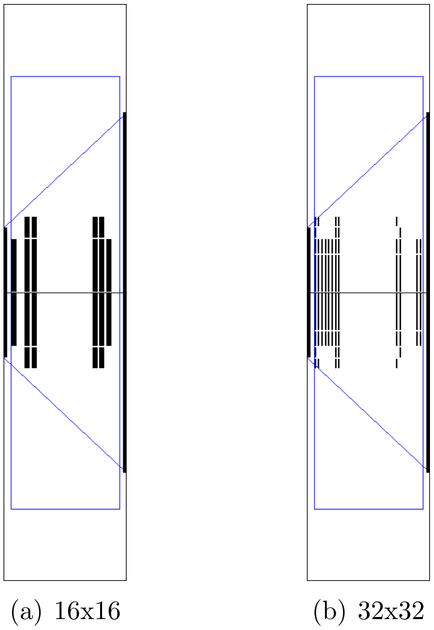
(a) 16x16

(b) 32x32

Figure 5.14: The best 16×16 MGGA shadow shield (Fitness = 0.96) vs. the best 32×32 MGGA shadow shield (Fitness = 0.967)

5.4.1 Conclusions from the 32×32 Grid for MGGA

Running on a larger search space demonstrated MGGA's power over GA even more than the 16×16 runs did. GA simply can't clean out the extra material fast enough to keep up with MGGA. MGGA was able to find a solution with 33 rings compared to GA's 517 rings. MGGA is using just 6.3% of the material that the GA solution has.

Run	Fitness	Rings
Run 1	0.8	50
Run 2	0.82	47
Run 3	0.8	50
Run 4	0.8	51
Run 5	0.79	52

Table 5.7: Results with a 16×16 grid for MGGA using the ByLocation fitness function

5.5 Results with a 16×16 Grid Using the ByLocation Fitness Function

The second fitness function for the shadow shield problem is the one in Equation 5.4 that requires the shield to beat the “heaviest” shield on flux at every detector location. Going into this run I expected the shields to be heavier, since they would require more material at the edges. I performed 5 runs each for MGGA and GA on the 16×16 grid to confirm this hypothesis and to see how MGGA performed with a different fitness function.

GA is run with 20 generations of 531 individuals. MGGA is run with the following phases:

- 2×2 grid with 10 individuals for 20 generations (200 candidates)
- 4×4 grid with 200 individuals for 20 generations (4000 candidates)
- 8×8 grid with 200 individuals for 20 generations (4000 candidates)
- 16×16 grid with 120 individuals for 20 generations (2400 candidates)

As with the MaxFlux runs I use a standard [Haupt & Haupt (1998); Mitchel (1998)] generational GA; I use tournament selection with a tournament size of 4, uniform crossover with a chance of 70%, random mutation with a chance of 20% and copy forward with a chance of 10%.

Run	Fitness	Rings
Run 1	0.45	140
Run 2	0.42	146
Run 3	0.39	155
Run 4	0.42	149
Run 5	0.42	148

Table 5.8: Results with a 16 × 16 Grid for GA using the ByLocation fitness function

The results of the runs are listed in tables 5.7 and 5.8. As in the MaxFlux fitness function case, the ByLocation fitness function tests are handily won by the MGGA over the GA. MGGA is using about 1/3 of the material that GA uses to create its best shield. The best MGGA result was from run 2 and resulted in a fitness of 0.82 using just 47 rings. This shield is pictured in Figure 5.15. The best result from GA is from run 1 with a fitness of 0.45. This shield is pictured in Figure 5.16.

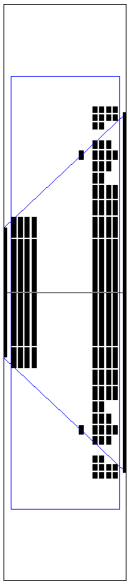

Figure 5.15: The best shield produced by MGGA for the ByLocation fitness function - Fitness = 0.82

As expected, these shields are heavier than their MaxFlux counterparts. MGGA is still creating a split shield, but now the two pieces of the shield are much heavier. One piece of the shield is also closer to the detector plane. As with the MaxFlux runs, looking at the average fitness per generation in the GA run shows that GA is

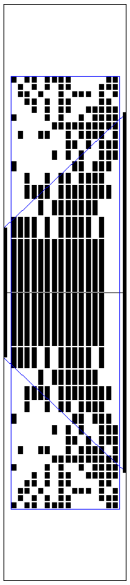

Figure 5.16: The best shield produced by GA for the ByLocation fitness function - Fitness = 0.45

progressing with each generation, but simply can't clean out material quickly enough.

5.5.1 MaxFlux vs. ByLocation Results

Perhaps the most interesting difference between the ByLocation results and the MaxFlux results is how GA protected the edges of the detector plane. We can see this graphically by looking at the flux as a function of detector radius. The fluxes for the best shields, plus their equivalent cone, plus a full shield are pictured in Figures 5.18 and 5.19.

The cone equivalent of the best shield fails to keep the flux down at the edges of the detector plane, causing it to fail the flux test. The cone equivalent to the best GA shield comes close because GA uses so much material that the cone is quite large, while the cone equivalent for the MGGA shield doesn't come close because so little material is used.

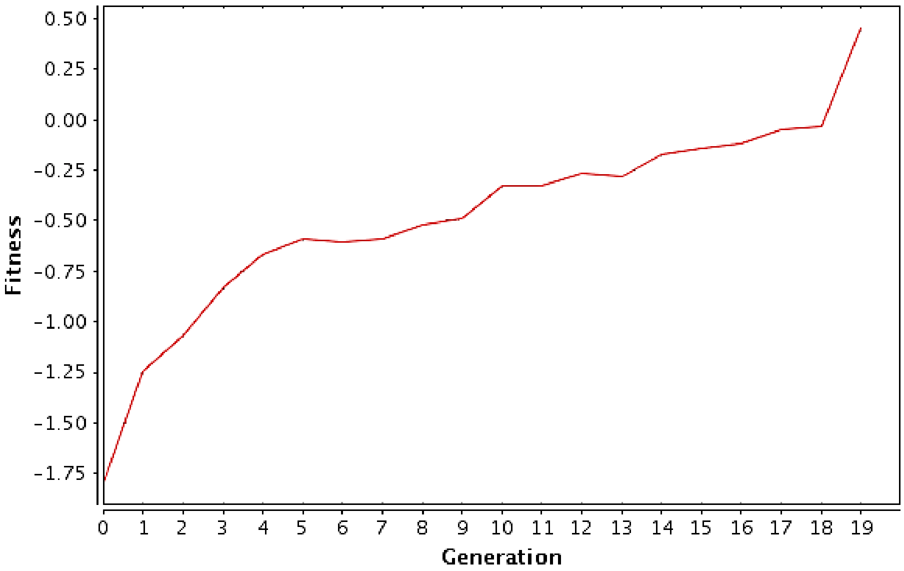

Figure 5.17: Average fitness vs. generation for a GA run with the ByLocation fitness function

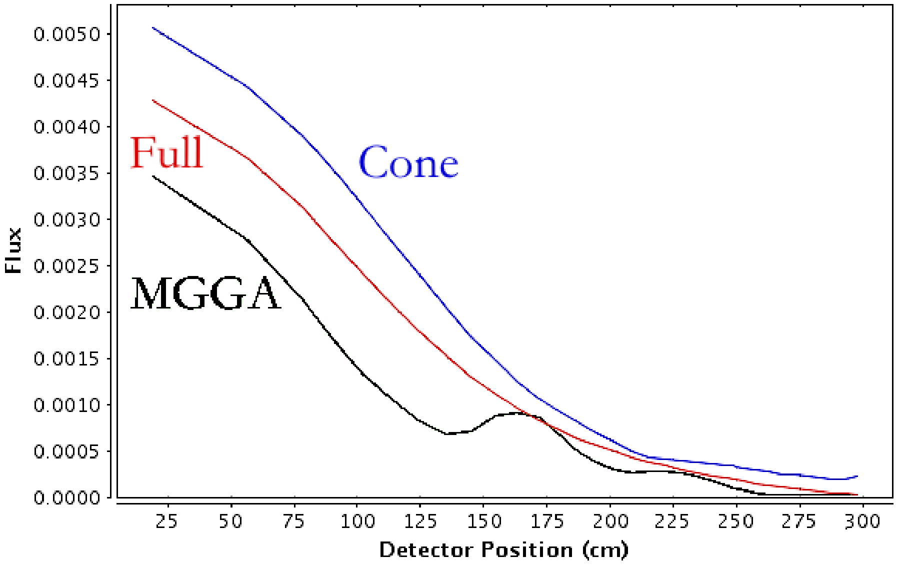

Figure 5.18: Fluxes for the best MGGA shadow shield using the ByLocation fitness test, equivalent cone and full shield

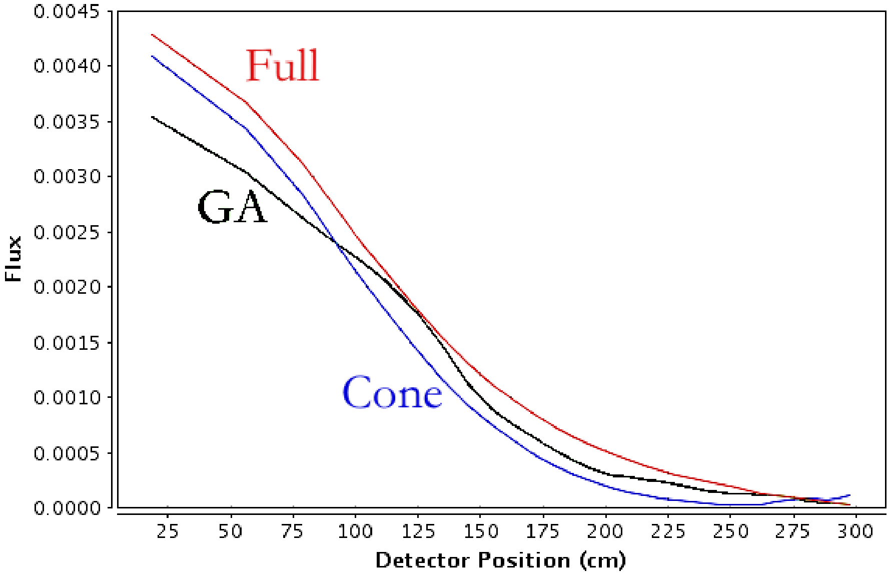

Figure 5.19: Fluxes for the best GA shadow shield using the ByLocation fitness test, equivalent cone and full shield

5.5.2 Conclusions from the ByLocation Fitness Function

Like the MaxFlux fitness function, MGGA is able to beat GA using the ByLocation fitness function and create a reasonable shield that uses only a small number of rings to beat the flux test. More importantly, it is able to do so with a much harder problem of lower dose across the entire detector plane.

5.6 Results with Single Point Crossover

One of the decisions I made at the beginning of my research into shadow shielding was to use Uniform Crossover. Uniform crossover did well with our test problem in Chapter III and should allow big changes in shields. Since we want a light shield, I suspected it would be good to allow GA to move and remove material quickly, which uniform crossover does. However, there is an open question: what if I had used standard single point crossover as described in Section 2.5.2.1? To answer this question I did three runs of MGGA using the MaxFlux fitness test and setup, where uniform crossover was replaced with single point crossover. I also did three similar runs of GA.

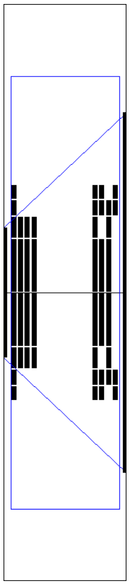

Figure 5.20: The best shadow shield from single point crossover for MGGA - Fitness = 0.91

Figures 5.20 and 5.21 show the results of the the best run from MGGA and GA with single point crossover. Both shields pass the flux test. Neither shield beats the best result from the Uniform Crossover runs, but neither is completely out of the running. It is worth noting that the MGGA shield wasn't able to clean up everything outside the shadow cone, while MGGA with uniform crossover, see Figure 5.4, was very good at this. MGGA scored 0.91 and 0.96, with single point and uniform crossover respectively, while GA scored .71 and 0.75. Uniform crossover did score better, by $5 - 10\%$ and I will use it for most of the remaining simulations in this dissertation.

5.7 Results with Non-Equal Mass Rings on a 16×16 Grid

As I mentioned in Section 5.3, all of the runs discussed up to this point have had rings of equal mass. This reduced the effect of mutation and crossover, since each element in a shield's gene had the same value for mass. Another way to model the

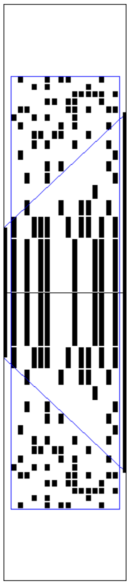

Figure 5.21: The best shadow shield from single point crossover for GA - Fitness = 0.71

problem was to keep the radial extent of the rings the same and let the masses change. I did several GA and MGGA runs for the MaxFlux fitness function where the rings have equal radial extent instead of equal mass. Using the same 300 cm maximum radius for a ring, this means that a chromosome using two radial values would have a ring from 0 to 150 *cm* and another from 150 *cm* to 300 *cm*. The outer ring in this case will be much heavier than the inner ring.

Figures 5.22 and 5.23 show the results of the first two runs. Both shields pass the flux portion of the fitness test. The MGGA run uses 29 cells of material and the GA uses 132 cells of material. The number of rings tells us more about noise, particularly outside the cone of interest, than it does about mass. We can see from the number of rings that MGGA is able to clean up the noisy rings that GA isn't. Running each of these simulations two more times produced the results from Tables 5.9 and 5.10.

If we visually compare the three shields MGGA was able to create using non-equal mass rings with the best shield from the equal mass geometry, pictured in Figure 5.24, we can see that MGGA is making progress toward the same type of solution each time. All three shields made from non-equal mass rings are split, and all three have material

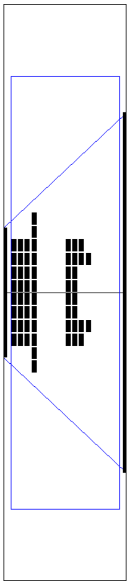

Figure 5.22: The best shadow shield from MGGA with non-equal rings - Fitness = 0.9675

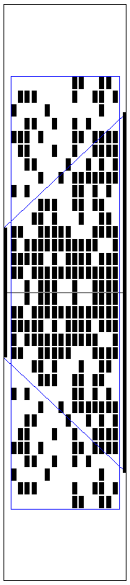

Figure 5.23: The best shadow shield from GA with non-equal rings - Fitness = 0.572

Run	Fitness	Rings
Run 1	0.968	29
Run 2	0.973	23
Run 3	0.974	24

Table 5.9: Results of running MGGA with non-equal mass rings on the shadow shield problem

Run	Fitness	Rings
Run 1	0.572	132
Run 2	0.57	133
Run 3	0.56	137

Table 5.10: Results of running GA with non-equal mass rings on the shadow shield problem

in the same area. At the same time, the three shields with non-equal mass rings differ in detail from the "best" MGGA shield from the earlier runs. The non-equal mass geometry drives the MGGA toward rings in the middle, which are lighter, and away from rings on the edges of the shield area, which are heavier. Fitness-wise, the non-equal rings are beating the equal mass rings. This appears to be because while the best equal mass solution required only 10 rings, the non-equal mass solutions can use twice as many rings and still have a lower mass. Moreover, by having more rings in the cone of interest the non-equal mass MGGA has more effective designs to choose from, and can create a more refined geometry near the axis. This refined geometry opens up streaming paths that allow neutrons to scatter away from the dose plan, to be lost radially into space.

At the same time, GA is having a harder time with the non-equal mass rings. All three runs have a fitness score around 0.57 while the GA runs with equal mass rings score around 0.72. If we visual compare the shields in Figure 5.25 which include the best shields from these three non-equal mass runs of GA with the best shield from the equal mass runs we see the root of the problem. The non-equal mass runs all contain much more material than the equal mass equivalent. One reason for this can be deduced by looking at the inner rings on these four shields. The GA using equal mass rings can protect a big area of the payload by reproducing in a way that adds material to the inner most ring (or disk). The non-equal mass geometry does not get as much of a flux benefit from the same mutations or crossovers. In fact, the non-equal mass geometry gets very small benefits each time it moves a ring of

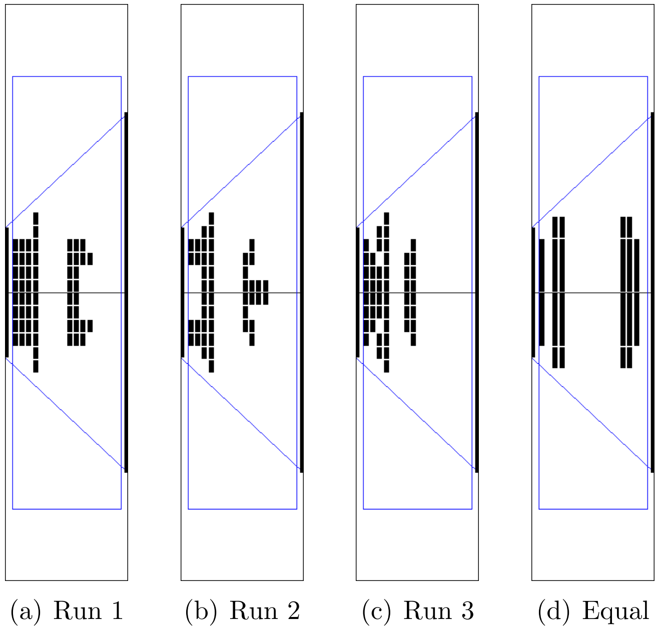
(a) Run 1 (b) Run 2 (c) Run 3 (d) Equal

Figure 5.24: The three best shadow shields with non-equal mass rings from MGGA (Fitness=0.968, 0.973 and 0.974) and the best shadow shield from MGGA for equal mass rings (Fitness=0.96)

material from the non-shadow area into the protective cone.

5.7.1 Comparing Equal and Non-Equal Mass Rings

I propose that MGGA can beat the GA so well on non-equal mass rings because of the way mutation and crossover effect the fitness. In the equal mass ring problem a single mutation will change the mass by the same amount regardless of which ring is mutated. In the non-equal mass ring problem a mutation can count for very different amounts depending on if a ring is changed near the axis or near the edge. While GA should ultimately work through this difference, this difference could add an extra selective pressure in the non-equal mass case. Essentially the non-equal mass rings may be making the fitness function less smooth, so shields that pass the flux test and are close in bits might be very far away from each other in fitness. For the equal mass ring problem, if two shields pass the flux test, and are close in bits, they are close in mass and therefore close in fitness.

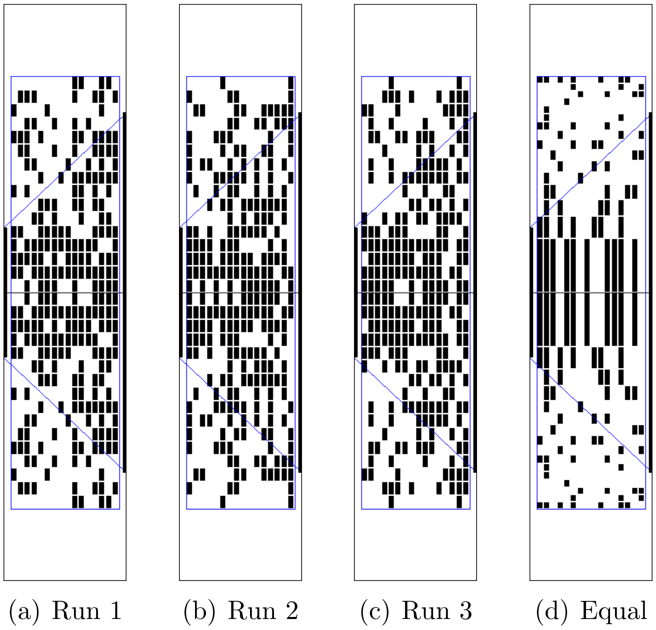
(a) Run 1 (b) Run 2 (c) Run 3 (d) Equal

Figure 5.25: The three best shadow shields with non-equal mass rings from GA (Fitness=0.572, 0.57 and 0.56) and the best shadow shield from GA for equal mass rings (Fitness=0.75)

To test this theory I wrote a tool to extract fitness difference for single mutations on shields where both the parent and child pass the flux test. By insuring that both parent and child pass the flux test, I am only looking at mutations effecting the mass part of the fitness test. Executing this tool on several runs from the non-equal mass and equal mass simulations I found that the non-equal mass rings do allow a larger maximum fitness change due to mutation, but that the average effect of this is about the same as for the equal mass ring case.

The biggest change due to mutation for the equal mass runs was 0.0039 compared to a best fitness of 0.96, while the biggest change for the non-equal mass runs was 0.0075 compared to a best fitness of 0.968. For the non-equal mass function this difference would be sufficient to move an individual from 0.968 to 0.975 which would beat the best shield from any of our non-equal mass MGGA runs.

Looking back at Figure 5.24 this effect makes sense. The non-equal mass rings result in very small rings near the axis, where most of the shielding needs to occur.

The MGGA is able to create more intricate designs that can allow for more scattering paths to let the neutrons out of the system. While the non-equal mass MGGA can find these small details in the primary shielding zone, the equal mass MGGA only has a very large ring to manipulate in the radial area.

In the end, it isn't obvious why GA is having a harder time with the non-equal mass ring geometry. One reasonable explanation for why GA is struggling relates to building blocks. When using equal mass rings, GA has to find building blocks containing the central ring in order to pass the flux test. This is a single gene and easy to find through mutation, crossover or randomly in the initial population. The non-equal mass scenario requires many more genes to be active at the core to pass the flux test. This makes creating the required building blocks more complex in the non-equal mass case. MGGA is able to overcome this complexity by finding good building blocks on the coarser grid and passing these building blocks into the higher resolution problem space. As a result, MGGA can generate a number of interesting and effective shields more easily than GA can.

5.7.2 Conclusions from the Non-Equal Mass Rings

As with the other fitness tests in this chapter, MGGA is doing a great job of finding solutions to the shadow shield problem. Despite the fact that GA has a harder time with the non-equal mass case, MGGA is still able to build good shields with no obvious design flaws.

5.8 Diversity and MGGA

As I suggested earlier, there is a question about how MGGA is effecting diversity. We can visually investigate this concern by looking at shields from the first generation of each phase in an MGGA run. Twenty-Five random shields, organized into five rows and five columns, from the first generation of each phase of the best run discussed in

Section 5.3 are pictured in Figure 5.26. Notice that randomly picking shields from the 2×2 phase resulted in only 6 different shields, of the 16 available shield encodings.

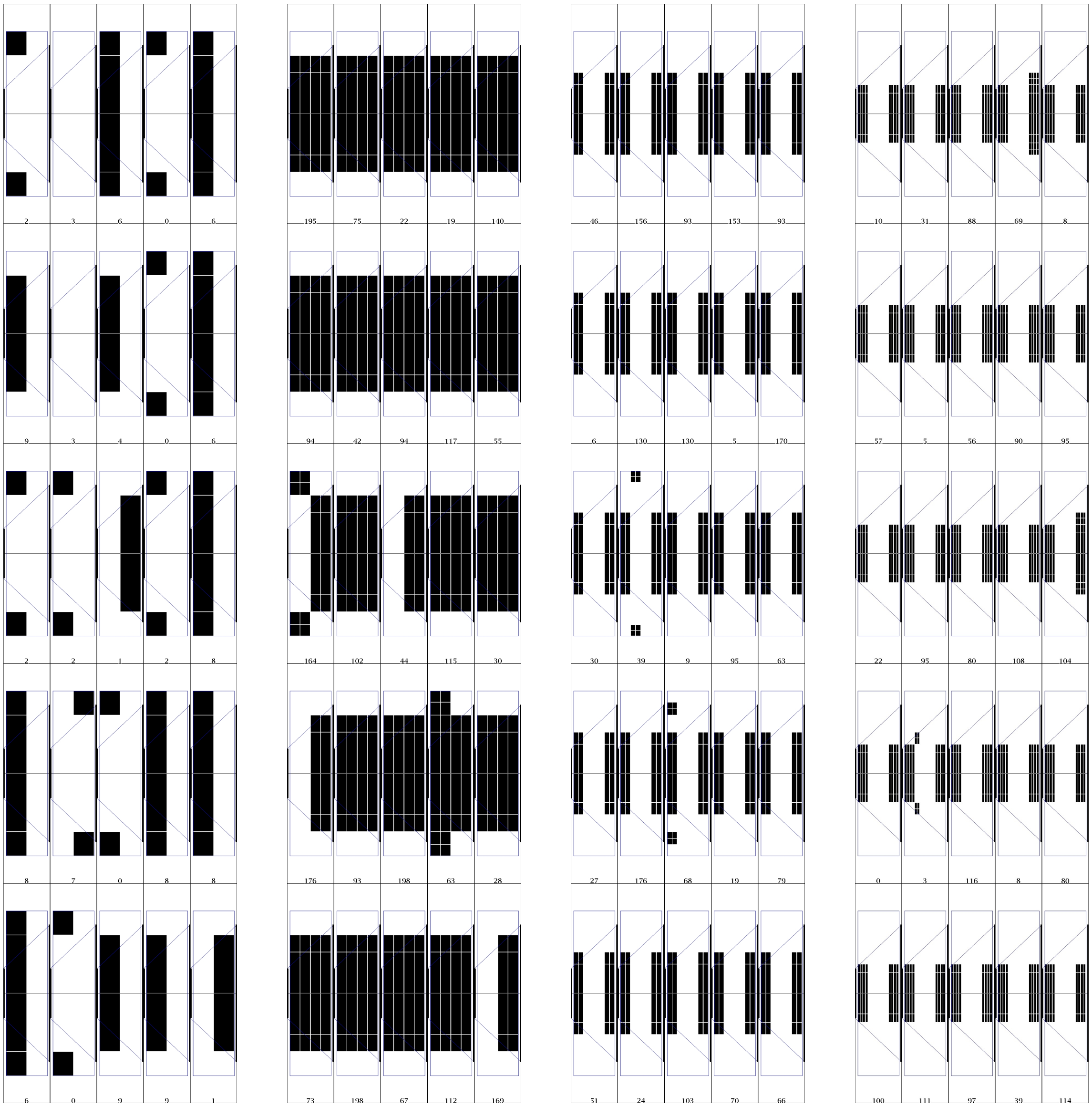

(a) 2×2 (b) 4×4 (c) 8×8 (d) 16×16

Figure 5.26: 25 random shadow shields from each phase in the winning MaxFlux MGGA run

It is easy to see that the later phases are not starting with a lot of diversity. The lack of diversity in the last phase is especially telling if we compare the starting population for the first generation of the 16×16 phase in the MGGA run with twenty-five random shields from the first generation of the best GA run from Section 5.3. Figure 5.27 shows the same twenty-five shields from Figure 5.26(d) as well as twenty-five shields from the first generation of the best GA run from the same results section.

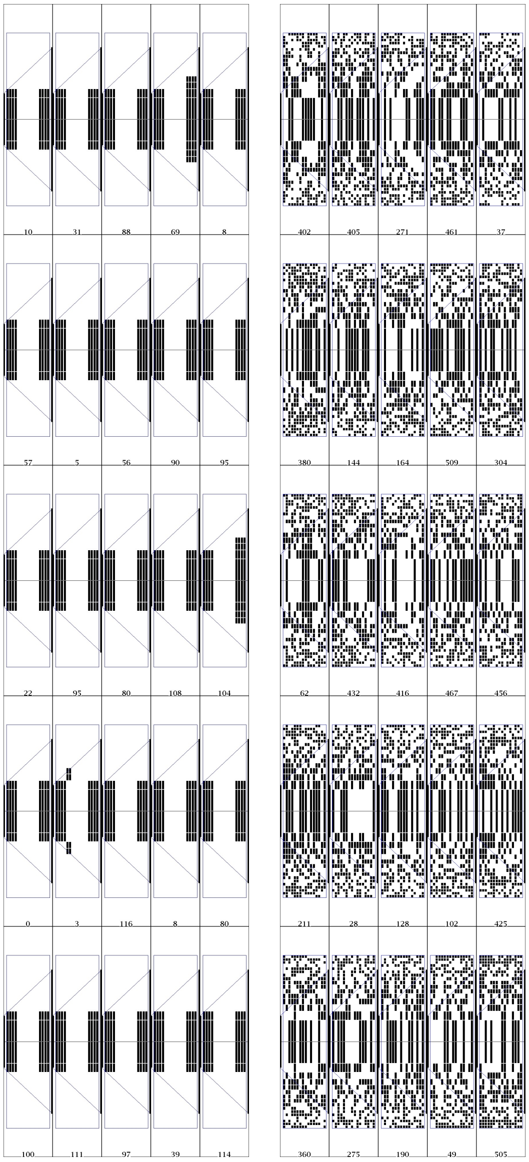

(a) MGGA

(b) GA

Figure 5.27: 25 random shadow shields from the first generation of the last phase of an MGGA run vs. shields from the first generation of a GA run

The GA starts with a much more diverse population. But part of the power of MGGA is that it is giving the next phase better building blocks, or good diversity, rather than simply feeding each phase with random diversity. MGGA is providing the final phase with a more limited set of good choices to optimize on, and thus reduces the amount of work the final GA phase has to perform to find a good solution. The question is, does it mean anything that we have low diversity going into the later phases? It doesn't seem to be hurting the results for the shadow shield problem. But in a problem with a large search space and many local maximum it could be a problem.

5.8.1 Measuring Diversity

We need an objective way to measure diversity. For the shadow shield problem I use a very simple diversity measure. Later, in Section 6.3.4.1, I will discuss a more statistical measure of diversity on a different problem.

Genetik caches the score of each unique chromosome, or individual. This cache knows the scores from all chromosomes in previous generations. When a new chromosome is scored, it checks to see if that same chromosome was used before, and if so, takes the score from the cache. Cache hits are inversely proportional to diversity, since zero cache hits would mean that all of the shields tested are unique in every generation, and a very high number of cache hits means that there are few unique shields to test. This simple method of measuring diversity as cache hits will overestimate diversity in most of our runs because we distribute the work of scoring to multiple machines. These machines do not communicate, so it is possible that within a generation the same individual's fitness score is tested more than once. Even with this leakage, measuring cache hits is a simple way to see how we are doing with diversity. Lots of cache hits means we are keeping the same individuals around across generations. Few cache hits means we are making new individuals to test. The cache is reset for each phase of an MGGA, so measuring diversity in MGGA will be a phase-by-phase process.

Using cache hits to measure diversity I looked at two possible techniques for improving diversity in MGGA. The first technique I investigated was to change the grid on which I initialized the MGGA for the shadow shield problem with the MaxFlux fitness function. The second technique was to inject diversity into the population during a translation phase using mutation.

5.8.2 An Investigation Into the Best Starting Phase

Analyzing Figure 5.26, it is clear that the 2×2 phase does not have a very large search space. There just aren't that many shields for GA to optimize toward. This means that coming out of that first phase with only a 2×2 grid might be starting with too simple a problem. We can investigate this idea by trying out MGGA with a later starting phase.

I did a MGGA run using the MaxFlux fitness function and the standard GA settings from Section 5.3, starting with the 4×4 grid instead of the coarser 2×2 one. The best solution from this run, pictured in Figure 5.28, was a shield with a fitness score of 0.957 using just 11 cells of material. This is only 1 cell more than the best run from the four phase MGGA run that started with a 2×2 grid. Figure 5.29 shows the same type of montage of twenty five random shields we looked at in the last section. Like the MGGA with four phases, the population appears to be converging quickly.

The next step was to do a run with only two phases of MGGA. The first phase used an 8×8 grid and the the last used the standard 16×16 grid. The other settings were the same as the other MaxFlux fitness function runs. This run produced a shield, pictured in Figure 5.30, with a fitness of 0.95 that used 12 cells of material. Figure 5.31 shows of twenty five random shields from the first generation of each phase.

Both of these limited phase runs tell us a lot about MGGA and GA in general.

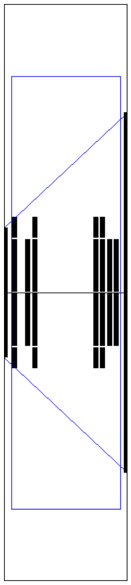

Figure 5.28: The best shadow shield from MGGA for the MaxFlux fitness function starting with a 4×4 grid - Fitness = 0.957

First, the run starting with an 8×8 grid shows how well GA was able to clean out the extra material. If we compare this to the GA starting with a 16×16 pictured in Figure 5.5 it is easy to see that our population size and generation count gave GA plenty of time to work on the smaller grid, but not quite enough on the larger grid. The results from the run starting with a 4×4 grid also shows that there may be a lower bound below which point MGGA doesn't gain value from coarser phases. In all cases we achieved a much better result with MGGA than with GA.

While changing the starting phase didn't have an effect on the result, it did have an effect on the diversity as measured by cache hits. Table 5.11 shows the cache hits by phase for these runs. The runs that started at a later phase had fewer cache hits in most cases. The run starting with the 8×8 grid had very few hits in the 8×8 phase. This is completely expected, and does show that in a problem where diversity is an issue, starting later could be a valid technique for keeping more diversity. One could conclude that diversity has no value, but I think that what we have really shown is that a lack of diversity was not a big problem for the shadow shield simulations. The

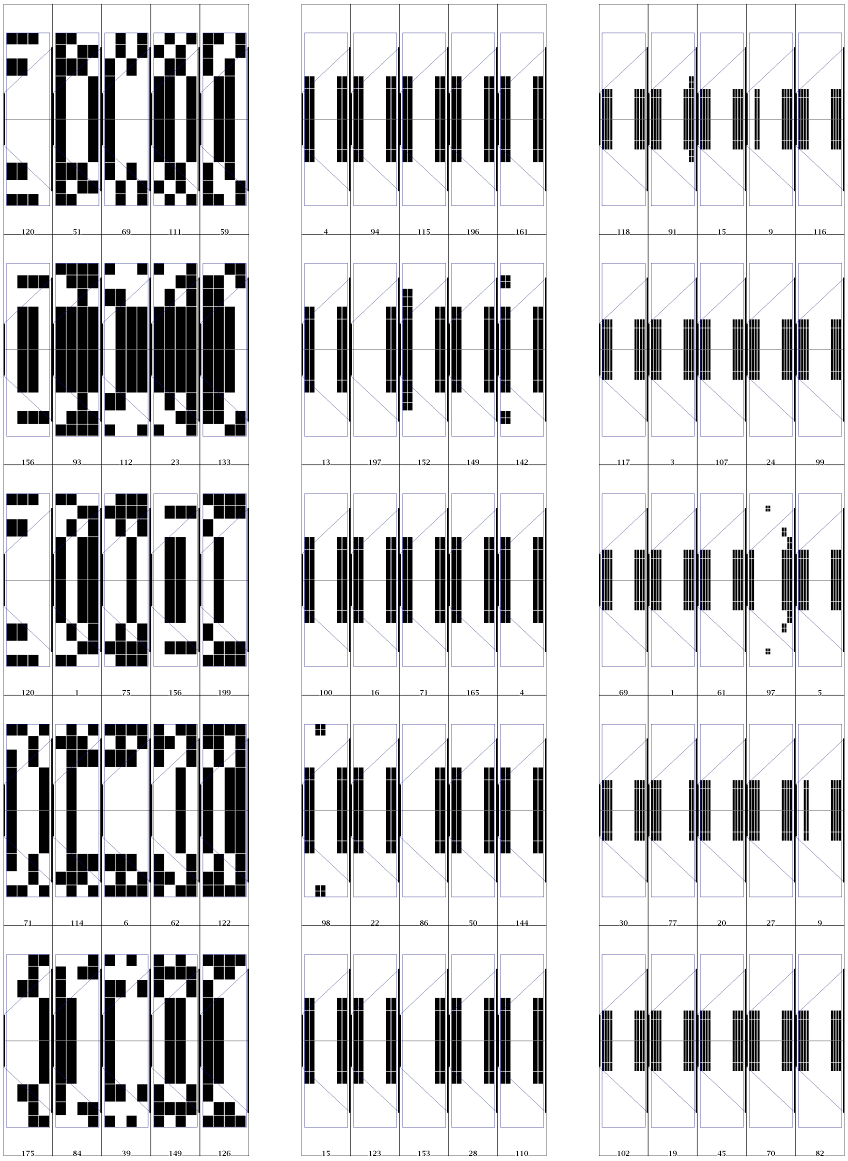

(a) 4x4

(b) 8x8

(c) 16x16

Figure 5.29: 25 random shadow shields from each phase in a MaxFlux MGGA run starting with a 4×4 grid

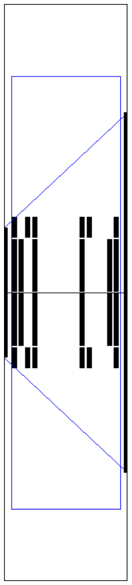

Figure 5.30: The best shadow shield from MGGA for the MaxFlux fitness function starting with a 8×8 grid - Fitness = 0.95

Grids	2×2	4×4	8×8	16×16
Four Grids	185	3422	3386	1815
Three Grids	N/A	2755	3392	1970
Two Grids	N/A	N/A	536	1613

Table 5.11: Cache hits by phase with different starting phases for MGGA on the shadow shield problem

MGGA was given sufficient resources and diversity, in the form of building blocks, to find good shields. In other words, we have shown that MGGA had sufficient diversity to do a good job. In the next section we will see what happens if we force more diversity into the MGGA.

5.8.3 Adding Diversity During Translations

Another idea for improving diversity in later phases is to create it artificially. GA uses mutation to add diversity into a stagnating population. Crossover can create diversity in populations that have enough diversity to drive it, but mutation can add diversity to even the most homogenous population. In this section I look at adding

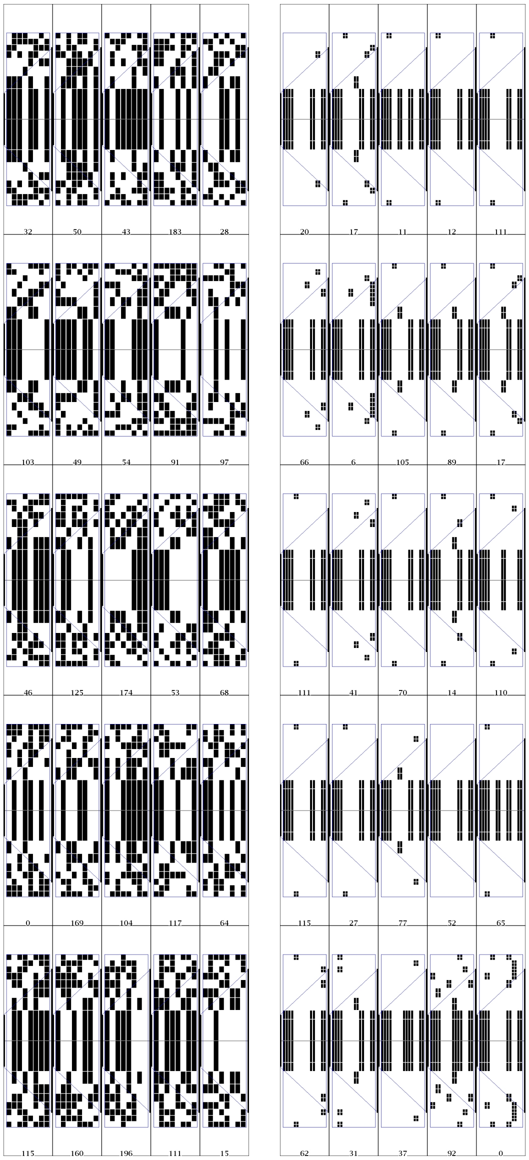

(a) 8x8

(b) 16x16

Figure 5.31: 25 random shadow shields from each phase in a MaxFlux MGGA run starting with an 8×8 grid

Mutations	Fitness	Rings
0	0.96	10
2	0.945	14
4	0.96	10
6	0.957	11

Table 5.12: The fitness and number of rings in the best shadow shields from MGGA with additional translation mutations

diversity between MGGA phases using mutation.

Unlike mutation as part of reproduction, the idea here is to force each individual that we translate from one phase of MGGA to the next to undergo some number of mutations. These mutations will force randomness and therefore diversity into the population. Regular mutation during reproduction performs the same roll but generally occurs at a lower rate, since tuning reproductive mutation to 100% would remove the copy and crossover operators.

To test this idea I did three runs with mutation during the translation phases. Every individual coming out of one phase is mutated before it is placed into the next phase. The setup was the same as the standard MaxFlux runs described in Section 5.3. Table 5.12 shows the results for the best run from with no interphase mutations, a run with 2 mutations per individual during the translation phase, a run with 4 mutations per individual and finally a run with 6 mutations per individual during the translation phase.

Based on these runs the mutation is not doing much to change the final result. While there is certainly some randomness going into the initial generation for each phase, it doesn't appear that the shadow shield problem is gaining anything from this additional randomness. Looking back at Section 5.8.2 this result is not surprising. If we added enough mutation between each phase translation it would cause the initial populations to all be random. The six mutation run here is approaching that case in the first phase translation that goes from a 2×2 grid to a 4×4 grid. The 4×4 grid only has 16 elements, and we can change 6 of them. Later phases are not as much

Mutations	2×2	4×4	8×8	16×16
No Mutations	185	3422	3386	1815
2 Mutations	184	3469	3392	1830
4 Mutations	183	3428	3258	1575
6 Mutations	184	3367	2915	1561

Table 5.13: Cache hits by phase with interphase mutation for MGGA on the shadow shield problem

effected. In some sense adding these mutations is equivalent to starting at a later phase for this problem space.

While the final result didn't changing much, mutation was adding diversity. Table 5.13 shows that we were getting fewer cache hits in the later generations when we add mutation, so I propose that it is creating diversity as we expected. The open question is: In what situation would a lack of diversity become a problem and when might it be helpful to add diversity using mutation during translations. This is one avenue of work to do in the future.

5.9 The Effect of MGGA on Time to Solution

Most of the runs in this chapter were designed to compare MGGA's performance versus GA based on the fitness score of the result. The total number of individuals tested was tuned to be about equal for the MGGA and GA configurations. All things being equal, we would expect MGGA and GA to run in the same amount of time for the same number of individuals. However, diversity and caching do come into play. As MGGA focuses in on solutions, it has to test fewer and fewer unique individuals. It is able to leverage the cache more heavily than GA.

To see this effect, we can look at the time spent scoring for both MGGA and GA. Tables 5.14 and 5.15 show the time spent scoring for three MGGA runs and three GA runs from Section 5.3. The three MGGA runs used an average of $244,042$ seconds to score unique individuals. The three GA runs used an average of $757,482$

Run	2×2	4×4	8×8	16×16	Total
Run 1	8,133	200,186	35,592	13,348	257,259
Run 2	7,271	143,297	34,831	12,804	198,203
Run 3	9,036	213,369	39,535	14,724	276,664

Table 5.14: Scoring time, by phase, for MGGA using the MaxFlux fitness function, in seconds

Run	Total
Run 1	989,989
Run 2	623,932
Run 3	658,525

Table 5.15: Scoring time for GA using the MaxFlux fitness function, in seconds

seconds. MGGA is spending only a third of the time that GA is scoring shields, and it generating much better answers.

5.10 Designing a Real Shield

The shields discussed in this chapter were very simplified. To figure out what we would need to do to design a real shield we need to break down some of my assumptions to see how we might work through them in a more realistic version of this problem.

Shield Geometry

The simple shadow shield used a cylinder with no support material. A real shield would have pipes, and other material in or around it, as well as structural supports. Using a full specification for the additional material we would identify a space where the shield would go. This space might be a cylinder with cutouts for non-shield material. The key point is that we identify the space where a shield might go.

Encoding the Problem

I used a very simple binary encoding. For a more realistic shield we would need to take the potential shield space and spit it into cells. For each cell we would define a material for that cell. If we want to model gamma and neutron radiation we could allow gamma shielding materials like tungsten as well as our LiH and other materials for neutrons. The GA could then use a string of integers for each chromosome, where the order of integers mapped to cell numbers and the values of the integers mapped to materials. By choosing the size and shape of the cells we could control how fine-grained a shield GA could produce.

Modeling the Physics

PARTISN provided good physics for our simplified shield. For a more realistic model we would probably need to use MCNP or another Monte Carlo code. As we will see in the next chapter, MCNP works fine with GA. Fitness functions don't really have restrictions in that way. Rather the GA user is limited by their computing resources. So while I used PARTISN and a simple model, someone with more computing time could use MCNP and a complex geometry.

Applying MGGA

While building a realistic fitness function is the first step, the MGGA user would also need to work out population sizes for this more accurate run. As with the physics question, sizing is mostly a question of computing resources. If the chromosomes encode hundreds of cells, then the population size will need to be in the thousands, at least. This will require significant computing time, potentially spread across a large cluster.

Each of the steps for applying MGGA to a more realistic shield scenario is addressable. The fundamental question would be one of computing resources. I think it is important to recognize that while MGGA provides a great way to explore the potential shield designs, it probably shouldn't be used to design the final shield at a production scale. A real shield will be constructed using standard milling machines which may not allow pieces to be added or removed as easily as they are in the simulation. I would posit that MGGA could be one step in the design process. MGGA would be used clarify the basic shield design. An engineering team would use that design and standard CAD/CAM tools to design the actual shield. This final design could be simulated to a very high resolution to confirm the MGGA results before construction.

5.11 Conclusions on the Shadow Shield Results

I performed a number of runs using both GA and MGGA to try and build a good solution to the shadow shield problem described in Section 5.2. Using the idea that we can score shields by how they compare to a "heaviest" shield, I built two fitness functions. The first scored shields on flux if they were unable to do at least as well as the heaviest shield did at its worst. This same function scored shields on their mass if they could beat a simple flux comparison with the heaviest shield. Using this MaxFlux fitness function, defined in Equation 5.3, MGGA was able to produce a number of excellent shield candidates. All of these shields demonstrated the value of splitting a shadow shield to allow particles to flow out of the system, supporting the conclusions in [Alpay & Holloway (2005)].

The second fitness function scored shields by trying to beat the heaviest shield at every detector location. Again, MGGA was up to the task and generated a number of shield candidates that passed the flux portion of this fitness test, given in Equation 5.4.

In both sets of trials, MGGA created a superior shield to GA using approximately the same number of fitness calculations and it did so in one third the time. This type of problem space seems to fit MGGA perfectly and MGGA should be considered a useful method for exploring possible shield designs in this type of geometry.

Exploring the value of MGGA further with a finer resolution and using the MaxFlux fitness function I was able to show that MGGA can handle a very large problem space, on the order of 2^{1024} shield candidates, and still produce reasonable results.

Altering the problem space by changing the shield rings from equal mass to non-equal mass, I showed that MGGA again finds better solutions than GA, and was even better at doing so in this problem space than the original one. MGGA appears to be fairly resilient to changes in the fitness function as long as the geometric scaling and translation phases are viable, which they all were for the shadow shield.

Finally, I explored a number of possible mechanisms for improving diversity in MGGA. The conclusions from these simulations indicate that diversity was not a problem and that having good building blocks going into the last phase of MGGA is what is important. If MGGA is not as sensitive to diversity issues as initially assumed it will make it an even more powerful tool for large problem spaces that can be organized into hierarchies.

Overall, MGGA did a great job building shadow shields. It surpassed GA with fewer computing resources in all cases. In the next two chapters I will see how MGGA performs when designing a shield and a filter using a more detailed physical simulation in the fitness test.

CHAPTER VI

Designing A Gamma Shield

6.1 Introduction

The goal of this chapter is to investigate MGGA in the context of designing a gamma radiation shield. Rather than look at simply blocking gamma rays, I also consider the concept of a wearable shield. Creating a shield that can be moved around is similar to the shadow shield problem in the last chapter. Movable or wearable shields have to balance shielding effectiveness versus mass. In the case of a wearable shield, the mass has a reasonable maximum on the order of 50kg for an unassisted human and something like 100kg for a human using an exoskeleton, [Robotics (2011)]. Given this tight mass constraint, GA may be a useful tool for finding novel shield designs. GA doesn't have any pre-conceived notions about good versus bad and may drive through unreasonable solutions to get to something better than a human might design.

The initial steps in designing a gamma shield is to look at what types of radiation we would need to worry about. There is a wide range of applications for gamma shields, ranging from x-ray technicians, to patients receiving radiation treatment, to a first responder dealing with a radiation dispersal device (RRD). Of these three, the first responder has perhaps broadest range of energies to shield against. In order to get a handle on this range of energies a first responder might encounter I looked at

Radioisotope	Gamma Energy (keV)	Intensity (%)	Dose (MeV/Bq-s)
Americium-241 (Am241)	26.3446	2.27	6.0×10^{-04}
	59.5409	35.9	0.02138
	125.3	0.00408	5.11×10^{-06}
Californium-252 (Cf252)	15.0	6.0	9.03×10^{-04}
Cesium-137 (Cs137)	283.5	5.8×10^{-4}	1.64×10^{-06}
	661.657	85.10	0.5631
Cobalt-60 (Co60)	1173.228	99.85	1.1715
	1332.492	99.9826	1.332260
Iridium-192 (Ir192)	295.95650	28.72	0.0850
	308.45507	29.68	0.0916
	316.50618	82.71	0.2618
	468.0688	47.81	0.2238
	604.41105	8.20	0.04956
	612.4621	5.34	0.03127
Plutonium-238 (Pu238)	13.6	10.2	0.00139
	43.498	0.0392	1.71×10^{-05}
Polonium-210 (Po210)	803.06	0.00103	8.3×10^{-06}
Radium-226 (Ra226)	186	3.59	0.00668

Table 6.1: Gamma emissions from high threat radioisotopes

an unpublished report [Schuster (2009)], that identified nine possible materials for an RRD. These materials are listed in Table 6.1 along with their more interesting radiation signatures. This list is based on [Ferguson *et al.* (2003)] and is verified in [IAEA (2002)].

Cobalt-60 jumps out of Table 6.1 for several reasons. First, it emits gammas with sufficient energy for pair production, [Chilton *et al.* (1984) pg. 43]. Second cobalt-60 is reasonably available, [Ferguson *et al.* (2003) page 13]. As a result of these two facts, I used cobalt-60 to set an upper limit for my high energy gamma sources. On the low end I mainly focus on energies at or above 50 kev, because shielding energies lower than this begins to require very little material, see Figure 6.4.

Shielding from gammas relies on electrons, [Shultis & Faw (2000) page 39]. An easy way to get a lot of electrons between a person and a gamma source is to use heavy elements, generally metals. Since mass will be a factor for a wearable shield, we

Material	Symbol	Density (gm/cm^3)
Tungsten	W	19.25
Lead	Pb	11.342
Bismuth	Bi	9.78
Tin	Sn	7.365
Antimony	Sb	6.697
Aluminum	Al	2.7

Table 6.2: A list of possible shield materials for gamma radiation shields

are going to look at a range of elements with various densities, starting with tungsten and moving down to aluminum. Tungsten will be the heaviest, and should be one of the best shielding materials. Aluminum will be the lightest, but may not have the electrons needed to perform well as a shield. The full list of materials we will consider for our shield are listed in Table 6.2.

As with the shadow shield, we will model places without shield material as vacuum, ignoring the shielding effect of air or structural material used to build the shield.

Looking at the literature we discovered a paper about optimizing non-Pb shields by [McCaffrey *et al.* (2009)]. McCaffrey and colleagues investigated a number of bi-layer shielding configurations with photon energies under 100 kev. Looking at Figure 4.5 we know that the K-edge, and other edges, provide zones at which different materials can alternate between which has the best cross section for a particular energy. McCaffrey found that using a low-Z/high-Z ordering was superior to the reverse for the energy ranges they tested. This result is good news for GA, it tells us that a smartly designed well-layered shield can beat lead, and gives us something to shot for. It also tells us that ordering can matter, giving GA even more design choices to work with. Ideally, low energy gammas will provide a fertile problem space for MGGA, but there is an open question of whether or not MGGA can help with high-energy shielding like the gammas from Cobalt-60.

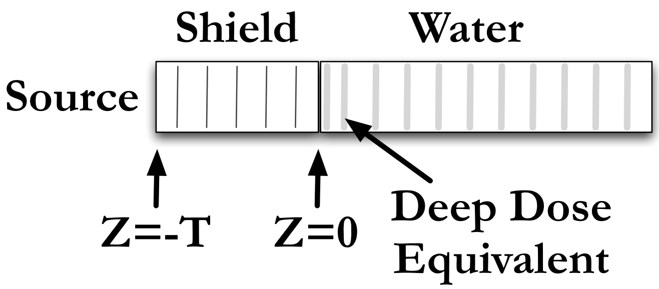

Figure 6.1: A slab geometry for gamma shield simulations

6.2 Initial Exploration

Consider the slab geometry pictured in Figure 6.1, for which I will describe several MCNP simulations. The geometry is defined in the X and Y directions by reflective walls at 0 and 10 centimeters. There is a circular source at $(5, 5, -T)$ with a radius of 5 cm. From the source to $Z = 0$ there is a shield of thickness T centimeters. The shield is split into some number of layers depending the MGGA or GA run's parameters. The positive Z direction is filled with water until $Z = 25.05$ cm. This water contains a series of 0.1 cm thick dose tallies. The first tally is 0.07 cm past the shield and provides a shallow dose tally. The second tally is centered 1 cm from the edge of the shield and is used to calculate a deep dose equivalent, [US Nuclear Regulatory Commission (2011)]. The remaining tallies are centered 5 cm from each other. The Z boundaries are both absorbing.

In the absence of a shield the absorbed dose should fall roughly exponentially into the water, and increase with energy. Figure 6.2 shows the results of an MCNP simulation for the unshielded water phantom. As expected, the dose at each tally goes down with depth, and goes up with energy.

Running this same simulation with the shield materials listed in Table 6.2 should result in a dose that decreases with the Z of the material and increases with the energy of the gamma radiation. Figure 6.3 shows the results of running MCNP for each of these possible shielding materials where the shield was 0.5 mm thick and the

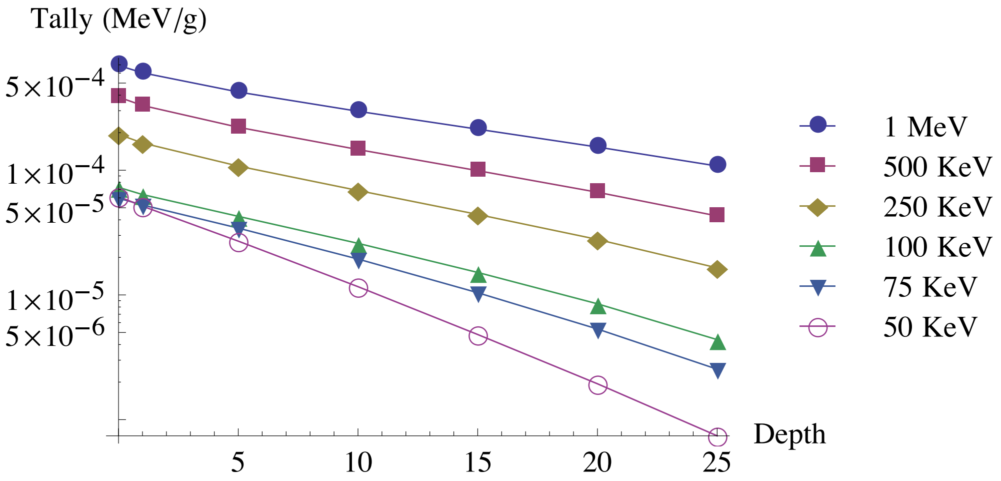

Figure 6.2: The vacuum tally vs. depth for various energies of gamma radiation in the slab geometry

energies ranging from 50 kev to 1 Mev, while Figure 6.4 shows the same data limited to energies under 100 kev.

At higher energies, this graph shows the expected behavior of higher Z performing better than lower Z. However, the lower energy region has some structure, suggesting that GA might be able to do something with shields at these lower energies, as per McCaffrey's paper.

6.2.1 High Z - Low Z

Duplicating McCaffrey's results requires layering two shielding materials. McCaffrey choose tungsten and antimony for their experiments so I have used the same materials. Looking at the cross-sections for these two materials, pictured in Figure 6.5, at the energies between 10 kev and 100 kev we can see there is a lot of structure. Photons that are absorbed by tungsten at 100 kev sometimes radiate out at tungsten's K-edge which borders an energy range at which antimony has a higher cross-section. Similarly, photons absorbed by antimony and re-emitted at its K-edge will fall into a region where tungsten has a higher cross-section.

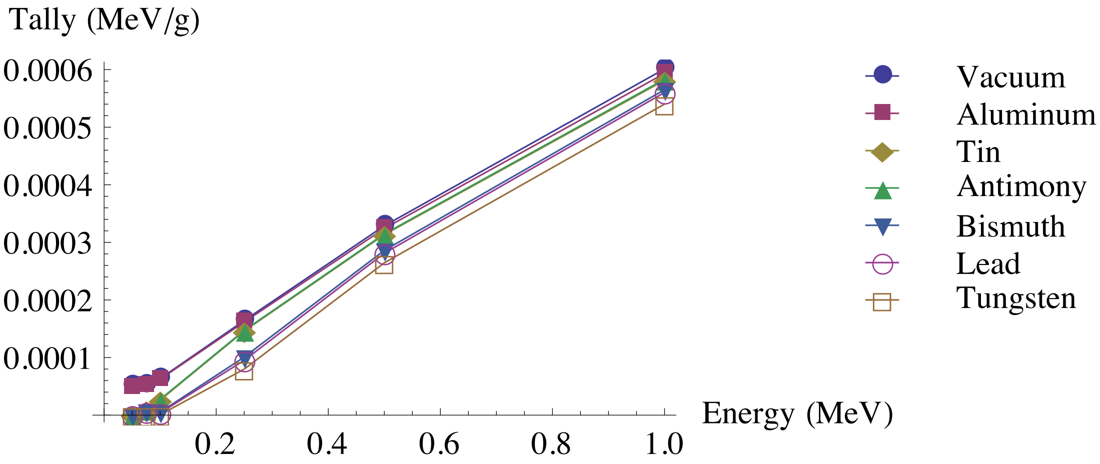

Figure 6.3: The dose for single material shields at a tally depth of 5 cm

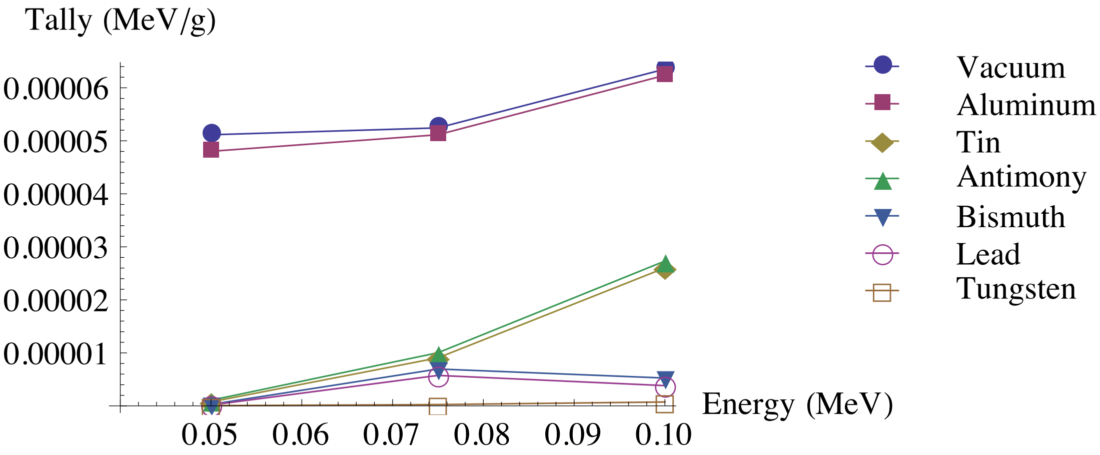

Figure 6.4: The dose for single material shields with energies under 100 kev

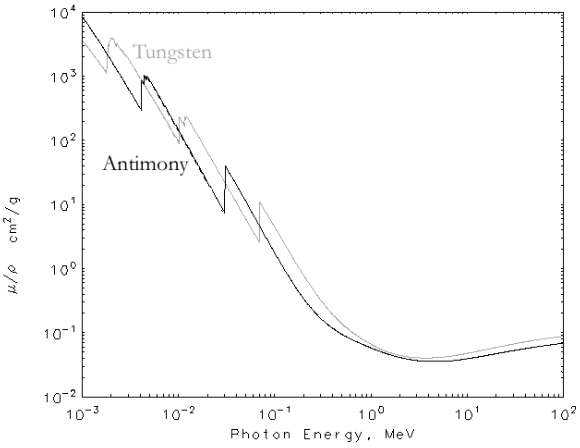

Figure 6.5: γ radiation cross-sections for Tungsten (gray) & Antimony (black), [National Institute of Standards and Technology (2011)]

I did two sets of MCNP runs, one used a source energy of 50 kev and the other used a source energy of 100 kev. Each set consisted of building a 16 layer shield with a variable number, from 0 to 15, of layers of tungsten or antimony. The remainder of the shield is built from the other material. For example, one run has 0 layers of tungsten and 16 layers of antimony and another has 5 layers of tungsten and 11 layers of antimony. This simulation was run in both directions. One set of results put tungsten, a high-Z material, closest to the source. The other put antimony, a low-Z material, closest to the source. In all cases the tally at 1 cm, corresponding to the Deep Dose Equivalent, was used to determine the dose.

The results for 50 kev are shown in Figure 6.6. These results match McCaffrey's in that the low-Z/high-Z structure did better than the high-Z/low-Z structure at this gamma energy.

Performing this same simulation with 100 kev gammas demonstrates another expected result, shown in Figure 6.7, which is that higher energy gammas are less affected by the high/low organization. This effect was also shown in McCaffrey's paper.

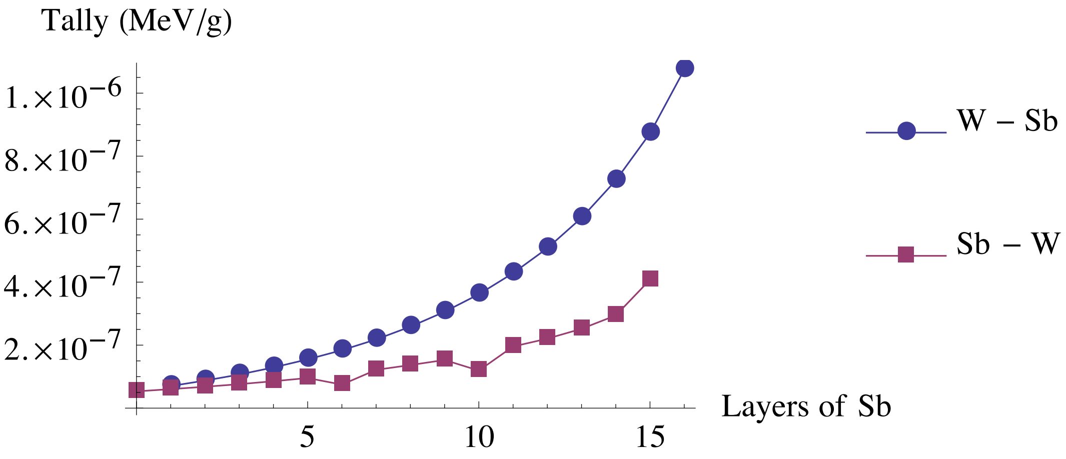

Figure 6.6: A comparison of tungsten and antimony layered shields at 50kev

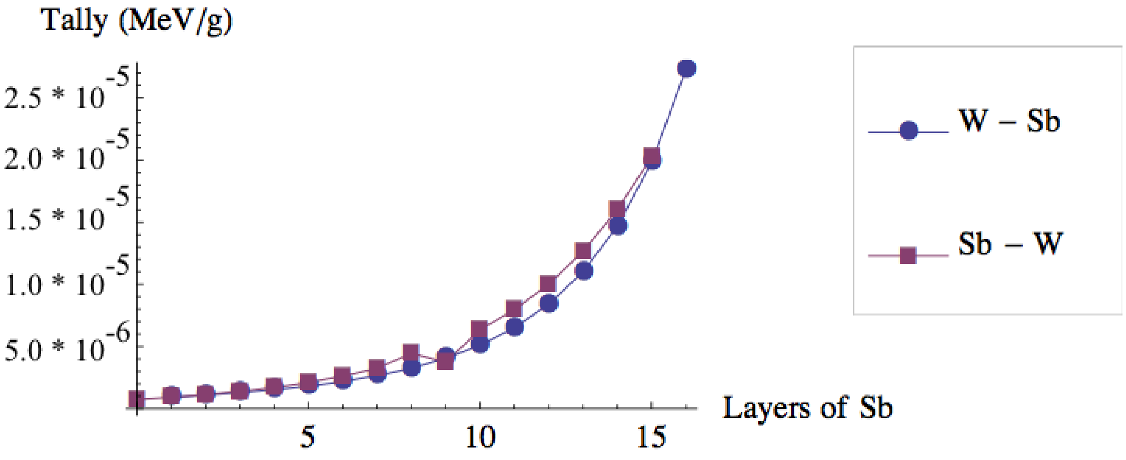

Figure 6.7: A comparison of tungsten and antimony layered shields at100kev

6.3 Designing a Gamma Shield with MGGA

Given that layering does effect the dose, what is the best shield we can construct from the materials in Table 6.2. MGGA and GA can help explore this problem and work toward building good shield. But first we have to create a fitness function that defines what good means.

6.3.1 Defining a Fitness Function

McCaffrey's paper compared the shields they tested against a fixed amount of lead on mass and dose. I copied this approach by defining a fitness function that tries to find a shield with a lower mass than one made from 0.5 mm of lead and then reduce the dose. Basically, the fitness function is trying to weigh less than a standard shield and then try to beat it on dose. The fitness of each shield, s, will be determined as follows:

1. Calculate the mass of a 0.5 mm shield made of lead, $m(S)$
2. Calculate the deep dose equivalent, $D(s)$, with shield s
3. Compare the mass with of shield s, $m(s)$ to the mass of the lead shield, $m(S)$:
    - If the shield is heavier than the lead shield, the fitness is $-(m(s)/m(S))$
    - Otherwise the fitness is $1 - (D(s) \times 1000)$

In other words, the fitness of shield s is

$$F(s) = \begin{cases} 1 - (D(s) \times 1000) & \text{if } m(s) < m(S) \\ -\frac{m(s)}{m(S)} & \text{otherwise.} \end{cases} \tag{6.1}$$

I am multiplying the tally, in MeV/g, by 1000 to make the fitness scores more human readable. Moreover, I am assuming that $D(s)$ is always less than 1/1000 so that a shield measured on dose is never assigned a score less than zero, and the scaling will not effect the ranking of two light shields, where $m(s) < m(S)$. This assumption was not violated in the runs described here.

While the fitness compares the deep dose after running a simulation using a shield s to the lead shield S, it is not always obvious what a particular fitness score means. To help understand the values of the shields better I calculate another value called *Dose Reduction Percentage.* Dose reduction of a shield s, compared to the lead shield S is defined as:

$$DoseReductionPercentage(s) = 100 * \left[1 - \frac{D(s)}{D(S)}\right] \tag{6.2}$$

Basically this is the percentage reduction in dose that the shield has over the lead shield.

6.3.2 Fitness and Error

When dealing with MCNP or any other physical simulation there will be error in the results. While I have tried to reduce the error to a small percentage of the total dose for these calculations, there is of course always a finite error. This means that running a stochastic simulation like MCNP on the same shield multiple times can result in different fitness scores (if independent random numbers are used). Moreover, it means that two shields with very close fitness scores may be equivalent within the error in the dose calculation. When running tournament selection, this equivalence is ignored. So one shield may have an advantage simply because the random number generator was kind to it in MCNP; in these cases we are effectively randomly selecting one of the shields. In the context of this dissertation, which is focussed on showing the value of MGGA versus GA for these types of problems, this potential inconsistency in the fitness functions is acceptable, but it does represent a possible area of research in the future.

6.3.3 Defining the Genetic Algorithm

Using the fitness function in Equation 6.1 I ran several simulations for GA and MGGA. The final geometry had a total of 16 layers, with seven possible materials in each layer, or $7^{16} = 3.32 \times 10^{13}$, or approximately 33 trillion possible shield configurations.

The GA was run with a population of 1000 for 20 generations. The MGGA was run with the following phases:

- 4 layers - 250 individuals per generation with 10 generations
- 8 layers - 500 individuals per generation with 15 generations
- 16 layers - 500 individuals per generation with 15 generations

Thus MGGA used 17,500 individuals while GA used 20,000.

To move between phases each layer was cut into two pieces for the next phase. From a shielding standpoint the shields were identical as they move between phases. The encoding for each shield was a string of integers, one for each layer. The integers were the numbers 0-6 indicating an index into the list of available materials: vacuum, tungsten, lead, bismuth, tin, antimony, and aluminum.

All GA was performed using tournament selection with a tournament size of 5. There was a 25% chance that the worst individual in a tournament would win to help preserve diversity. Reproduction relied on uniform crossover 70% of the time, mutation of a single layer 20% of the time and copying 10% of the time. Uniform crossover allowed each child to use the materials for any layer from either parent, however, I created two children for each crossover reproduction, these two children were the result of reversing the coin flip for each gene in uniform crossover.

Energy (KeV)	Fitness	Dose Reduction Percentage	Algorithm
50	0.99996	79.69	GA
50	0.99994	67.7	MGGA
75	0.99905	83.54	GA
75	0.99908	84.09	MGGA
100	0.9973	31.02	GA
100	0.9967	15.57	MGGA
125	0.9911	6.118	GA
125	0.9906	0.0021	MGGA
150	0.9796	1.313	GA
150	0.9793	0.158	MGGA
175	0.9642	1.379	GA
175	0.9637	0.082	MGGA
200	0.9459	1.319	GA
200	0.9453	0.203	MGGA

Table 6.3: Results of MGGA and GA for a 1mm Shield vs 0.5mm of lead in the slab geometry

6.3.4 Results for a 1 mm Shield Compared to 0.5 mm of Lead

I initially ran GA with a shield thickness of $T = 0.5$ mm and a lead shield thickness of 0.5 mm. But this value for T was very constraining. GA was pressured to always use lead for every layer since lead met the mass requirement as well as performing well on the dose. The solution to this constraint, used by McCaffrey as well, was to give the GA more space to build a shield. In the simulations listed in Table 6.3 the GA was given a shield thickness $T = 1$ mm, but was still compared to the mass of 0.5 mm of lead. This allowed the GA to use more layers of lighter elements if it choose to.

Figure 6.8 shows the winning shields for GA and MGGA at 50 kev. Both shields have the low-Z/high-Z layout we expected from McCaffrey's research, which means that GA and MGGA are matching the physical experiments. At this energy the GA run beat MGGA by almost 10% on dose reduction. The question is, why?

Both the GA and MGGA shields use tin, antimony and bismuth in place of lead. Table 6.4 shows a breakdown of the materials, by layer, for each of these shields.

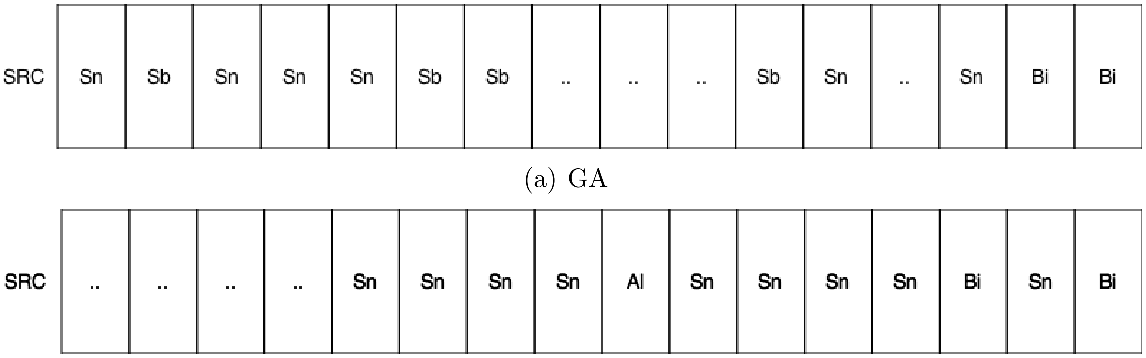

(a) GA

(b) MGGA

Figure 6.8: The best GA and MGGA gamma shields at 50 kev

Material	Density	GA Layers	MGGA Layers
Bismuth	9.78	2	2
Tin	7.365	6	9
Antimony	6.697	4	0
Aluminum	2.7	0	1

Table 6.4: Layers of material for the best GA and MGGA shields at 50kev

The big difference is that MGGA used a layer of aluminum, and the GA used some antimony instead of tin. This change to antimony saved a bit of mass and allowed GA to include the higher density material instead of aluminum and still beat the mass requirement. The lead shield has a mass of 56.71kg. The GA shield has a mass of 56.58kg and the MGGA shield has a mass of 55.34kg. Clearly the MGGA could have used a bit more mass, while GA was very efficient.

To try to understand why MGGA is losing from an algorithmic perspective, lets look at the dose over time for each run. Figure 6.9 shows the best shield's dose for each generation versus the dose of the lead shield. Keep in mind that this graph does not take into account mass, so the shields in the early generations may have lead and tungsten and weigh more than the lead shield. The MGGA graph uses vertical lines to distinguish the three phases of MGGA. What is particularly interesting about these graphs is that they show MGGA is having trouble reducing the dose until very late in the process. This could mean that MGGA is focused on reducing mass or that

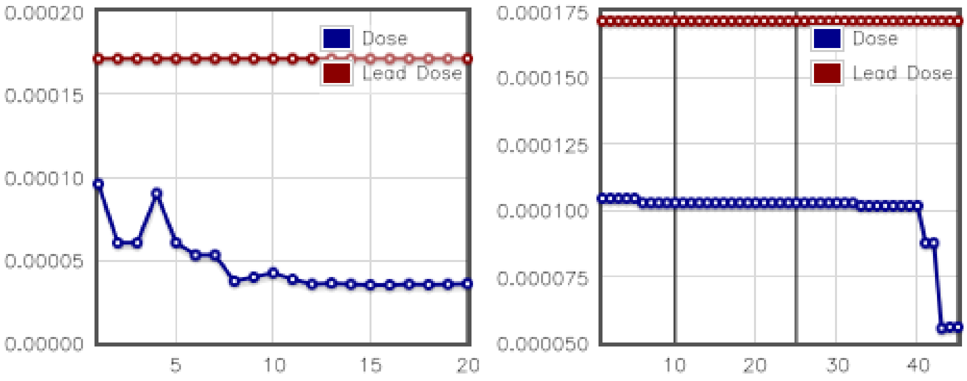

(a) GA

(b) MGGA

Figure 6.9: Dose as an F6 tally for GA and MGGA at 50 kev

MGGA has stagnated.

Figure 6.10 gives us some more insight into the problem. MGGA quickly finds that an all tin shield beats the lead shield on mass, and begins scoring on dose. Unfortunately, it takes several generations into the final phase for MGGA to start putting bismuth into the shield. This could be due to the mass of bismuth in the earlier phases. Although bismuth could certainly be used in phases one and two, MGGA did not appear to pick a shield with bismuth and paid a higher dose cost as a result. Once bismuth was included MGGA was moving toward a shield that would match the GA one.

MGGA appears to be stagnating on this tin-based solution and is taking a long time to get out of it. One way to see if this is the case is to look at diversity.

6.3.4.1 Diversity

In Section 5.8 we measured diversity using cache hits. Another way to measure diversity is to look at variance of individuals. Figure 6.11 shows a graph of diversity using variance as a measure for the MGGA run at 50 kev. The diversity is calculated using the following algorithm:

- For each gene, calculate the “mean” value. So if half the individuals have a 2

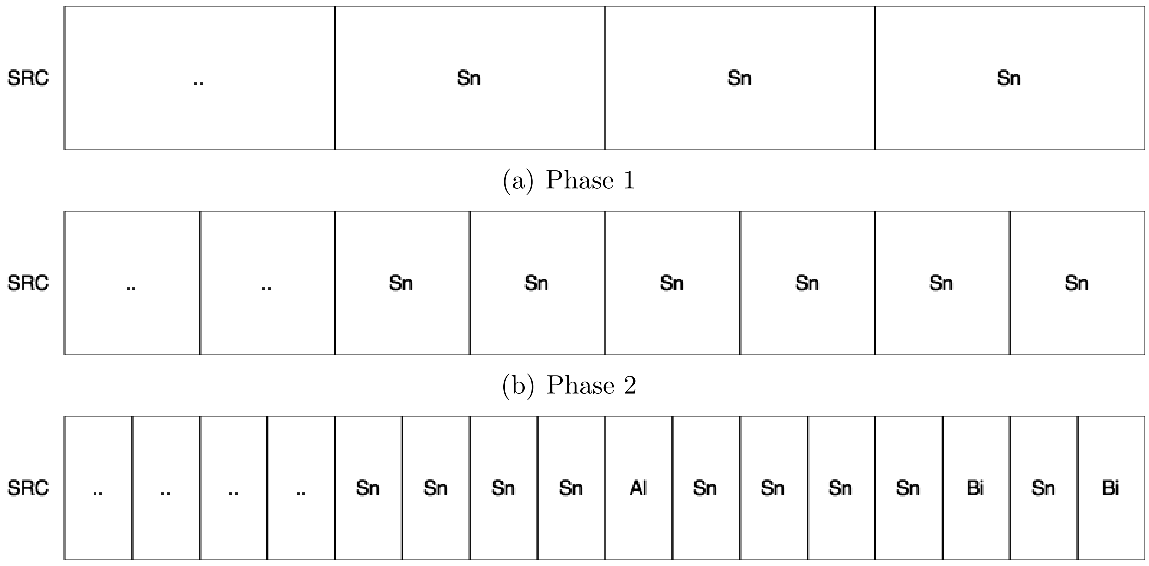

(a) Phase 1

(b) Phase 2

(c) Phase 3

Figure 6.10: The best gamma shields at 50 kev for MGGA by phase

for their first gene and half are 0 for their first gene the mean is 1 for the first gene. This is a true mean, we just add up the values for the i^{th} gene for each individual and divide by the number of individuals.

- For each individual calculate the distance for each gene from the mean and square this value.
- Sum over all individuals and genes
- Divide by the population size × the number of genes

Note that this algorithm normalizes the result by the population size and number of genes so that we can compare diversity between the MGGA phases.

The diversity based on this calculating for the two 50 kev runs is pictured in Figure 6.11.

From these graphs, we can see that MGGA starts with reasonable diversity compared to GA in the first phase, where there are fewer possible individuals. The second phase is able to add some diversity back, but this is quickly reduced. It is only late

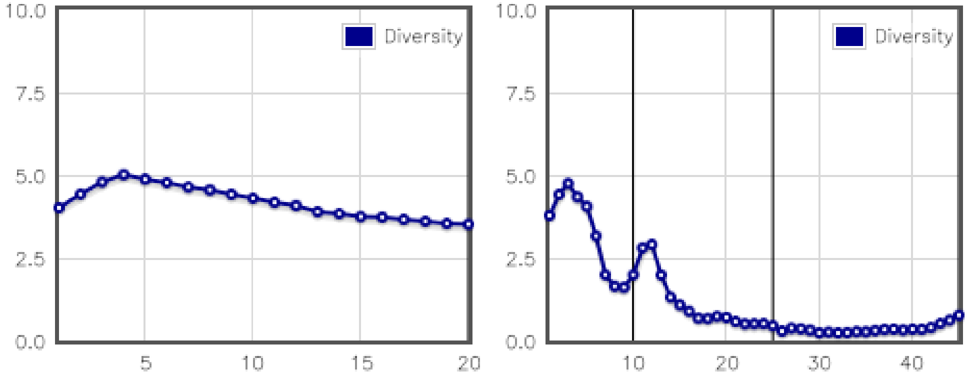

(a) GA

(b) MGGA

Figure 6.11: Diversity for GA and MGGA runs at 50 kev

into phase three that mutation and crossover are able to starting adding diversity into the MGGA population, by which point the MGGA population has stagnated at a pretty low level compared to the equivalent GA population.

Based on this diversity plot and the shields from Figure 6.8 I think that MGGA was hitting a local maxima for the fitness and having trouble getting out of it using mutation on only 20 percent of the children. Two ways to test this in future work would be to provide more resources to MGGA or use mutation between phases.

At 75 kev the MGGA run beat the GA run by a small amount. Looking at the two best shields, pictured in Figure 6.12, two things jump out. First, the low-Z/high-Z order is not being maintained. Second, both GA and MGGA are starting to rely on some heavier elements like tungsten, bismuth and lead.

This trend toward higher Z materials is not unexpected and will become even more pronounced at higher energies. Similarly it is not unreasonable that the ordering preference is changing. Based on McCaffrey's paper and the results pictured in Figure 6.7 the value of ordering should go down with energy.

Figure 6.13 shows how MGGA arrived at its best shield, showing the top shields from each of the three phases. Keeping in mind that these shields do not necessarily have any sort of parent-child relationship, it is easy to see that MGGA found tungsten

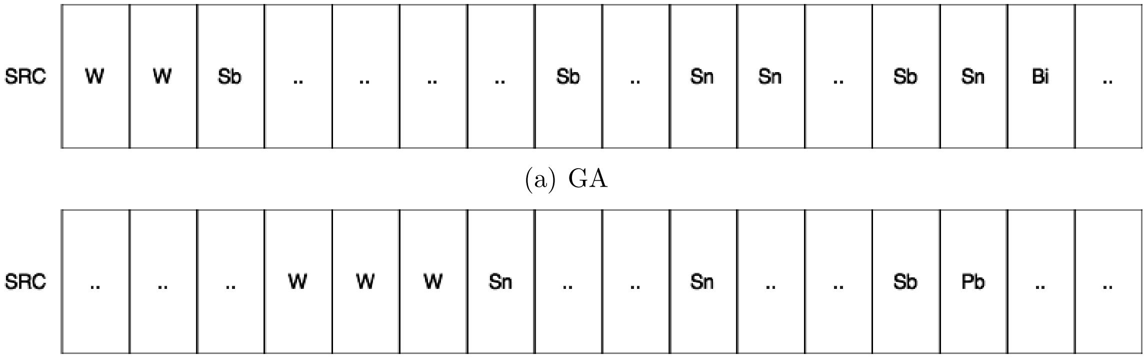

SRC	W	W	Sb	..	..	..	..	Sb	..	Sn	Sn	..	Sb	Sn	Bi	..

(a) GA

SRC	..	..	..	W	W	W	Sn	..	..	Sn	..	..	Sb	Pb	..	..

(b) MGGA

Figure 6.12: The best GA and MGGA shields at 75 kev

early and was optimizing after that. The mass of the lead comparison shield was 56.71kg, the masses of the respective shields from each MGGA phase are 54.875, 56.652 and 56.57. While the GA produced a shield with a mass of 56.54kg. As we might expect, the heavier shield is the better shield, just like it was at 50 kev.

Moving up to 100 kev the two best shields, pictured in Figure 6.14, show that GA has really started to rely on the High-Z materials. Moreover, MGGA is headed toward just making a lead shield. In fact at 150 kev, pictured in Figure 6.15, MGGA builds the lead shield and GA builds a bismuth shield with one layer of lead.

It is worth noting that the bismuth shield is able to be nine layers, while the all lead can only be eight, and still meet the mass test. This is what allows the bismuth shield to score slightly higher.

Interestingly the best shield at 175 kev and 200 kev is the same for GA and MGGA as it is at 150 kev. Of course the layer orders are different, but the number and overall content of the layers are the same.

6.3.5 Changing the MGGA

To try to get a handle on why MGGA is having trouble beating GA for this problem space, I took a look at giving MGGA a bigger problem space to work in.

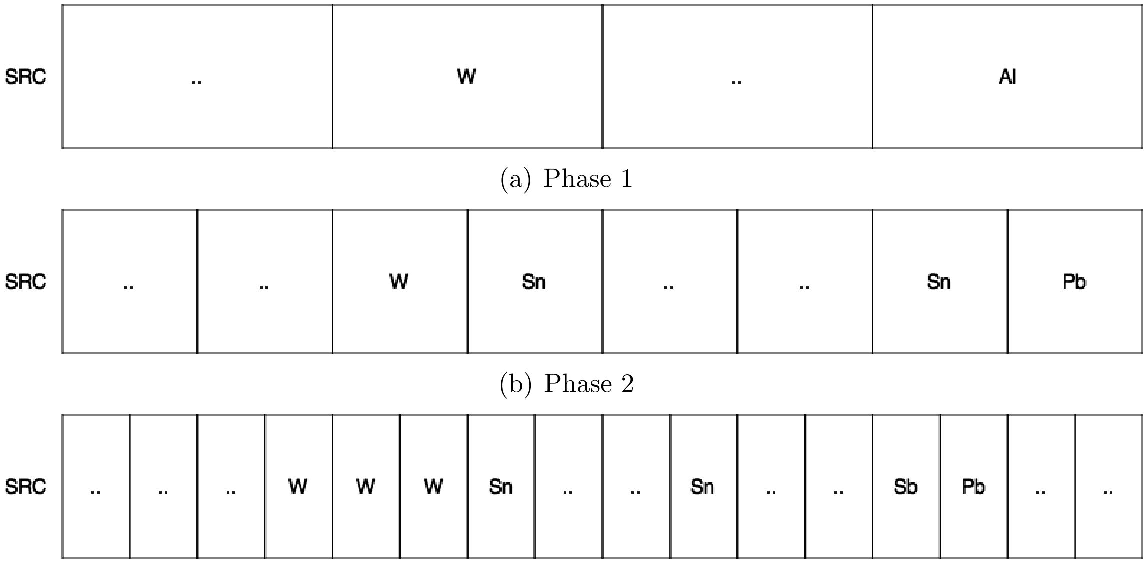
SRC .. W .. Al
SRC .. .. W Sn .. .. Sn Pb
SRC .. .. .. W W W Sn .. .. Sn .. .. Sb Pb .. ..

(a) Phase 1

(b) Phase 2

(c) Phase 3

Figure 6.13: The best gamma shields at 75 kev for MGGA by phase

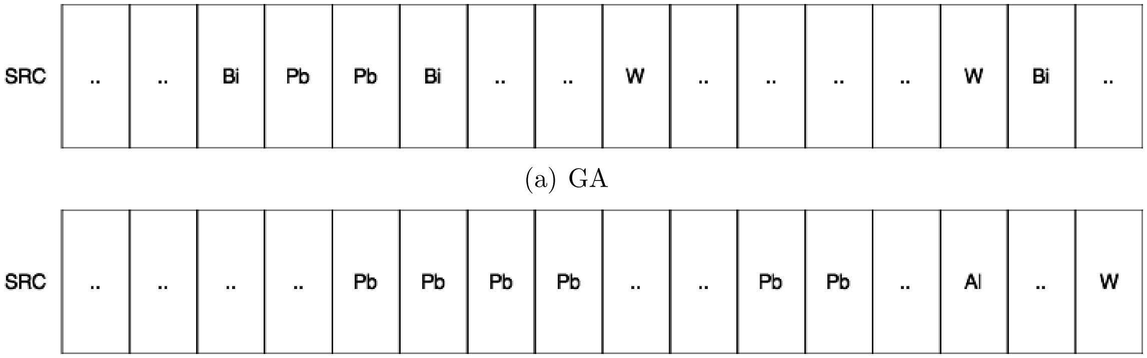
SRC .. .. Bi Pb Pb Bi .. .. W .. .. W Bi ..
SRC .. .. Pb Pb Pb Pb .. .. Pb Pb .. Al .. W

(a) GA

(b) MGGA

Figure 6.14: The best gamma shields at 100 kev

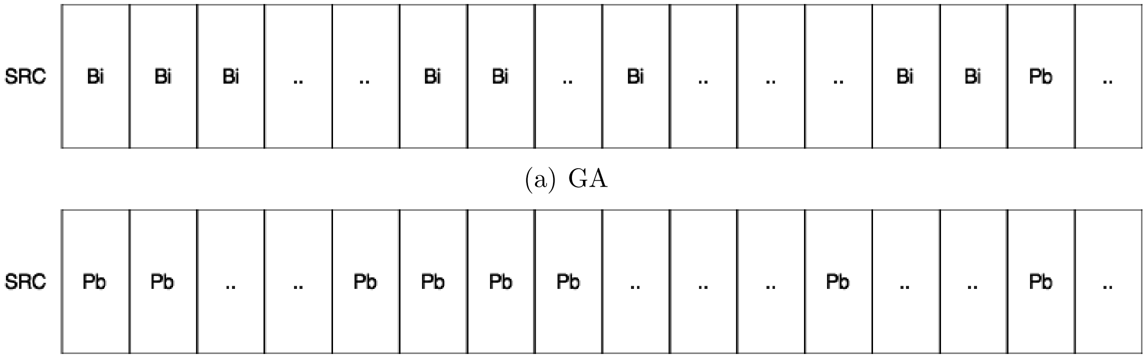
SRC
Bi Bi Bi .. .. Bi Bi .. Bi .. .. .. Bi Bi Pb ..
SRC
Pb Pb .. .. Pb Pb Pb Pb .. .. .. Pb .. .. Pb ..

(a) GA

(b) MGGA

Figure 6.15: The best gamma shields at 150 kev

This seems counter intuitive. But I posit that MGGA has two properties that must be balanced. First, like GA, MGGA cannot work if it is over constrained. If the population or generation size is too small the basic algorithm can't work. But unlike GA, MGGA performs sub-setting of the problem space in the earlier phases. It is possible that MGGA gets over constrained at the later phases by wasting resources during earlier phases. In a real world problem this may not happen, but in this discussion, where we are trying to compare the two, the resource counts for GA are always from a bigger problem space, while MGGA is forced to use some fitness test resources on smaller problem spaces. If we tune the MGGA wrong we might not get good results.

To test this theory I ran the MGGA version of our problem at 50 kev and 1 mm thickness, with phases set to 8, 16 and 32 layers [1]. Again the mass is compared to lead at 0.5 mm, as in Equation 6.1. The final problem space has twice the layers of the original run. This new version of the problem used a population of 500 and a generation count of 15 for each phase. This resulted in a total of 22,500 individuals tested. The original test used only 20,000 individuals for GA, so MGGA is using more resources for this test.

[1] These runs had a bug in the materials cards for MCNP. A low density cobalt foam was used instead of aluminum. While this effected the intermediate shield populations, it did not show up in the best shield.

In the original MGGA the best score was 0.99994, while the best score from GA was 0.99996. The new MGGA runs I did for 32 layers matched the GA best score. Where the earlier MGGA had trouble matching GA, the finer resolution MGGA has no problem keeping up with it. Figure 6.16 shows the best shield from these finer grid runs.

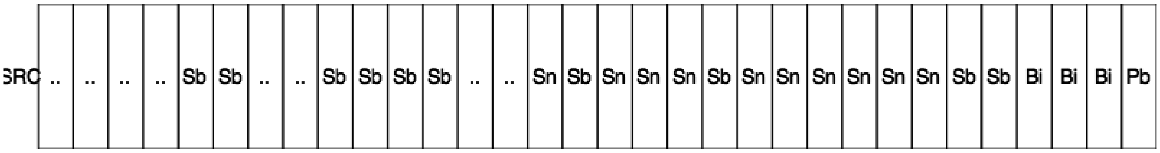

SRC	..	..	..	..	Sb	Sb	..	..	Sb	Sb	Sb	Sb	..	..	Sn	Sb	Sn	Sn	Sn	Sb	Sn	Sn	Sn	Sn	Sn	Sn	Sb	Sb	Bi	Bi	Bi	Pb

Figure 6.16: 50kev MGGA shield with 32 layers

This shield demonstrate the low-Z/high-Z configuration we expect. It uses tin and antimony close to the source and bismuth or lead closer to the target. The shield also has eight empty layers, which is the same empty space as the 16 layered version. Essentially the 32 layer version seems to have been more successful at avoiding pitfalls, or bad choices, but is otherwise similar to the winning GA shields from the smaller space.

6.3.5.1 Conclusions for the 1 mm Shield

We can draw several conclusions from the results on the 1 mm shield compared to a 0.5 mm shield made of lead. First, something is holding MGGA back in comparison to pure GA. Perhaps it is a local minima. Perhaps it is a lack of diversity. Both algorithms are creating good shields, but MGGA seems to fall into some sort of trap that it can't get out of. As we have seen in the earlier chapters this could be a resource problem. The second conclusion is that GA, and as a result MGGA, are struggling to beat lead as the energies increase. This may be due to the thickness of the shields. In the next section I will increase the shield size to test this hypothesis. Finally, we can conclude that GA and MGGA do provide value for designing shields for low-energy

Energy (KeV)	Fitness	Dose Reduction Percentage	Algorithm
200	0.99987	11.2	GA
200	0.99984	−7.15	MGGA
300	0.99083	4.47	GA
300	0.9900	−3.51	MGGA
400	0.9588	2.39	GA
400	0.9569	−2.15	MGGA
500	0.913	1.64	GA
500	0.91	−1.47	MGGA

Table 6.5: Results of MGGA and GA for a 1cm Shield vs 0.5cm of lead in the slab geometry

gammas. In a later section I will test this conclusion in a more realistic geometry with a more detailed human phantom.

6.3.6 Results for a 1 cm Shield Compared to 0.5 cm of Lead

To see if GA can find good shields at higher energies I gave MGGA and GA more shielding material. Table 6.5 shows the results of running the GA and MGGA on the same geometry, but allowing for a 1 cm shield. This shield is ten times thicker than the previous one. To make the comparison fair, the lead shield being compared to is 0.5 cm thick. From these results, GA is clearly beating MGGA. Something about the MGGA is preventing it from finding good solutions for these high energies. At the same time, the effectiveness of GA is going down with energy, and we can expect that at higher energies GA will become less and less skilled at beating the lead shield, or there simply isn't a better shield to be found with the materials we are testing.

To get an idea for what is happening let's look at the new 200 kev results pictured in Figure 6.17. GA found a shield with 8 layers of bismuth and 1 of lead. At the same energy, MGGA found a shield with 7 layers of lead and 1 of bismuth. The runs at 300 kev, 400 kev and 500 kev all produced the same shields for both GA and MGGA. Just like the 1 mm result, MGGA is getting stuck on a lead based shield.

In Figure 6.18 we can see that MGGA is trying to be smart in the first phase.

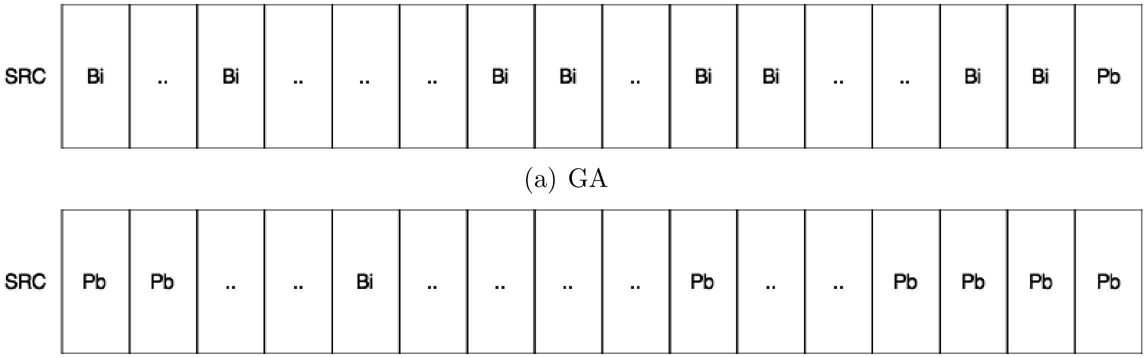
SRC Bi .. Bi .. .. .. Bi Bi .. Bi Bi .. .. Bi Bi Pb
SRC Pb Pb .. .. Bi .. .. Pb .. .. Pb Pb Pb Pb

(a) GA

(b) MGGA

Figure 6.17: The best gamma shields at 200 kev with 1 cm shields

It finds a shield with lead and bismuth, which meets the mass goal and has lots of electrons to reduce dose. In phase two, the MGGA tries to continue this process and again picks lots of lead and a little bismuth. Again this will meet the mass goal. The problem is that MGGA doesn't seem to figure out that switching to mostly bismuth is ok for the mass goal and the dose. Perhaps this switch doesn't get propagated into later generations because switching to bismuth could, depending on the total shield, create a higher dose. A higher dose would lead to a lower fitness and reduces the chance that the shield will win a tournament and reproduce.

6.3.7 Conclusions for the 1 cm Shield

GA is able to beat a lead shield at moderate energies, between 200 kev and 500 kev using a thicker shield. MGGA is getting stuck at these energies. Future work might look into why MGGA is getting stuck and how we might force it to move forward, perhaps by injecting diversity using interphase mutation.

6.4 The ORNL Phantom

The ORNL phantom, [Oak Ridge National Laboratory (2011)], defines a man, pictured in Figure 6.19, with two legs, numerous internal organs, a neck and a head. The

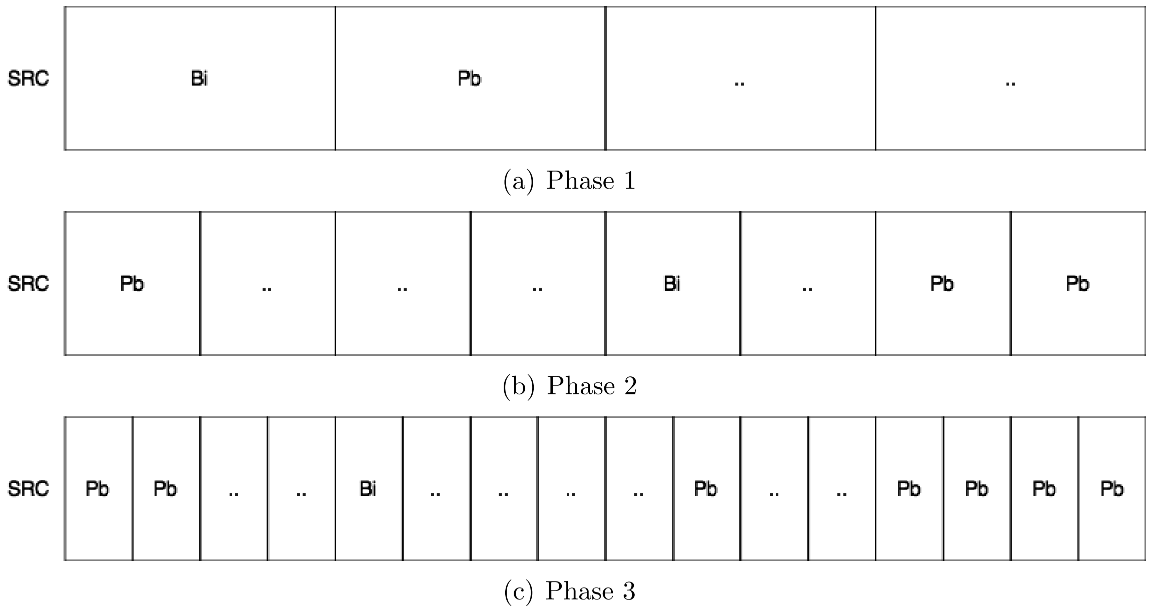

(a) Phase 1

(b) Phase 2

(c) Phase 3

Figure 6.18: The best gamma shields at 200 kev for MGGA by phase, at 1 cm

phantom also defines a skeleton and differentiates the skin from the other elements of the body.

The first step for using this phantom is to define a shield geometry. The shield is defined as a set of layers outside the torso split into horizontal rings and angular sections, as shown in Figure 6.20. The results discussed below do not use the rings or sections, and instead focus on layering. The phantom also contains a simple helmet around the head that provides layers in the radial direction and another set of layers on top of the head. The helmet is the same thickness as the shield, determined by the parameters discussed below.

After testing the initial file, I turned it into a template so that the GA could replace the material for each shield section using simple text replacement. The ORNL template contained a number of tallies. Using the values in [Shultis & Faw (2000)] I redesigned the tallies to match the ICRP and NCRP dose weighting scheme. A tally multiplier card is used to multiply the output of these tallies by the appropriate weighting. The final dose tally is simply a sum over the tallies defined in the input

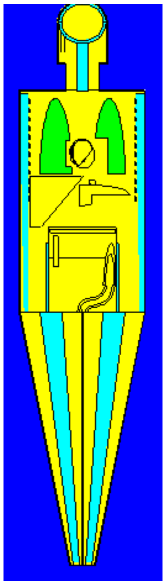

Figure 6.19: The ORNL phantom

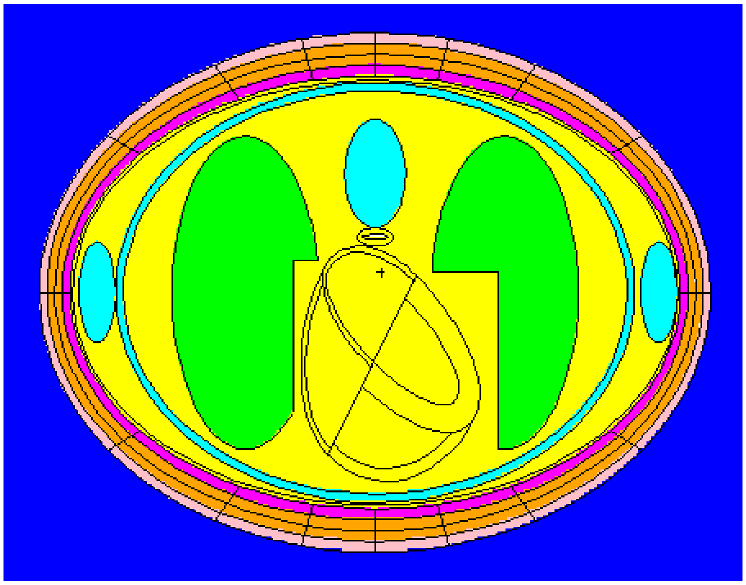

Figure 6.20: The shield cross section for the ORNL phantom layered shield

	1000000	5000000	10000000	20000000	30000000	40000000	50000000
lungs	5.6	5.7	5.6	5.6	5.6	5.6	5.6
skin	0.48	0.48	0.48	0.48	0.48	0.48	0.48
liver	2.0	2.1	2.2	2.2	2.2	2.2	2.2
stomach	5.8	5.4	5.5	5.8	5.8	5.8	5.8
bladder	2.0	2.0	1.9	2.1	2.2	2.2	2.2
esophagus	1.8	2.1	2.0	2.0	2.1	2.1	2.1
colon	4.8	5.1	5.1	5.2	5.3	5.3	5.3
thyroid	0.98	0.86	0.92	0.9	0.92	0.93	0.94
bone	0.44	0.44	0.44	0.44	0.44	0.44	0.44
remainder	1.7	1.7	1.7	1.7	1.7	1.7	1.7
gonads	8.9	11	9.3	9.5	9.5	9.3	9.3
Run Time	25.63s	1.98m	4.00m	7.64m	14.21m	18.83m	19.08m

Table 6.6: A comparison of tally ($\times 10^{-9}$) versus particles run at various tally locations in the ORNL phantom

file. There is one potential problem with the current scheme. The bone tally does not account for bone marrow. This may alter the importance of some regions of the body in a final shield design.

6.4.1 Determining the Number of Particle Histories to Run

The MCNP file from ORNL used a spherical source at head level. I altered the file to use a cylindrical source that surrounded the body. Using this input file I ran some tests to see how the tally definitions responded under different numbers of particles. GA would need to run MCNP thousands of times and I had limited computing resources. Therefore I wanted to find the find the smallest acceptable number of histories MCNP could run to get a reasonable result. Table 6.6 shows a summarized version of this investigation. In order to fit the table into this document all numbers were truncated, not rounded, and all uncertainties are removed. The times were calculated on a Macbook Pro running MCNP in single threaded mode.

Figure 6.21 is a graph of the tallies for the thyroid, gonads and bladder as a function of the number of histories run. These are three of the tallies that changed the most when the number of particles was changed. Some tallies, like skin, had almost no change in response to the particle count. These plots all show the weighted dose, for a single tally, as a function of the number of histories on the entire MCNP simulation. The error bars are derived from the uncertainties as output by MCNP.

Using the plots of tally versus particles, including those in Figure 6.21, we decided to use fifteen million particles as the number of particle histories to run. This history count reduced the changes as shown in Table 6.6 to less than 10 percent, while allowing the simulations to complete in approximately six minutes. Time is an important driving force.

6.4.2 Analyzing Tallies

Next I looked at the tallies to see which ones were going to drive the total dose. The tally information for a test run is listed in 6.7. This table focuses on the percentage of the total dose for each tally.

Several things jump out of this tally summary. First, the gonads are almost 50% of the total dose. Second, bone and soft tissue, in the form of the remainder, account for over a third of the dose. These two insights turn out to be extremely important because our original shield geometry did not extend to cover the gonads or legs. This means that a large part of the ORNL dose is being calculated on unshielded areas.

6.4.3 Updating the Simulation

Using this understanding of the ORNL simulation I altered the MCNP file to focus GA on shielding the parts of the body that it could, make the source more realistic and maximize the chance that a particle created at the source would hit the phantom. These changes, listed below, are pictured in Figure 6.22. In both cases particles going through the ceiling are ignored once they leave the system.

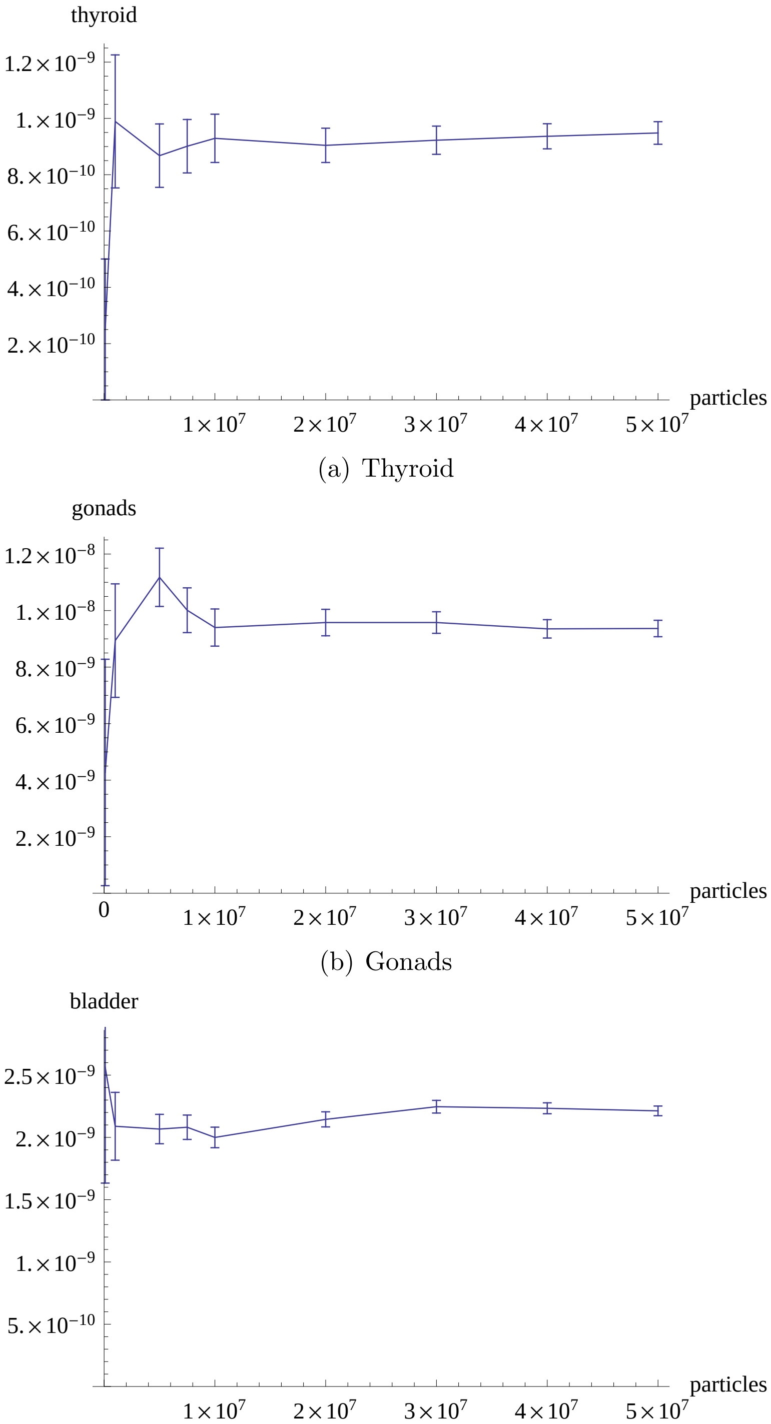

(a) Thyroid

(b) Gonads

(c) Bladder

Figure 6.21: Plots for 3 tallies in the ORNL phantom: dose equivalent vs. particle count

Table 6.7: MCNP tallies from an ORNL phantom run at 75kev

Tally	% of Total Dose	Error %
Lungs	2.519	2.88
Skin	2.9845	0.18
Liver	0.4739	4.07
Stomach	1.200	6.619
Bladder	2.400	3.75
Esophagus	1.283	5.28
Colon	3.378	2.56
Thyroid	3.967	4.25
Bone	13.519	0.32
Remainder/Soft Tissue	22.630	0.18
Gonads	45.641	2.85

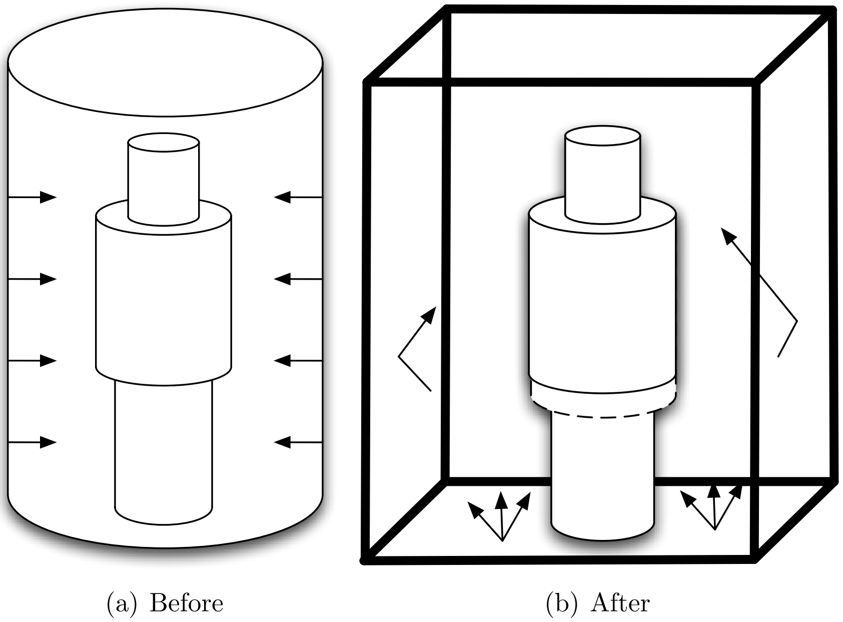
(a) Before (b) After

Figure 6.22: ORNL-based geometry before and after optimizations

- The shield was made longer, so that it covered the gonads. The shield was still open at the bottom, but provides protection from the sides.

- The source was changed to a ground source, which simulates ground covered with a contaminant emitting keV range gammas.

- The "walls" were made reflective to emulate a larger space. However, that larger space is being modeled as having other ORNL phantoms with shields on, not as empty space. The walls are $3m$ from the Z axis, in the positive X, negative X, positive Y and negative Y directions.

- The legs were removed from the skin, bone and soft tissue tallies, but remain in the geometry.

Removing the legs allows the GA to focus on shielding the torso and head, not trying to lower the dose on the legs which are unshielded. One small secondary task in removing the legs from the ORNL model was calculating the volume assigned to the

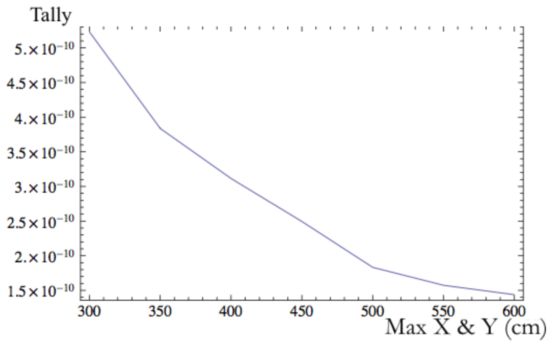

Figure 6.23: Dose on the ORNL phantom as a function of the XY reflective wall positions

skin covering the legs versus other skin. To calculate the volume of the skin covering the legs I used a simple monte carlo approximation of the volume. I created a small program that modeled the space around the skin covering the legs. This program picked random points and calculated if they were in the skin or not. Then I used a ratio of hits-to-misses and compared it to the ratio of volume in the space to volume of the skin. The result converged quickly and resulted in about 40% of the total skin volume being assigned to the leg skin.

The second important change from the original ORNL geometry is the addition of reflective walls. This will increase the percentage of particles that hit the phantom. Figure 6.23 shows how the dose is effected for a lead shield as the XY position of the reflective walls is increased.

As we would expect the dose goes down as the total area of the simulation goes up, since fewer reflected particles collide with the phantom. While this effect is important, it should not effect the overall MGGA or GA results, since the simulation is simply modeling a world with many shielded people in a grid.

6.4.4 Defining a Fitness Function

The layered ORNL phantom shield fitness function will try to meet a mass goal and then reduce the dose. The mass goal will be the mass of $0.5mm$ of lead in the shield area. This is a standard shield material, so we are basically trying to weigh less than a standard shield and then try to beat it on dose. The fitness of each shield will be determined as follows:

1. Calculate the mass of the shield made of lead, $m(S)$
2. Calculate the mass of the shield based on the MCNP output file volume information, $m(s)$
3. Calculate the dose with the shield, $D(s)$ by summing up all of the weighted tallies from the MCNP output
4. Compare the mass with the shield to the mass of the lead shield
   - If the shield is heavier than the lead shield, the fitness is $-(m(s)/m(S))$
   - Otherwise the fitness is $1 - D(s)$

In other words, the fitness of shield s is

$$F(s) = \begin{cases} 1 - D(s) & \text{if } m(s) < m(S) \\ -\frac{m(s)}{m(S)} & \text{otherwise} \end{cases} \tag{6.3}$$

6.4.5 Defining the Genetic Algorithm

Using this fitness function I ran several simulations for GA and MGGA. The final geometry had a total of 2 helmet layers on the side, 2 helmet layers on the top, and 32 torso layers. There are seven possible materials, listed in Table 6.2, in each layer. The total number of possible shields is therefore, $7^{36} = 2.65 \times 10^{30}$, where 7 is the number of materials and their are $32 + 2 + 2$ volumes to fill in.

The GA runs had 20 generations of 1000 individuals. The MGGA was run with the following phases:

- 8 layers - 500 individuals per generation with 15 generations
- 16 layers - 500 individuals per generation with 15 generations
- 32 layers - 500 individuals per generation with 15 generations

To move between phases, each layer was cut into two pieces. From a shielding standpoint the shields were identical as they move between phases. All of the runs used two helmet layers for all phases.

All GA was performed using tournament selection with a tournament size of 5. There was a 25% chance that the worst individual in a tournament will win to help preserve diversity. Reproduction relied on uniform crossover 70% of the time, mutation 20% of the time and copying 10% of the time. Uniform selection allowed each child to use the materials for any layer from either parent, however, I created two children for each uniform crossover reproduction, as discussed previously.

6.4.6 MGGA and GA Results

I ran several MGGA simulations, two each for 50 kev, 75 kev and 100 kev. The best results are listed in 6.8. The 75 kev run is reminiscent of the results from the simple geometry in 6.3. Looking at the three best shields, pictured in 6.24, keep in mind that the source is on the right, and the phantom on the left. The helmet is not pictured here, but contained very little material in all 3 cases. The helmet is discussed in detail in Section 6.4.7.

At 50 kev we see the expected low-Z/high-Z organization with bismuth near the torso and tin or antimony closer to the source. The 75 kev shield uses more high-Z material, tungsten in particular, compared to the lower energy shield. We saw this same behavior in the simple geometry. The 100 kev shield piles on even more high-Z material, including lead, but still beats the lead mass, by using bismuth as a lighter

Table 6.8: Summary of results with the ORNL phantom at 50 kev, 75 kev and 100 kev with GA and MGGA

Energy	Shield Thickness	Dose Reduction Percentage	Lead Thickness	Algorithm
50 keV	1 mm	11.368	0.5 mm	MGGA
50 keV	1 mm	10.98	0.5 mm	GA
75 keV	1 mm	66.894	0.5 mm	MGGA
75 keV	1 mm	65.4	0.5 mm	GA
100 keV	1 mm	27.622	0.5 mm	MGGA
100 keV	1 mm	22.65	0.5 mm	GA

alternative. The 100 kev shield only saves 0.097 percent in mass, so the MGGA is doing a great job of balancing mass versus dose to get a 27% dose reduction. Some of this savings is coming from the helmet.

6.4.7 The Helmet

The ORNL phantom includes a two layer helmet in two pieces. There is a cylindrical section around the head with a cutout for the face, and a round top, as pictured as Figure 6.25. If designed by a person, the helmet would probably contain material on the sides and the top. But, since the top should receive little, if any radiation, the GA should remove the top. This is almost exactly what happened. The 50 kev solution used a single layer of lead on the sides of the helmet and a single layer of tin on the top. The 75 kev solution used a single layer of antimony on the side and had no top. The 100 kev solution used a single layer of lead on the side, and had no top.

By removing the top, GA was able to save mass that could be used to shield the torso. The volume for the top of the helmet is approximately 65 cm^3, the volume of the sides of the helmet is approximately 88 cm^3 and the volume of the torso shield

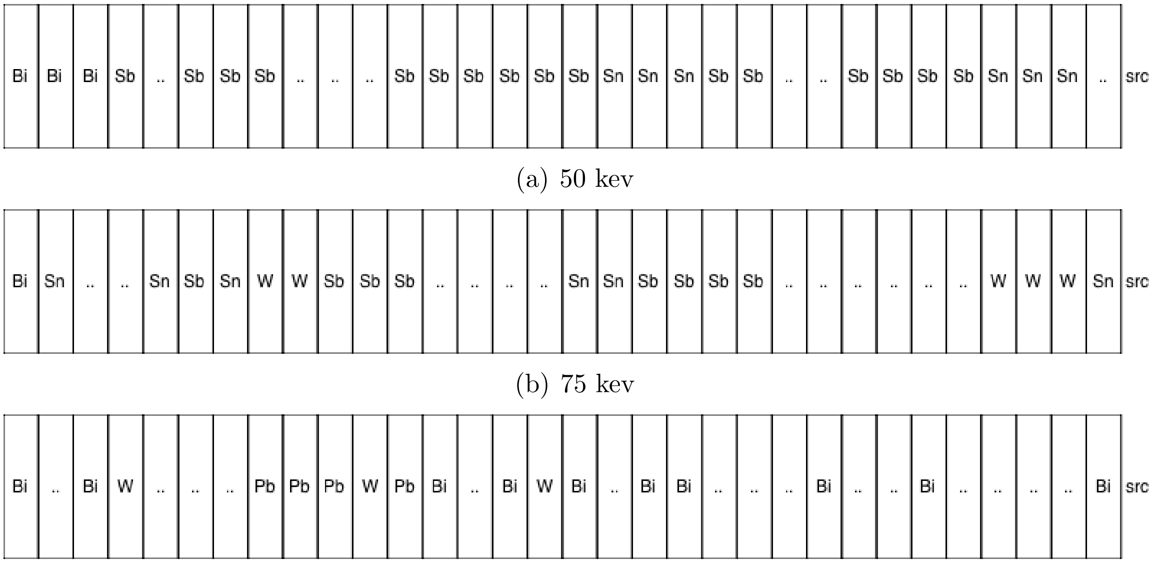
Bi Bi Bi Sb .. Sb Sb Sb .. .. .. Sb Sb Sb Sb Sb Sb Sn Sn Sn Sb Sb .. .. Sb Sb Sb Sb Sn Sn Sn .. src
Bi Sn .. .. Sn Sb Sn W W Sb Sb Sb .. .. Sn Sn Sb Sb Sb Sb .. .. W W W Sn src
Bi .. Bi W .. .. .. Pb Pb Pb W Pb Bi .. Bi W Bi .. Bi Bi .. .. .. Bi .. .. Bi .. .. Bi src

(a) 50 kev

(b) 75 kev

(c) 100 kev

Figure 6.24: The best gamma shields for ORNL with MGGA

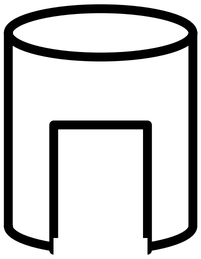

Figure 6.25: The helmet (without a top) for the ORNL phantom

is slightly over 800 cm^3. Keeping in mind that the lead used for comparison is one half of the thickness as the shield GA designed, including on the helmet, the GA was able to save at most 371 and 501 gm on the top and sides of the helmet respectively, compared to a mass for the torso shield of about 4,536 gm. This means that the GA can use almost 10 percent more mass to shield the torso by removing the top of the helmet.

6.4.8 Comparing GA and MGGA for the ORNL Phantom

Looking at the results at 100 kev and comparing them to the results from the simple geometry in Table 6.3 we see that MGGA is doing better than GA for this more complex geometry. While GA beat MGGA in the simple geometry, MGGA is winning on the more complex problem. In fact, MGGA was able to reduce the dose to 7.38×10^{-10} while GA had a dose of 8.011×10^{-10}. This is in comparison to a lead shield dose of 1.035×10^{-9}. While the two best shields may be within the uncertainty of MCNP, MGGA used approximately 6,122 minutes running MCNP to arrive at this answer while GA used approximately 7,377 minutes running MCNP. This means that MGGA used only 83% as much computing time as GA while achieving somewhat better shield designs in each case.

Comparing the two best shields visually, from Figure 6.26, they are quite similar. GA has a single layer of low-Z material that may be adding just enough to the dose for it to lose to MGGA.

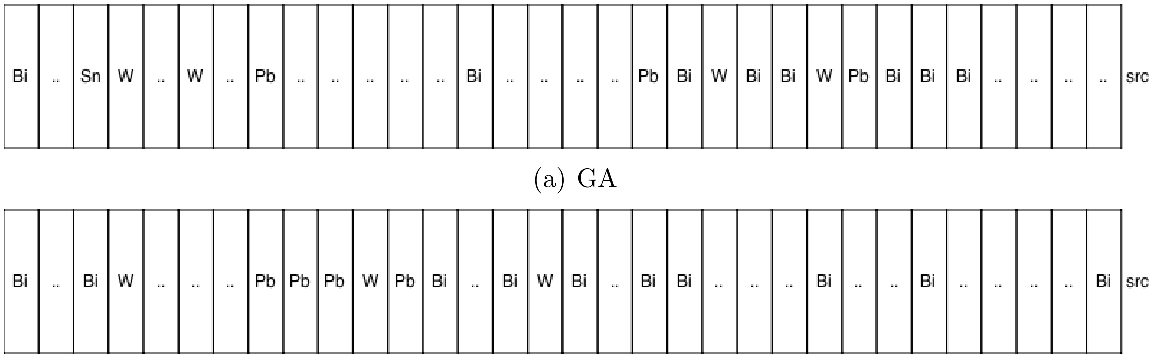

(a) GA

(b) MGGA

Figure 6.26: A comparison of MGGA and GA gamma shields for the ORNL phantom at 100 kev

6.5 The ORNL Phantom at High-Energy

Prior to looking at low energy gamma shielding, I did a fairly extensive look at high energy gamma shielding, [Asbury & Holloway (2011)]. This exploration started with a simple geometry, moved to a minimal human phantom and ended with running MGGA and GA on the ORNL phantom with greater than $1MeV$ photons. The fitness function for these simulations was different than the one used in this chapter. It set a dose goal based on a heavy shield and then tried to reduce mass once the goal was met.

The results from these simulations were not interesting. Essentially GA and MGGA used high-Z materials to lower the dose, and then would remove what they could to reduce mass. The shields were generally tungsten or lead, leading to the conclusion that while GA and MGGA are a useful tool at low energies where optimally layering can do better than lead, they are less useful at higher energies where pair-production and Compton scattering dominate the photon shield interactions.

6.6 Conclusions

I performed several MGGA and GA runs with both a simple geometry and a human-like phantom. Simulations at low energies showed that there is value in creating layered shields, while simulations at higher energies showed little value for layering. As we would hope, MGGA and GA are able to create good shields for gamma radiation as they did for the shadow shield. Moreover, MGGA and GA perform well with a complex geometry. Both algorithms were able to create shields in a complex geometry that were similar to shields in a simple geometry.

These results are a good indicator that GA and MGGA can work on this type of problem, despite the severe resource constraints we were working under. MGGA struggled with high energy gamma problems, where there may not be a good solution, but it was able to do a great job on a very complex geometry using the ORNL phantom. While GA beat MGGA on a simple geometry, MGGA surpassed GA as the problem space grew. Moreover, MGGA saved more than 10 percent of the computing resources used by GA. MGGA is able to provide good ideas for shield designs.

In the next chapter I will discuss how MGGA performs when designing a gamma radiation filter.

CHAPTER VII

Designing A Filter

7.1 Introduction

When doing imaging during radiotherapy a cone beam tomography system is sometimes used. This system uses an x-ray source that emits a cone of x-rays towards and through a patient, and then images the x-rays on a detector plane below the patient. These detector plates are solid state devices that have a limited dynamic range and which can saturate when exposed to too high a radiation fluence. Because the patient is generally thick in the middle, and thin at the edge, a sufficient fluence to image the center of the patient often results in saturation and poor imaging at the edge of the patient.

Figure 7.1 shows the total flux of x-rays from a 120 keV source falling on an image plane after passing through a 15cm radius water phantom. Note the high flux near the edge of the image, where, if sufficient flux is used to image the center, the detector can be expected to saturate. In addition, the edge of the phantom results in scattered radiation falling in the center of the image plane, and the resulting higher scattered to total radiation near the center also contributes to a poorer image there, as shown in Figure 7.2 [Kanamori *et al.* (1985)].

In order to minimize these effects a bow-tie filter is often used [Mail *et al.* (2009)]. Such a filter is an x-ray absorber that is usually shaped like a bowtie, see Figure 7.3.

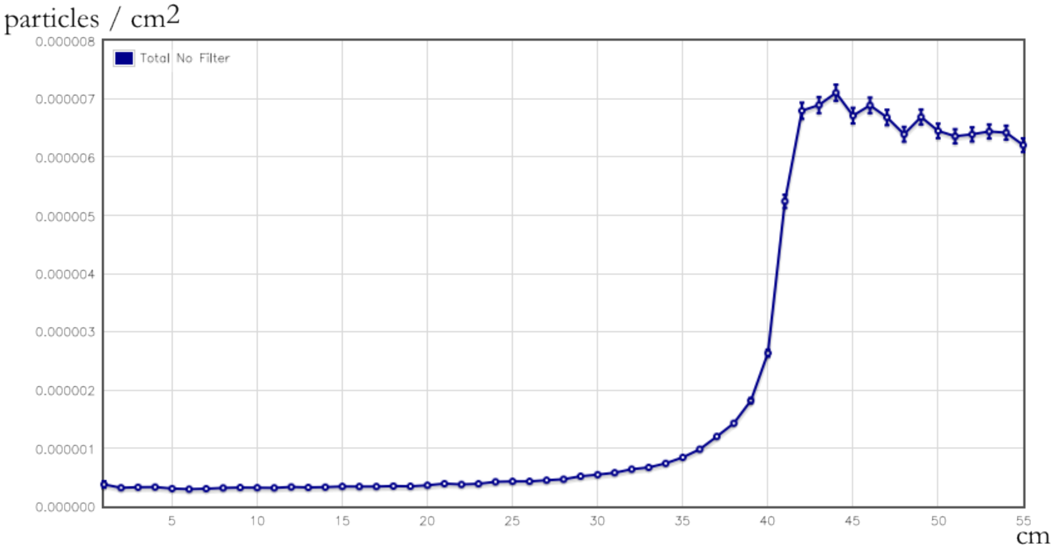

Figure 7.1: The total flux vs. detector radius at 120 kev

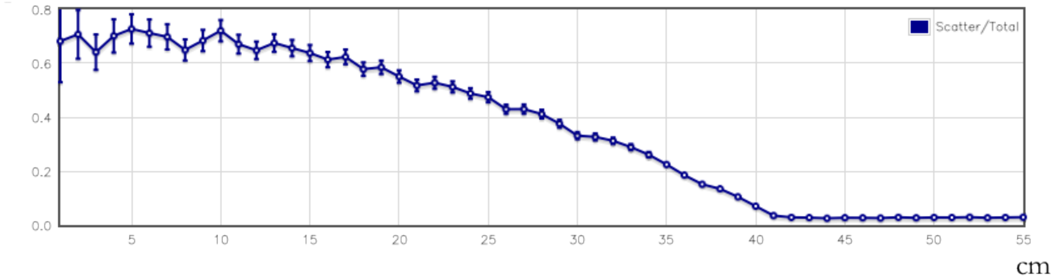

Figure 7.2: The scatter/total fluence ratio vs. detector radius at 120 kev

Essentially, the goal of these filters is to reduce the fluence at the edge of the phantom, where high flux is not needed for imaging. This also reduces the relative amount of scattered radiation in the center of the image, because excess scattering at the edge is reduced.

In this section we will explore the optimal design of such a filter by seeking a filter design that makes the ratio of the scattered to the total flux nearly constant [Kwan *et al.* (2005)]. In fact, we will maximize

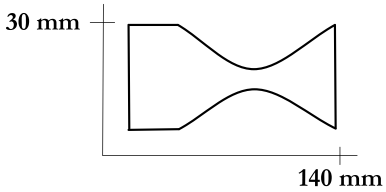

Figure 7.3: Representative bowtie filter cross-section

$$F(s) = 1 - \frac{1}{\Delta r} \int \left(\frac{\phi_s(r)}{\phi_t(r)} - \left\langle \frac{\phi_s}{\phi_t} \right\rangle \right)^2 dr \tag{7.1}$$

where Δr is the detector ring size, ϕ_s is the fluence of scattered particles and ϕ_t is the total fluence at a detector. This is 1 minus the variance of the scattered to total flux ratio. This quantity will approach 1 as the scattered to total flux ratio becomes constant (and this will occur only if the scattered to unscattered flux ratio becomes constant). However, this objective function will also prevent the total flux from becoming zero, which is important: if we allow the total flux to become small then the optimal solution will simply be a filter that blocks all radiation.

In this chapter we will explore GA and MGGA as a method to design a filter to maximize this objective function.

7.2 The Problem Setup

Consider a cylindrical space, pictured in Figure 7.4, with a vertical axis along the Z direction. This graphic shows a source at the top, a small filter space split into grid sections, a large spherical phantom, and a target plane. The target plane is split into cells that are associated with MCNP tallies. We can think of these tallies as the detectors for a radiography system.

The phantom represents a target which the radiation is being used to image. It is split into vertical sections which are used for variance reduction by increasing the particle importance at each boundary. The problem is symmetric around the axis, so

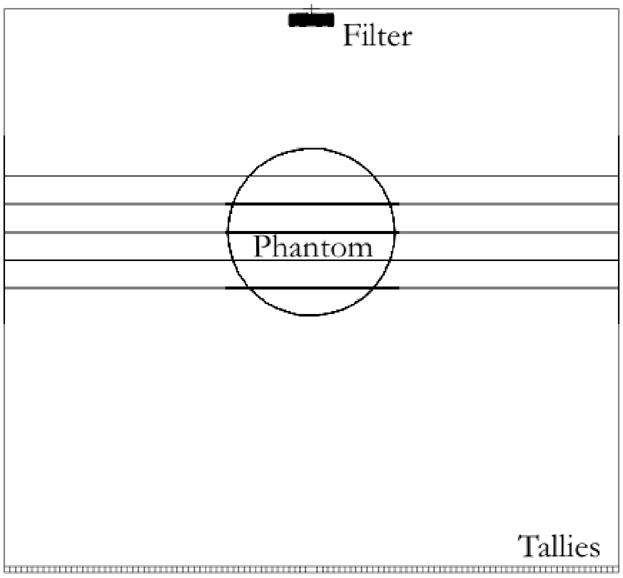

Figure 7.4: Geometry for a bowtie filter with a spherical phantom

all filters will be symmetric.

The source is a disk 1 mm in diameter. The source will generate mono-energetic photons. Results for the two energies of 120 kev, [Kanamori *et al.* (1985)], and 160 kev are discussed below. Photons that leave the space are forgotten. The filter is 4 cm in radius, placed 1 cm from the source, with a maximum potential thickness of 2 cm. The detectors are at 100 cm from the source, and extend out to 55 cm from the axis. Each detector is 1 cm of radial extent, 1 cm thick, contains vacuum and uses an F4 flux average tally. The spherical phantom is 15 cm in radius, and is centered at 40 cm.

It is worth noting that the detectors are not all the same surface area. The outer targets have a bigger surface area than the inner detectors. However, the flux averaging performed by the MCNP F4 tally accounts for this by computing a volume averaged fluence per source particle. The detectors are configured to tally two different energy bins. One energy bin is set to capture everything less than 99 percent of the source energy. The second bin is set to capture everything from 99 percent to 100 percent of the source energy. Using these two bins we can determine scattered, primary and total fluence at each detector.

Our goal, from Equation 7.1 and expressed in the following fitness algorithm, will be to minimize the variance of the scattered fluence to total fluence ratio across the detector plan. This goal, loosely taken from [Mail *et al.* (2009)], will reduce the dose to the patient by minimizing the impact of scattered (noisy) photons.

1. Determine the total flux for each detector using the MCNP tally
2. Determine the scattered flux at each detector, using the energy bin related to all energies less than 99 percent of the source energy
3. If there is no flux at a detector, give the filter a fitness score of 1 minus 1000 times the number of detectors with no flux
4. Calculate the scatter to total ratio at each detector, and include it in a variance calculation
5. Score the filter as one minus the variance squared, better filters approach a score of 1 from below

In other words, the fitness of shield s is

$$F(s) = \begin{cases} 1 - 1000 \times \text{count of zero tallies} & \text{if any tallies are zero} \\ 1 - \frac{1}{N}\sum_{i=0}^{N}\left(\frac{\phi_s(i)}{\phi_t(i)} - \langle\frac{\phi_s}{\phi_t}\rangle\right)^2 & \text{otherwise} \end{cases} \tag{7.2}$$

I performed several GA simulations with this fitness function with the filter split into 16 layers and 16 bands, for a total of 256 elements. Each GA run had a population of 1125 individuals, and executed for 20 generations. A total of $22,500$ individuals are tested for each GA run. The MGGA used three phases:

- 4×4 - 500 individuals per generation with 15 generations
- 8×8 - 500 individuals per generation with 15 generations

- 16 × 16 - 500 individuals per generation with 15 generations

This results in a total of 22,500 individuals tested for each MGGA run. Thus the MGGA and GA have an equal number of individuals to try.

To move between phases for MGGA, each cell was cut into four equal pieces. From a shielding standpoint the shields were identical as they move between phases. The encoding for each shield was a string of integers, one for each cell.

All GA was performed using tournament selection with a tournament size of 5. There was a 25% chance that the worst individual in a tournament would win to help preserve diversity. Reproduction relied on uniform crossover 70% of the time, mutation of a single layer 20% of the time and copying 10% of the time. Uniform crossover allowed each child to use the materials for any layer from either parent, however, I created two children for each crossover reproduction, these two children were the result of reversing the coin flip for each gene in uniform crossover.

7.3 Results at 120kev

Normally bowtie filters are milled from a single material. I did one MGGA run with vacuum and aluminum as the only choices for each cell in the filter. This MGGA run designed the filter pictured in Figure 7.5 with a fitness of 0.981.

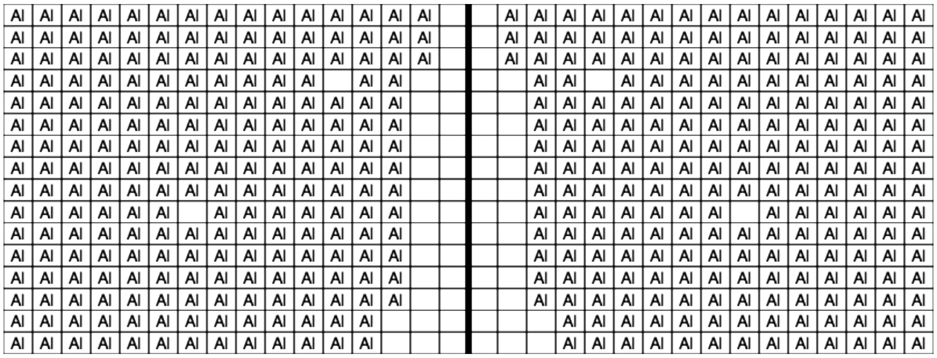

Al	Al	Al	Al	Al	Al	Al	Al	Al	Al	Al	Al	Al	Al	Al			Al	Al	Al	Al	Al	Al	Al	Al	Al	Al	Al	Al	Al	Al	Al
Al	Al	Al	Al	Al	Al	Al	Al	Al	Al	Al	Al	Al	Al	Al			Al	Al	Al	Al	Al	Al	Al	Al	Al	Al	Al	Al	Al	Al	Al
Al	Al	Al	Al	Al	Al	Al	Al	Al	Al	Al	Al	Al	Al	Al			Al	Al	Al	Al	Al	Al	Al	Al	Al	Al	Al	Al	Al	Al	Al
Al	Al	Al	Al	Al	Al	Al	Al	Al	Al	Al		Al	Al					Al	Al		Al	Al	Al	Al	Al	Al	Al	Al	Al	Al	Al
Al	Al	Al	Al	Al	Al	Al	Al	Al	Al	Al	Al	Al	Al					Al	Al	Al	Al	Al	Al	Al	Al	Al	Al	Al	Al	Al	Al
Al	Al	Al	Al	Al	Al	Al	Al	Al	Al	Al	Al	Al	Al					Al	Al	Al	Al	Al	Al	Al	Al	Al	Al	Al	Al	Al	Al
Al	Al	Al	Al	Al	Al	Al	Al	Al	Al	Al	Al	Al	Al					Al	Al	Al	Al	Al	Al	Al	Al	Al	Al	Al	Al	Al	Al
Al	Al	Al	Al	Al	Al	Al	Al	Al	Al	Al	Al	Al	Al					Al	Al	Al	Al	Al	Al	Al	Al	Al	Al	Al	Al	Al	Al
Al	Al	Al	Al	Al	Al	Al	Al	Al	Al	Al	Al	Al	Al					Al	Al	Al	Al	Al	Al	Al	Al	Al	Al	Al	Al	Al	Al
Al	Al	Al	Al	Al	Al		Al	Al	Al	Al	Al	Al	Al					Al	Al	Al	Al	Al	Al	Al		Al	Al	Al	Al	Al	Al
Al	Al	Al	Al	Al	Al	Al	Al	Al	Al	Al	Al	Al	Al					Al	Al	Al	Al	Al	Al	Al	Al	Al	Al	Al	Al	Al	Al
Al	Al	Al	Al	Al	Al	Al	Al	Al	Al	Al	Al	Al	Al					Al	Al	Al	Al	Al	Al	Al	Al	Al	Al	Al	Al	Al	Al
Al	Al	Al	Al	Al	Al	Al	Al	Al	Al	Al	Al	Al	Al					Al	Al	Al	Al	Al	Al	Al	Al	Al	Al	Al	Al	Al	Al
Al	Al	Al	Al	Al	Al	Al	Al	Al	Al	Al	Al	Al	Al					Al	Al	Al	Al	Al	Al	Al	Al	Al	Al	Al	Al	Al	Al
Al	Al	Al	Al	Al	Al	Al	Al	Al	Al	Al	Al	Al							Al	Al	Al	Al	Al	Al	Al	Al	Al	Al	Al	Al	Al
Al	Al	Al	Al	Al	Al	Al	Al	Al	Al	Al	Al	Al							Al	Al	Al	Al	Al	Al	Al	Al	Al	Al	Al	Al	Al

Figure 7.5: The best aluminum MGGA filter at 120kev (source at the top) - 0.981

Figure 7.6 shows the scatter-to-total fluence ratio against the detector radius of both this best filter and when no filter is present. From this graph we can see that MGGA built a filter that does a good job of flattening the scatter-to-total ratio.

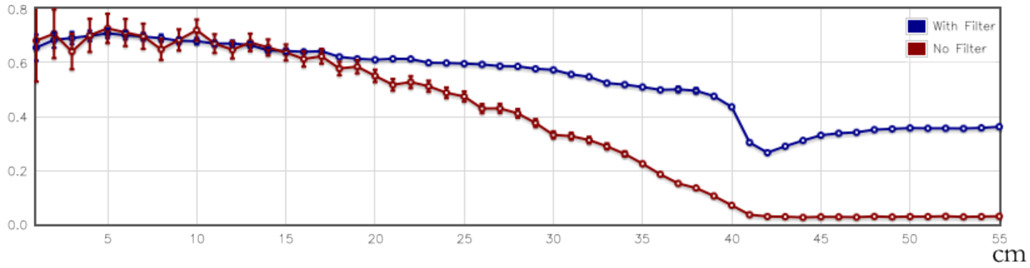

Figure 7.6: The scatter-to-total fluence ratio for the aluminum MGGA filter at 120kev

This is a great result. But can GA do better if it can take advantage of more materials, with K-edges located at different energies, as it did in the previous chapter? Figure 7.7 shows the cross sections for titanium and aluminum. These two materials are reasonable for making a filter, and provide some interesting overlaps in their cross section values. I did several runs of both GA and MGGA using these new choices. Each cell could be vacuum, titanium or aluminum, resulting in a total search space of 3^{256} or 1.39×10^{122} possible filters.

The GA and MGGA runs at 120kev produced the results listed in Table 7.1. In all cases, the MGGA beat GA. Moreover, MGGA produces an arguably simpler filter, due to the way MGGA builds from a coarse grid to a finer one. This can be seen if we look at the best MGGA filter, pictured in Figure 7.8, and the best GA filter, pictured in Figure 7.9. Note, the symmetry of these filters is caused by the geometry, not the Genetic Algorithm.

Both filters have a similar macroscopic structure. Both have little material down the axis, surrounded by a core of titanium. The cells along a diagonal from the top inner radius to the bottom corner have either aluminum or sparse titanium. The MGGA result shows an empty block about half way out in radius, while the GA filter

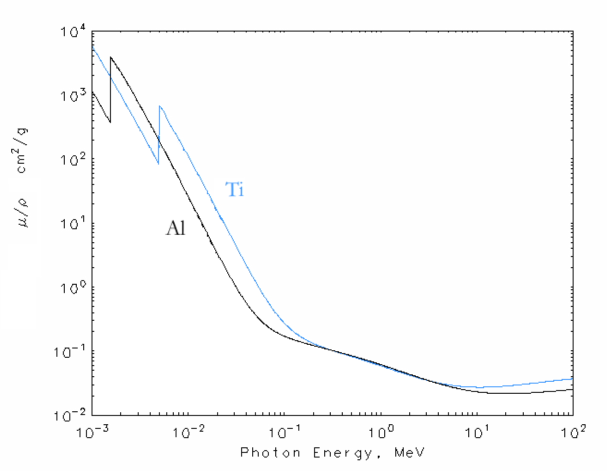

Figure 7.7: γ radiation cross-sections for Titanium (gray) & Aluminum (black), [National Institute of Standards and Technology (2011)]

Run	MGGA	GA
Run 1	0.99776	0.99641
Run 2	0.99754	0.99652
Run 3	0.99742	0.99640

Table 7.1: Results for GA and MGGA on the bowtie filter problem at 120kev

Al	Al	Al	Al	Al	Al	Al	Al	Al	Al	Al	Al	Ti	Ti	Ti			Ti	Ti	Ti	Al	Al	Al	Al	Al	Al	Al	Al	Al	Al	Al	Al
Al	Al	Al	Al	Al	Al	Al	Al	Al	Al	Al	Al	Ti	Ti	Ti			Ti	Ti	Ti	Al	Al	Al	Al	Al	Al	Al	Al	Al	Al	Al	Al
Al	Al	Al	Al	Al	Al	Al	Al	Al	Al	Al	Al	Ti	Ti					Ti	Ti	Al	Al	Al	Al	Al	Al	Al	Al	Al	Al	Al	Al
Al	Al	Al	Al	Al	Al	Al	Al	Al	Al	Al	Al	Ti	Ti					Ti	Ti	Al	Al	Al	Al	Al	Al	Al	Al	Al	Al	Al	Al
Al	Al	Al	Al	Al	Al	Al	Al	Al	Al	Al	Al	Ti	Ti					Ti	Ti	Al	Al	Al	Al	Al	Al	Al	Al	Al	Al	Al	Al
Al	Al	Al	Al	Al	Al	Al	Al	Al	Al	Al	Al	Ti	Ti					Ti	Ti	Al	Al	Al	Al	Al	Al	Al	Al	Al	Al	Al	Al
Al	Al	Al	Al	Al	Al	Al	Al	Al	Al	Al	Ti	Ti	Ti					Ti	Ti	Ti	Al	Al	Al	Al	Al	Al	Al	Al	Al	Al	Al
Al	Al	Al	Al	Al	Al	Al	Al	Al	Al	Al	Ti	Ti	Ti	Al			Al	Ti	Ti	Ti	Al	Al	Al	Al	Al	Al	Al	Al	Al	Al	Al
Al	Al	Al	Al	Al	Al	Al	Al		Ti	Ti	Ti	Ti	Ti					Ti	Ti	Ti	Ti	Ti		Al	Al	Al	Al	Al	Al	Al	Al
Al	Al	Al	Al	Al	Al	Al	Al	Ti		Ti	Ti	Ti	Al					Al	Ti	Ti	Ti		Ti	Al	Al	Al	Al	Al	Al	Al	Al
Al	Al	Al	Al	Al	Al	Al	Al	Al	Al	Ti	Ti	Ti	Ti					Ti	Ti	Ti	Ti	Al	Al	Al	Al	Al	Al	Al	Al	Al	Al
Al	Al	Al	Al	Al	Al	Al	Al	Al	Al	Ti	Ti	Ti	Ti					Ti	Ti	Ti	Ti	Al	Al	Al	Al	Al	Al	Al	Al	Al	Al
Al	Al	Al	Al						Ti	Ti	Ti	Ti	Ti					Ti	Ti	Ti	Ti	Ti						Al	Al	Al	Al
Al	Al	Al	Al						Al	Ti	Ti	Al	Ti	Al			Al	Ti	Al	Ti	Ti	Al						Al	Al	Al	Al
Al	Al	Al	Al					Ti	Ti	Ti	Ti								Ti	Ti	Ti	Ti						Al	Al	Al	Al
Al	Al	Al	Al					Ti	Ti	Ti	Ti								Ti	Ti	Ti	Ti						Al	Al	Al	Al

Figure 7.8: The best MGGA filter at 120kev (source at the top) - 0.997

Al	Ti	Al	Ti	Ti	Ti	Ti			Al	Al			Ti	Ti			Ti	Ti			Al	Al			Ti	Ti	Ti	Ti	Al	Ti	Al
Ti	Al	Ti	Al	Ti		Al	Al	Ti	Al	Ti	Al	Al	Ti	Ti			Ti	Ti	Al	Al	Ti	Al	Ti	Al	Al		Ti	Al	Ti	Al	Ti
Ti	Al		Ti	Ti	Ti	Al	Ti	Ti	Al	Al	Al	Al	Ti	Ti			Ti	Ti	Al	Al	Al	Al	Ti	Ti	Al	Ti	Ti	Ti		Al	Ti
Ti		Al	Al	Al		Ti	Ti			Al	Al	Ti	Ti	Al			Al	Ti	Ti	Al	Al			Ti	Ti		Al	Al	Al		Ti
Al	Ti	Al	Al		Al	Ti	Al	Al	Ti			Ti	Ti	Al			Al	Ti	Ti			Ti	Al	Al	Ti	Al		Al	Al	Ti	Al
Ti	Al		Al		Al	Al	Ti	Al		Al	Al	Ti	Ti					Ti	Ti	Al	Al		Al	Ti	Al	Al		Al		Al	Ti
Ti	Al	Al	Ti	Al	Ti	Ti	Ti	Al	Al	Ti	Al	Ti	Ti	Al			Al	Ti	Ti	Al	Ti	Al	Al	Ti	Ti	Ti	Al	Ti	Al	Al	Ti
Ti	Al	Al		Ti	Ti	Ti					Ti	Ti	Ti					Ti	Ti	Ti					Ti	Ti	Ti		Al	Al	Ti
Ti	Al		Al	Ti	Ti	Ti		Ti	Al	Al	Ti	Ti	Al					Al	Ti	Ti	Al	Al	Ti		Ti	Ti	Ti	Al		Al	Ti
Al	Al	Al		Ti	Al	Al		Al	Al	Ti	Ti	Ti	Al	Al			Al	Al	Ti	Ti	Ti	Al	Al		Al	Al	Ti		Al	Al	Al
Al	Al		Al	Ti		Al			Al		Ti	Ti	Ti					Ti	Ti	Ti		Al			Al		Ti	Al		Al	Al
Al		Al		Ti	Ti		Al	Al	Al	Ti	Ti	Ti							Ti	Ti	Ti	Al	Al	Al		Ti	Ti		Al		Al
Al	Al		Al	Ti	Al				Al	Ti	Ti	Ti							Ti	Ti	Ti	Al				Al	Ti	Al		Al	Al
				Ti	Al		Ti		Al	Ti	Ti	Ti	Al					Al	Ti	Ti	Ti	Al		Ti		Al	Ti				
Ti	Al	Ti		Al					Al	Ti	Ti	Al	Al					Al	Al	Ti	Ti	Al					Al		Ti	Al	Ti
		Ti					Al	Al	Ti	Ti	Ti									Ti	Ti	Ti	Al	Al					Ti		

Figure 7.9: The best GA filter at 120kev (source at the top) - 0.996

is sparse in this area. To get a handle on the possible reasons behind these designs, lets look at the scattered-to-total fluence ratio for the best filter from MGGA. This data, along with the same ratio when no filter is present, is pictured in Figure 7.10.

When there is no filter, the scatter-to-total ratio goes down with the detector radius. Geometrically this can be expected. The source is very small and on the axis, while the phantom is in the center, so particles near the axis have a higher chance of scattering in the phantom than particles farther from the axis that pass through less or no phantom. A perfect filter would create a flat line for the scatter-to-total ratio. While the best MGGA doesn't reach this goal, it does do a great job of flattening the scatter-to-total ratio.

The filter has two ways to change the scattered-to-total value at each tally. The

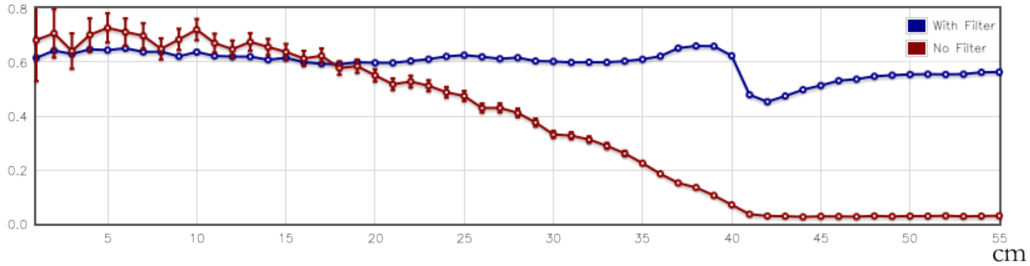

Figure 7.10: The scatter-to-total fluence ratio for the best MGGA filter at 120kev

filter can increase the scattered particles hitting that tally and the filter can reduce the total number of particles hitting that tally. With these two mechanisms in mind, reconsider the graphs in Figure 7.10 and look at Figure 7.11 which shows the total, primary and scatter radiation separated out for both the filtered and non-filtered cases.

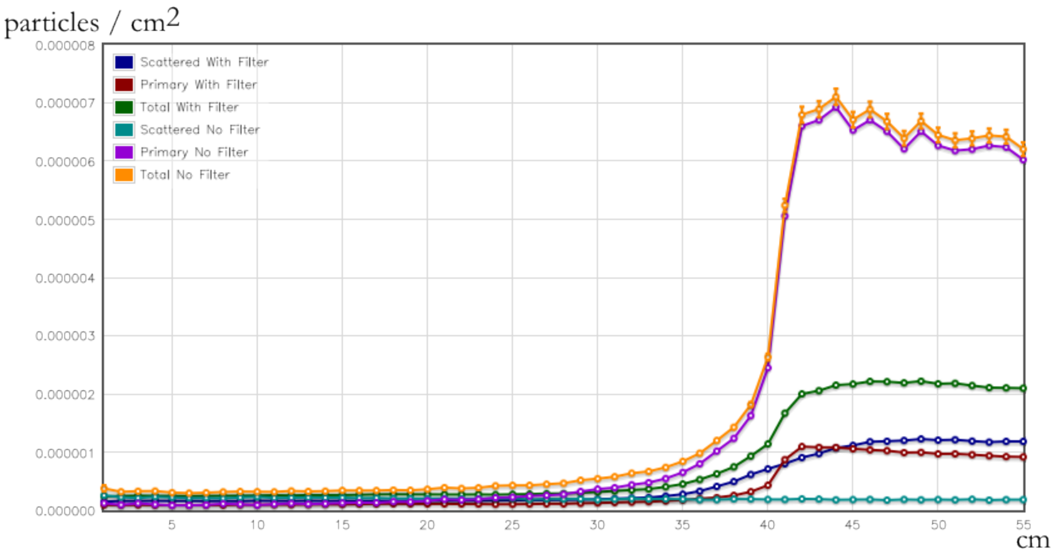

Figure 7.11: The scatter, primary and total tallies with and without the best MGGA filter at 120kev

The filter slightly lowered the scatter-to-total ratio near the axis, and significantly raised the scatter-to-total ratio towards the edge. Looking at the raw data, the filter greatly reduced the total fluence near the edge of the detector plane. The filter also raised the scattered fluence near the edge of the detector plane. Together, these two changes altered the ratio enough to bring it closer to the ratio at the center.

There is an interesting feature of the plot of scatter-to-total ratio that looks a bit like a bump followed by a valley. This feature occurs at the same radius, around 40 cm, as the large change in total fluence in the unfiltered case. This is the image of the edge of the phantom. A ray leaving the source, would hit the phantom tangentially at (13.9054,34.375). Taking this point, and using similar triangles, I determined that the source starts hitting the detector plane directly, without hitting the phantom, at 40.45 centimeters. This radius exactly matches the big drop in scatter-to-total ratio, and leads to a conclusion that the edge of the phantom is causing this bump. The GA filter shows the same type of feature at the same place, as pictured in Figure 7.12.

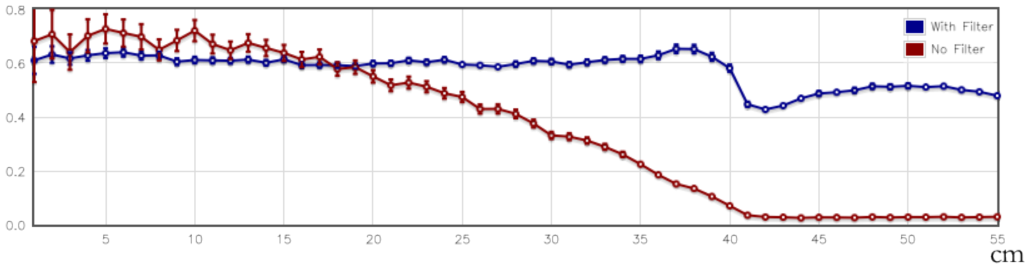

Figure 7.12: The scatter-to-total ratio for the best GA filter at 120kev

Both GA and MGGA were able to beat the pure aluminum filter designed by MGGA using titanium and aluminum. Despite the gigantic nature of the search space, MGGA is constructing interesting well-scoring filters. Moreover, MGGA is using approximately 3,143 minutes to find its best filter compared to approximately 6,183 minutes for GA. MGGA is using almost half of the computing resources as GA to find a better, more manufacturable filter.

Run	MGGA	GA
Run 1	0.99470	0.99366
Run 2	0.99472	0.99365
Run 3	0.99473	0.99357

Table 7.2: Results for GA and MGGA on the bowtie filter problem at 160 kev

7.4 Results at 160 kev

The GA and MGGA runs at 160*kev* produced the results listed in Table 7.2. Again, the MGGA beat the GA. MGGA also produced a simpler filter. This can be seen if we look at the best MGGA filter, pictured in Figure 7.13, and the best GA filter, pictured in Figure 7.14.

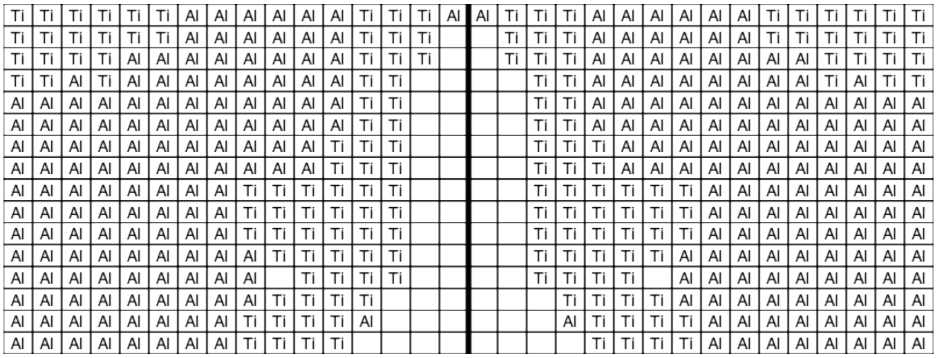

Ti	Ti	Ti	Ti	Ti	Ti	Al	Al	Al	Al	Al	Al	Ti	Ti	Ti	Al	Al	Ti	Ti	Ti	Al	Al	Al	Al	Al	Al	Ti	Ti	Ti	Ti	Ti	Ti
Ti	Ti	Ti	Ti	Ti	Ti	Al	Al	Al	Al	Al	Al	Ti	Ti	Ti			Ti	Ti	Ti	Al	Al	Al	Al	Al	Al	Ti	Ti	Ti	Ti	Ti	Ti
Ti	Ti	Ti	Ti	Al	Al	Al	Al	Al	Al	Al	Al	Ti	Ti	Ti			Ti	Ti	Ti	Al	Al	Al	Al	Al	Al	Al	Al	Ti	Ti	Ti	Ti
Ti	Ti	Al	Ti	Al	Al	Al	Al	Al	Al	Al	Al	Ti	Ti					Ti	Ti	Al	Al	Al	Al	Al	Al	Al	Al	Ti	Al	Ti	Ti
Al	Al	Al	Al	Al	Al	Al	Al	Al	Al	Al	Al	Ti	Ti					Ti	Ti	Al	Al	Al	Al	Al	Al	Al	Al	Al	Al	Al	Al
Al	Al	Al	Al	Al	Al	Al	Al	Al	Al	Al	Al	Ti	Ti					Ti	Ti	Al	Al	Al	Al	Al	Al	Al	Al	Al	Al	Al	Al
Al	Al	Al	Al	Al	Al	Al	Al	Al	Al	Al	Ti	Ti	Ti					Ti	Ti	Ti	Al	Al	Al	Al	Al	Al	Al	Al	Al	Al	Al
Al	Al	Al	Al	Al	Al	Al	Al	Al	Al	Al	Ti	Ti	Ti					Ti	Ti	Ti	Al	Al	Al	Al	Al	Al	Al	Al	Al	Al	Al
Al	Al	Al	Al	Al	Al	Al	Al	Ti	Ti	Ti	Ti	Ti	Ti					Ti	Ti	Ti	Ti	Ti	Ti	Al	Al	Al	Al	Al	Al	Al	Al
Al	Al	Al	Al	Al	Al	Al	Al	Ti	Ti	Ti	Ti	Ti	Ti					Ti	Ti	Ti	Ti	Ti	Ti	Al	Al	Al	Al	Al	Al	Al	Al
Al	Al	Al	Al	Al	Al	Al	Al	Ti	Ti	Ti	Ti	Ti	Ti					Ti	Ti	Ti	Ti	Ti	Ti	Al	Al	Al	Al	Al	Al	Al	Al
Al	Al	Al	Al	Al	Al	Al	Al	Al	Ti	Ti	Ti	Ti	Ti					Ti	Ti	Ti	Ti	Ti	Al	Al	Al	Al	Al	Al	Al	Al	Al
Al	Al	Al	Al	Al	Al	Al	Al	Al		Ti	Ti	Ti	Ti					Ti	Ti	Ti	Ti		Al	Al	Al	Al	Al	Al	Al	Al	Al
Al	Al	Al	Al	Al	Al	Al	Al	Al	Ti	Ti	Ti	Ti							Ti	Ti	Ti	Ti	Al	Al	Al	Al	Al	Al	Al	Al	Al
Al	Al	Al	Al	Al	Al	Al	Al	Ti	Ti	Ti	Ti	Al							Al	Ti	Ti	Ti	Ti	Al	Al	Al	Al	Al	Al	Al	Al
Al	Al	Al	Al	Al	Al	Al	Al	Ti	Ti	Ti	Ti									Ti	Ti	Ti	Ti	Al	Al	Al	Al	Al	Al	Al	Al

Figure 7.13: The best MGGA filter at 160kev (source at the top) - 0.994

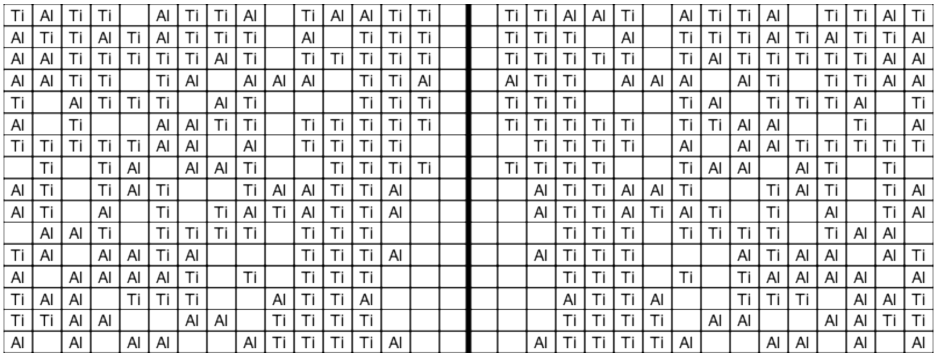

Ti	Al	Ti	Ti		Al	Ti	Ti	Al		Ti	Al	Al	Ti	Ti			Ti	Ti	Al	Al	Ti		Al	Ti	Ti	Al		Ti	Ti	Al	Ti
Al	Ti	Ti	Al	Ti	Al	Ti	Ti	Ti		Al		Ti	Ti	Ti			Ti	Ti	Ti		Al		Ti	Ti	Ti	Al	Ti	Al	Ti	Ti	Al
Al	Al	Ti	Ti	Ti	Ti	Ti	Al	Ti		Ti	Ti	Ti	Ti	Ti			Ti	Ti	Ti	Ti	Ti		Ti	Al	Ti	Ti	Ti	Ti	Ti	Al	Al
Al	Al	Ti	Ti		Ti	Al		Al	Al	Al		Ti	Ti	Al			Al	Ti	Ti		Al	Al	Al		Al	Ti		Ti	Ti	Al	Al
Ti		Al	Ti	Ti	Ti		Al	Ti				Ti	Ti	Ti			Ti	Ti	Ti				Ti	Al		Ti	Ti	Ti	Al		Ti
Al		Ti			Al	Al	Ti	Ti		Ti	Ti	Ti	Ti	Ti			Ti	Ti	Ti	Ti	Ti		Ti	Ti	Al	Al			Ti		Al
Ti	Ti	Ti	Ti	Ti	Al	Al		Al		Ti	Ti	Ti	Ti					Ti	Ti	Ti	Ti		Al		Al	Al	Ti	Ti	Ti	Ti	Ti
	Ti		Ti	Al		Al	Al	Ti			Ti	Ti	Ti	Ti			Ti	Ti	Ti	Ti			Ti	Al	Al		Al	Ti		Ti	
Al	Ti		Ti	Al	Ti			Ti	Al	Al	Ti	Ti	Al					Al	Ti	Ti	Al	Al	Ti			Ti	Al	Ti		Ti	Al
Al	Ti		Al		Ti		Ti	Al	Ti	Al	Ti	Ti	Al					Al	Ti	Ti	Al	Ti	Al	Ti		Ti		Al		Ti	Al
	Al	Al	Ti		Ti	Ti	Ti	Ti		Ti	Ti	Ti							Ti	Ti	Ti		Ti	Ti	Ti	Ti		Ti	Al	Al	
Ti	Al		Al	Al	Ti	Al				Ti	Ti	Ti	Al					Al	Ti	Ti	Ti				Al	Ti	Al	Al		Al	Ti
Al		Al	Al	Al	Al	Ti		Ti		Ti	Ti	Ti							Ti	Ti	Ti		Ti		Ti	Al	Al	Al	Al		Al
Ti	Al	Al		Ti	Ti	Ti			Al	Ti	Ti	Al							Al	Ti	Ti	Al			Ti	Ti	Ti		Al	Al	Ti
Ti	Ti	Al	Al			Al	Al		Ti	Ti	Ti	Ti							Ti	Ti	Ti	Ti		Al	Al			Al	Al	Ti	Ti
Al		Al		Al	Al			Al	Ti	Ti	Ti	Ti	Al					Al	Ti	Ti	Ti	Ti	Al			Al	Al		Al		Al

Figure 7.14: The best GA filter at 160 kev (source at the top) - 0.993

The filters produced for 160*kev* are very similar to the ones produced for 120*kev*.

Looking at the scatter-to-total ratio in Figure 7.15 and Figure 7.17 we can see that the MGGA filter is doing a great job of reducing the variance for this source energy.

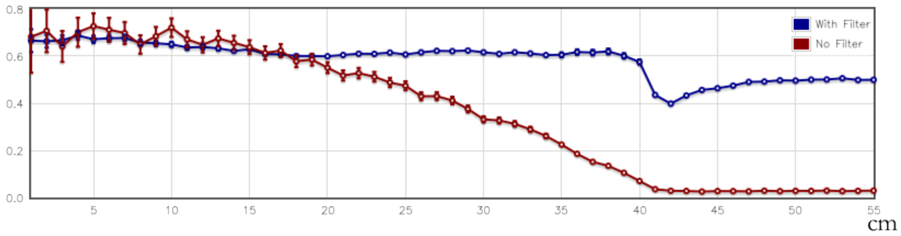

Figure 7.15: The scatter-to-total ratio for the best MGGA filter at 160kev

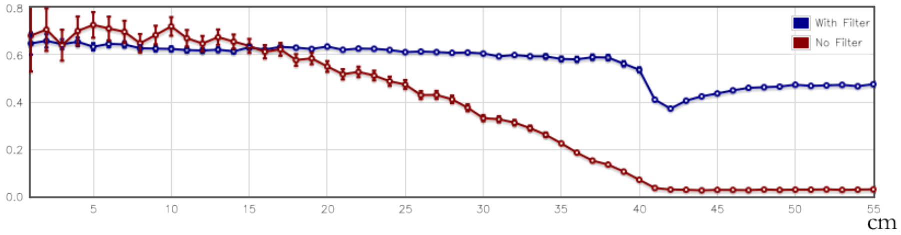

Figure 7.16: The scatter-to-total ratio for the best GA filter at 160kev

Comparing the scatter and total tallies for 160kev, picutred in Figure 7.17, to the same values at 120kev, from Figure 7.11, we see that the filter is trying to accomplish the same changes to the total and scatter radiation to move the ratio toward a straight line.

7.5 Conclusions

I performed two sets of MGGA runs one at 120 kev and one at 160 kev. In each case, MGGA was tasked with designing a bow tie filter that shaped the radiation coming from a source and passing through a water phantom before hitting a detector plane.

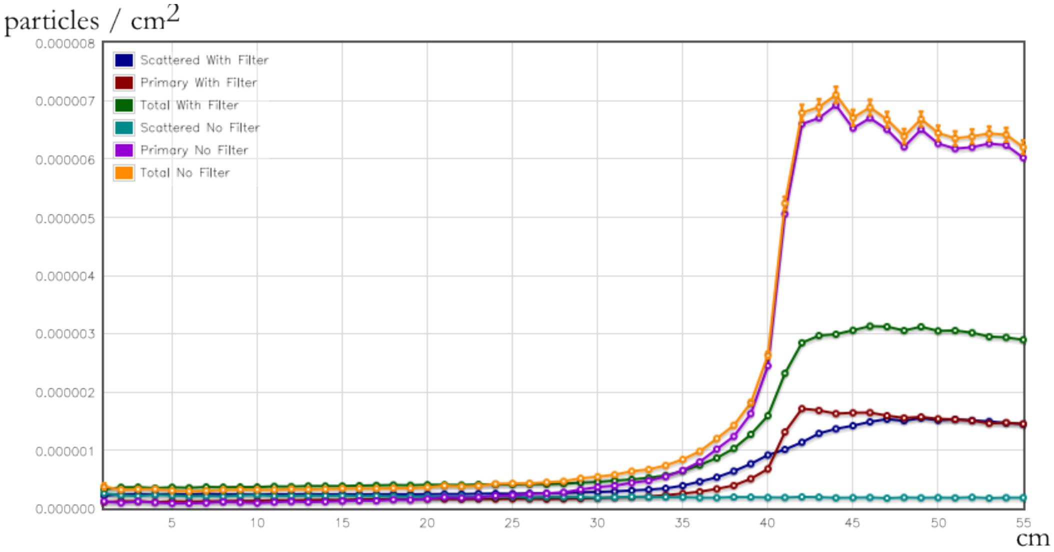

Figure 7.17: The scatter and total tallies for the best MGGA filter at 160kev

Both MGGA and GA produced very good filters for this problem space. Considering that the fitness test for this application was quite different than the others presented in this dissertation, this is a great result. The MGGA was able to balance the need to raise the scattered particles as a ratio of the total, as opposed to just raising or lower a single value. Moreover, MGGA was able to do so with a fairly small number of resources, testing only 22,500 individuals out of a total of 1.39×10^{122} possible filters, and beat GA at the same time. MGGA also beat GA on resources used, making it the clear winner.

The results of this simulation suggest that MGGA would be a useful tool to apply in filtering applications.

CHAPTER VIII

Summary And Conclusions

As I stated in the introduction, shielding is a simple concept. Something bad is moving toward something good and we want to protect the good from the bad. Unfortunately, shielding against radiation is often a problem that involves more than just stopping the bad stuff, we also have to think about mass, cost, secondary radiation effects and other factors.

This dissertation is a study in how a new form of genetic algorithms, called Multi-Grid Genetic Algorithms, can be used to explore the space of possible shields and help engineers design better shields. More importantly, MGGA is about helping engineers find unexpected solutions, solutions that a human may not have considered.

8.1 The Toolbox

The primary tool discussed in this dissertation are genetic algorithms. Chapter II discussed what genetic algorithms are, and provides a basic idea of how they solve problems. Using GA required configuring numerous parameters and defining fitness functions. The goal of a Genetic Algorithm is ultimately to find a solution that has the best score from the fitness function. One disadvantage of genetic algorithms is that they want to run the fitness function numerous times. The fitness functions in this dissertation all involved performing a radiation transport simulation with a code like MCNP. These codes can take minutes, hours or even days to run. As a result, the fitness function becomes a time constraint.

To help address this time constraint I pursued several avenues of research. First, I created a genetic algorithm library that would allow me to scavenge time on a computing cluster. Over the course of my research I moved through several cluster implementations, each move altering the optimal implementation for the genetic algorithm code. I began with a very modular implementation that broke the problem into a series of jobs that could be farmed out onto the cluster. The GA code saved the state for each job in a way that allowed the entire process to be restarted, from the last un-scored generation, on error. This very modular implementation was able to evolve into a much simpler single job model that leveraged *MPI* for MCNP on a set of reserved nodes in the cluster.

The second way I optimized resources was by optimizing the scoring process. The GA library uses caching to minimize retesting of the same individuals. This caching takes two forms, remembering scores of individuals that are copied forward and looking for identical individuals so they only have to be scored one time. The library also included an implementation of pre-calculation which allowed me to avoid scoring individuals that were never selected for the next generation. Unfortunately, while novel, pre-calculation turned out to add more complexity than value to the code.

Finally, I created a new form of genetic algorithm called *Multi-Grid Genetic Algorithms* which leverages geometric considerations to move the algorithm to a good solution more quickly, using fewer calls to the fitness function. MGGA was described in Chapter III and used for each problem I described in this dissertation. MGGA beat GA in almost every scenario I ran, and always used fewer computing resources, showing that it is a strong addition to the optimization toolkit.

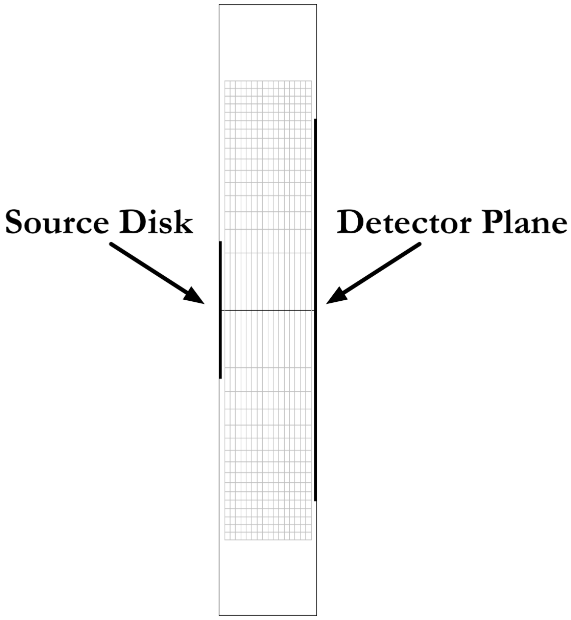

Figure 8.1: Geometry of a shadow shield problem

8.2 The Scenarios

Take, for example, the challenge of building a shadow shield for a space mission powered by a nuclear reactor, see Figure 8.1. The reactor will be generating neutrons that could easily damage sensitive equipment in the payload. Whatever the shield is made from will have to be launched into space, a process that is dependent on mass and can be very expensive. On the good side, the shield can be leaky, in that sense that it doesn't have to surround the reactor. It only needs to protect the payload. Despite having a simple geometry the solution to this problem must balance shielding quality versus mass, cost and other factors.

In Chapter V I discussed how Genetic Algorithms were able to provide insight into new ways to design a shadow shield that leveraged scatter to create a light and efficient shield. These insights included the concept of splitting the shield, replicating the results of [Alpay & Holloway (2005)], but also showed that the split shield can contain more intricate design elements to open up even more radiation stream paths as seen in Figure 8.2.

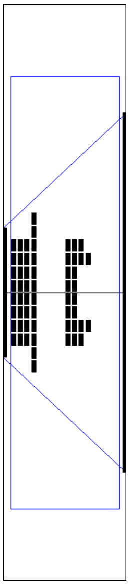

Figure 8.2: MGGA built shadow shield

A completely different shielding problem is the design of a shield for radiation workers and first responders, like the one modeled in Figure 8.3. In this application the shield should be *wearable* or at least movable. Moreover, it should focus on shielding against the primary dangers, generally gamma radiation, a first responder will encounter.

In Chapter VI I used MGGA to explore the possibility of protecting a person from γ-rays. At lower energies, under 150 kev, where the the differing atomic physics of different elements comes into play, MGGA was able to design a novel layered shield that beat a lead shield on dose by over 66% while keeping the same mass, see Figure 8.4. This suggests that new, more effective, shields can be designed using lighter materials, perhaps in a slightly thicker, but not higher weight, format. As with the shadow shield, MGGA is providing possible insights into shield designs that may not have been previously explored.

The final problem I looked at involved the concept of a *bowtie filter*. These filters are used in CT scanners and other devices to control the intensity of radiation incident on the detector plane. This problem doesn't suffer from mass restrictions but does

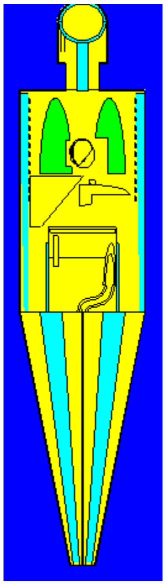

Figure 8.3: Advanced phantom for a radiation worker

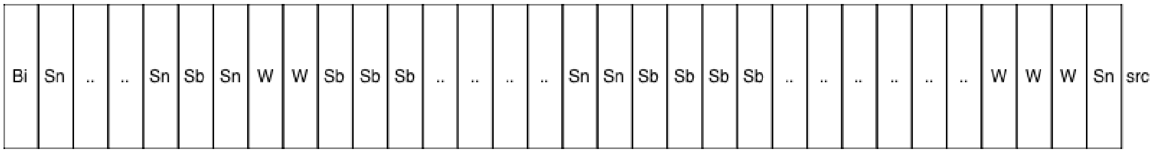

Figure 8.4: MGGA designed shield For 75KeV gamma rays

present a different type of challenge. Rather than trying to shield the target from all radiation, we are trying to shape the incident radiation.

Al	Al	Al	Al	Al	Al	Al	Al	Al	Al	Al	Al	Ti	Ti	Ti			Ti	Ti	Ti	Al	Al	Al	Al	Al	Al	Al	Al	Al	Al	Al	Al
Al	Al	Al	Al	Al	Al	Al	Al	Al	Al	Al	Al	Ti	Ti	Ti			Ti	Ti	Ti	Al	Al	Al	Al	Al	Al	Al	Al	Al	Al	Al	Al
Al	Al	Al	Al	Al	Al	Al	Al	Al	Al	Al	Al	Ti	Ti					Ti	Ti	Al	Al	Al	Al	Al	Al	Al	Al	Al	Al	Al	Al
Al	Al	Al	Al	Al	Al	Al	Al	Al	Al	Al	Al	Ti	Ti					Ti	Ti	Al	Al	Al	Al	Al	Al	Al	Al	Al	Al	Al	Al
Al	Al	Al	Al	Al	Al	Al	Al	Al	Al	Al	Al	Ti	Ti					Ti	Ti	Al	Al	Al	Al	Al	Al	Al	Al	Al	Al	Al	Al
Al	Al	Al	Al	Al	Al	Al	Al	Al	Al	Al	Al	Ti	Ti					Ti	Ti	Al	Al	Al	Al	Al	Al	Al	Al	Al	Al	Al	Al
Al	Al	Al	Al	Al	Al	Al	Al	Al	Al	Al	Ti	Ti	Ti					Ti	Ti	Ti	Al	Al	Al	Al	Al	Al	Al	Al	Al	Al	Al
Al	Al	Al	Al	Al	Al	Al	Al	Al	Al	Al	Ti	Ti	Ti	Al			Al	Ti	Ti	Ti	Al	Al	Al	Al	Al	Al	Al	Al	Al	Al	Al
Al	Al	Al	Al	Al	Al	Al	Al		Ti	Ti	Ti	Ti	Ti					Ti	Ti	Ti	Ti	Ti		Al	Al	Al	Al	Al	Al	Al	Al
Al	Al	Al	Al	Al	Al	Al	Al	Ti		Ti	Ti	Ti	Al					Al	Ti	Ti	Ti		Ti	Al	Al	Al	Al	Al	Al	Al	Al
Al	Al	Al	Al	Al	Al	Al	Al	Al	Al	Ti	Ti	Ti	Ti					Ti	Ti	Ti	Ti	Al	Al	Al	Al	Al	Al	Al	Al	Al	Al
Al	Al	Al	Al	Al	Al	Al	Al	Al	Al	Ti	Ti	Ti	Ti					Ti	Ti	Ti	Ti	Al	Al	Al	Al	Al	Al	Al	Al	Al	Al
Al	Al	Al	Al						Ti	Ti	Ti	Ti	Ti					Ti	Ti	Ti	Ti	Ti						Al	Al	Al	Al
Al	Al	Al	Al						Al	Ti	Ti	Al	Ti	Al			Al	Ti	Al	Ti	Ti	Al						Al	Al	Al	Al
Al	Al	Al	Al					Ti	Ti	Ti	Ti									Ti	Ti	Ti	Ti					Al	Al	Al	Al
Al	Al	Al	Al					Ti	Ti	Ti	Ti									Ti	Ti	Ti	Ti					Al	Al	Al	Al

Figure 8.5: The best MGGA filter at 120kev (source at the top)

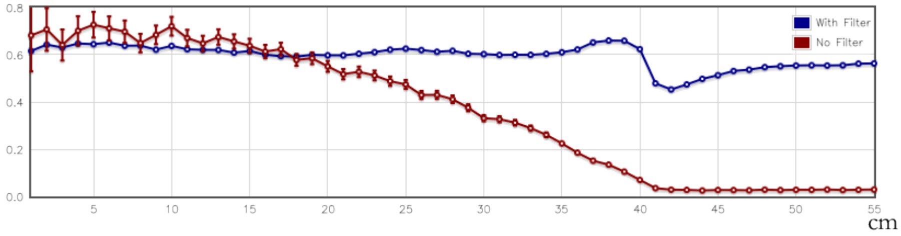

Figure 8.6: The scatter-to-primary ratio for the best MGGA filter at 120kev

MGGA used vacuum and multiple materials to flatten the primary radiation incident on the detector at several different energies. Consider the filter designed by MGGA and pictured in Figure 8.5. This filter able to do a great job of flattening the scattered to total ratio for 120 kev gamma radiation hitting a target plane as shown in Figure 8.6. One important aspect of this filter, due to the way MGGA works through phases, is that the resulting filter is more manufacturable than one created by GA alone.

8.3 Presentations and Publications

During the process of writing this dissertation I participated in a number of conferences and smaller opportunities to present my work. Early on I presented an hour long talk to students in the NERS department on biologically inspired optimization algorithms. This presentation was a good start and provided me with some initial thoughts on which algorithms would be worth trying on the shielding problems. I tried ant colony and particle swarm optimization on several simple problems and presented those concepts and results at this talk. While these techniques are both very interesting and powerful, they didn't seem to be a good fit for the shielding applications, so I focused on genetic algorithms.

In 2009 I presented the work Dr Holloway and I did on shadow shields to the International Conference on Mathematics, Computational Methods & Reactor Physics in a talk entitled *Multi-Grid Genetic Algorithms for Space Shield Design*, [Asbury & Holloway (2009a)]. The same year I presented our initial work on the wearable shield to the Chemical and Biological Defense Science and Technology Conference in a paper entitled *Optimization of Gamma Radiation Shielding by Genetic Algorithms*, [Asbury & Holloway (2009b)].

In 2011 I presented my results on low energy gamma rays to the International Conference on Mathematics, Computational Methods & Reactor Physics, in a paper entitled *Designing Shields for KeV Photons with Genetic Algorithms*, [Asbury & Holloway (2011)]. This paper included the initial results, but did not include my final revised ORNL geometry results.

8.4 Future Work

There is still work to be done on MGGA. First, there is more research to do in terms of how we can tune MGGA. In particular, the gamma shield problem was able to stymie MGGA at some energies. It would be interesting to see if this is related to diversity and if adding mutations between phases would help. This question of when diversity matters and how is a generally important one.

I ignored error when using the results from PARTISN and MCNP to produce fitness scores. There is an interesting line of research here, that could look at how error could be used or propagated into the fitness calculation to create more fair tournaments, or reproductive choices. For example, given two shields with very close fitness scores, if the error is not taken into account the one with the higher fitness would win a tournament. But if the error in the transport computation is taken into account we might more fairly select between the shields, or we might automatically refine the computation of fitness in these cases.

The applications I looked at could continue to be extended. The shadow shield geometry can be expanded to include support material and the simulations could add secondary radiation, in particular gamma rays. The fitness function for this shield could be altered to penalize free standing rings, making the shield more manufacturable. The gamma shield problem offers a wide variety of research paths in extending the ORNL geometry and looking at more types of radiation, while the filter problem could be extended to more closely mimic a CT scanner.

8.5 Conclusions

The MGGA results from this dissertation are very positive. The split shadow shield was validated and expanded to include more intricate paths for scattered neutrons to escape the shield. A simple lead shield was defeated for low energy gamma radiation, providing insight into the possibility of using layered materials to create lighter and more protective shields for radiation workers. Finally, MGGA was able to build a manufacturable bow-tie filter with two materials.

More importantly, in almost every case MGGA created a better scoring individual than GA with fewer computing resources. In some cases, MGGA was able to use half the resources as GA to create a superior result. By leveraging the hierarchical nature of a problem, MGGA was also able to create more structured and subjectively cleaner solutions. The shadow shield was less noisy than its GA equivalent. The bow-tie filter created by MGGA was more manufacturable than the one created by GA. For these three problems, and likely for similar ones, MGGA is a powerful complement for plain GA.

Ultimately, MGGA is a great new tool for shield designers. GA and MGGA are constrained by computing resources, limiting the "realism" that can be included in their fitness functions. But this limitation does not make them useless. Rather it places them earlier in the design process where MGGA is able to explore a huge problem space and suggest counter intuitive solutions with a reasonable computing cost. These ideas can then be pursued using standard design and simulation techniques to create better radiation shields.

APPENDICES

APPENDIX A

Genetik

A.1 A Quick Introduction to Genetik

This appendix describes the high level design and features of Genetik, a set of Java libraries I wrote to explore optimization techniques for this dissertation. The primary goal of Genetik was to provide an extensible library for exploring optimization routines, especially GA, for nuclear engineering problems. Genetik is in some ways over-engineered for the problems discussed in this dissertation, but the flexibility provided by Genetik's design was fundamental in implementing MGGA and supporting batch GA on a cluster.

To allow for the greatest range of topics, Genetik was originally designed to support both genetic algorithms and genetic programming, where the chromosomes represent runnable computer programs. To make GP simple and consistent with GA I wrote a small stack-based language called Sting. Sting is interpreted, with an intermediate format designed for use in genetic programming. Sting is based on languages like Forth, Postscript and Push. All of the chromosomes for Genetik 1.0 were defined as Sting programs. Sting allows data constants, so for a chromosome containing binary data the Sting program might be something like “0 0 1 0”. However, this format can be confusing since it reverses constants due to Sting’s nature as a stack language.

In order to make Genetik more usable by others, I created an updated version, 2.0, that replaced the Sting syntax with a pluggable chromosome type. This simplified the process of reading chromosomes as text.

The Genetik library contains a number of sub-packages that define major features. Some of these include:

crossover Classes that define GA crossover operators, renamed to operations in 2.0

generator Classes that define different ways to generate a population, including phase-based generation used for MGGA

insertion Classes that define different ways to insert individuals into a population

driver Utility classes for running Genetik, including on a cluster

optimize Core optimization algorithm implementations

population Classes that define population holders

precalc Implementation of the pre-calculation routines (1.0 only)

reporting Classes to help build reports from Genetik Runs

scaling Classes that can be used to scale raw scores before the fitness is calculated

selection Classes that define the various GA selection schemes

terminate Classes that define termination conditions for runs

Combined these packages represent numerous options for running GA or other optimization algorithms. Genetik library includes optimizers that use GA, HillClimbing, Random Change, Particle Swarm and Simulated Annealing to find the best solution in a generational context. The crossover package includes single point and uniform crossover. Finally, Genetik supports random, rank, roulette, tournament, truncation and stochastic selection.

A.2 Running Genetik 1.0

Genetik 1.0 uses two XML configuration files to define what it will do. These files define the concept of a run group and the optimization to perform. For legacy reasons the run group file is generally called run.xml and the the optimization description is called evdesc.xml.

The following XML describes the basic format for a run.xml file.

```
<genetik>
    <run_desc>
        .. parameters for the run ..
        .. an array of run definitions ..
        <run>
            .. parameters for a single run ..
        </run>
        .. other runs ..
    </run_desc>
</genetik>
```

Basically a run group is a collection of runs. The group has some configuration, including a name used to create the folder where results are stored. Each run can also have parameters. However, these parameters are expressed as substitutions into the evdesc.xml file. By default, all settings for a run are in the associated evdesc.xml file.

The runs in a run group can be in one of two styles. In the most simple case a run group has a collection of unrelated runs. This feature is used to run multiple copies of the same run, or to perform multiple runs with slightly different parameters.

The second case for a run group is to have a collection of runs that form an MGGA. In this case, each run represents a phase of the MGGA.

The evdesc.xml file contains all of the parameters for a run. When a run group is executed, the substitutions for that run are performed in the default evdesc.xml file and the new file is saved for that run. This insures that we have the evdesc.xml file used to actually run each phase of an MGGA or each run in a multi-run simulation.

The following is an example evdesc.xml file, and shows how the various GA parameters are set.

```
<genetik>
    <evolution_desc>
  <initial_operations>256</initial_operations>
  <max_operations>256</max_operations>

  <generationpop>4000</generationpop>
  <maxgenerations>40</maxgenerations>

  <optimize_raw_score_calculations>false</optimize_raw_score_calculations>
  <break_if_solution_found>false</break_if_solution_found>
  <max_terminal_fitness>10000000</max_terminal_fitness>
  <max_terminal_fitness>10000000</max_terminal_fitness>

  <save_generations>true</save_generations>
  <backup_stack>false</backup_stack>
  <clone_on_push>false</clone_on_push>
```

```
<is_binary_problem>true</is_binary_problem>


<topntosave>5</topntosave>


<tournamentsize>5</tournamentsize>


<reproductionprob>.1</reproductionprob>
<crossoverprob>.7</crossoverprob>
<mutationprob>.2</mutationprob>


<crossovertries>5</crossovertries>
<crossover_class_name>com.sasbury.genetik.crossover.UniformCrossover</crossover_
<optimizer_class_name>com.sasbury.genetik.optimize.GenetikEvolver</optimizer_cla


<available_operations>
    <op>%</op>
</available_operations>


<wildcardmin>0</wildcardmin>
<wildcardmax>256</wildcardmax>


<available_fitness_tests>


    <fitnesstest_desc>
        <classname>CurveFitTest</classname>
    </fitnesstest_desc>
```

```
  </available_fitness_tests>
    </evolution_desc>
</genetik>
```

Fitness tests in Genetik 1.0 are implemented by extending the FitnessTest class. Subclasses need to implement a a single method that takes the results from a Sting program, interprets them as a chromosome and scores that chromosome. The following example is the code from the curve fit example's fitness function. The utility method extractIntegerProgramResults is used to remove the integers from the program that represent our chromosome. Then the mean square is calculated, scaled and returned. If an error occurs, a very bad fitness of -1000 is returned. Also, the user data on the program is set. This data will be saved to disk and can be useful for debugging purposes.

```
public double calculateRawScore(ExecutionContext context)
{
    double retVal = -1000.0;

    try
    {
        int[] data = Genetik.extractIntegerProgramResults(context);
        int size = data.length;//should be odd, so we can split better

        double scale = 1.0/(size-1);
        double sum = 0.0;

        for(int i=0,max=size;i<max;i++)
        {
            double x = scale * (double)i;
            double y = scale * (double) data[i];
            double f = f(x);
            double diff = Math.abs(f-y);
            sum += (diff*diff);
        }

        double ms = sum/size;

        retVal = 1-(1000*ms);//spread out the ms some

        ((Program)context.getProgram()).setUserData("Mean Square: "+ms);
    }
    catch(Exception exp)
    {
        Application.instance().debug(exp);
    }

    return retVal;
}
```

Genetik 1.0 included code to run in batch mode on the University of Michigan cluster as well as on the command line or embedded in another Java application.

A.3 Running Genetik 2.0

Genetik 2.0 was a re-write of Genetik 1.0 with a focus on simplifying the configuration files and making it easier to extend. At the time, Dr. Holloway and I were thinking that someone else might be using the library and I wanted to make it more accessible.

One of the key changes was moving from XML to the Java properties file format. This is a key-value format. Genetik uses a simple rule to handle array like values. One key will contain a comma separated list of values. These values are used to construct other keys. This construct is exemplified with the runs key in the properties list below. This example is an actual description file, combining the run.xml and evdesc.xml roles, for a gamma shield simulation.

```
#
#
# Core settings
#
runs=4_bands,8_bands,16_bands
chromosome=com.sasbury.genetik.chromosomes.IntegerChromosome
minimum_gene=0
maximum_gene=6
phase_translator=com.sasbury.experiment.xraylayers.FixedLayersFitnessTest
phase_selection=com.sasbury.genetik.selection.TournamentSelection
#
# 4 band run settings
#
4_bands.population=250
4_bands.generations=10
4_bands.genes=4
4_bands.shield_layers=4
#
# 8 band run settings
#
```

```
8_bands.population=500
8_bands.generations=15
8_bands.genes=8
8_bands.shield_layers=8
8_bands.generator=com.sasbury.genetik.generator.PhaseBasedGenerator
#
# 16 band run settings
#
16_bands.population=500
16_bands.generations=20
16_bands.genes=16
16_bands.shield_layers=16
16_bands.generator=com.sasbury.genetik.generator.PhaseBasedGenerator
#
# General test settings
#
tests=xraylayers
xraylayers.class=com.sasbury.experiment.xraylayers.FixedLayersFitnessTest
particles=2250000
energy=0.05
thickness=0.1
lead_compare_thickness=0.05
#
# Reporting settings
#
customRelativeClass=com.sasbury.experiment.xraylayers.FixedLayersFitnessTest
customReportingBase=/com/sasbury/experiment/xraylayers/
```

```
customReporting=layers_ind.html,layers_sum.html,lead_dose.js
customSummaryFragment=layers_sum.html
customIndFragment=layers_ind.html
#
# MCNP settings
#
mcnp_cmd=mpirun,mcnp5.mpi,i=%INPFILE%
#
# Cluster settings
#
cluster_id=.nyx.engin.umich.edu
class_path=~/genetik/lib/phd.jar
estimated_time=200:00:00
procs=46
job_qos=hagar_flux
job_queue=flux
account=hagar_flux
```

Some items worth noting in this run description are the way a set of MGGA runs are defined using the key array value array of keys pattern is used. Also, properties can be passed to the fitness functions, like the command line for MCNP. Genetik 1.0 used an XML based reporting scheme. The 2.0 library moved to an HTML+Javascript scheme that allows custom web pages and files to be included. These appear the "Reporting Settings" section of the example. Genetik 2.0 also provided a simple way to pass information about the cluster, which is appears at the bottom of this file.

Perhaps the biggest change that 2.0 made is how chromosomes are stored. In 1.0 the chromosomes are Sting programs. In 2.0 they are objects that can be anything. This simplifies problems where the chromosome is just an array of numbers.

The following code block shows the code for the shortest path fitness function. This function implements both the scoring code and the code to translate from one phase of MGGA to the next.

Genetik 2.0 also included a feature that allowed each element in the GA, including fitness functions, to validate the run properties before the simulation started. The shortest path does nothing for these validation steps, and they are hidden.

```
package com.sasbury.experiment.shortestpath;

import com.sasbury.genetik.*;
import com.sasbury.genetik.chromosomes.*;
import com.sasbury.genetik.driver.*;
import com.sasbury.genetik.population.*;

public class ShortestPathFitTest
 implements FitnessTest, ChromosomeTranslator
{
    public static int[] adjustData(int[] data)
    {
        int[] newData = new int[data.length+2];

        newData[0] = 0;
        newData[newData.length-1] = (newData.length-1);

        for(int i=0,max=data.length;i<max;i++)
        {
            newData[i+1] = data[i];
        }
        return newData;
    }

    public static double calcBestScore(int size)
    {
        double scale = 1.0/(size-1);
        double sum = 0.0;

        for(int i=0,max=size-1;i<max;i++)
        {
            double x1 = scale * (double)i;
            double y1 = scale * (double)i;
            double x2 = scale * (double)(i+1);
            double y2 = scale * (double)(i+1);

            sum += Math.sqrt((x2-x1)*(x2-x1) + (y2-y1)*(y2-y1));
        }

        return 1-sum;
    }

    ... Validation ...

    public Chromosome translate(Chromosome old
                                , Run fromRun, Run toRun)
    {
        IntegerChromosome intChromo = (IntegerChromosome)old;
        int[] values = intChromo.getGenes();
        IndividualGenerator generator = (IndividualGenerator)
           toRun.createObject(GenetikConstants.GENERATOR);
        IntegerChromosome newChromo = (IntegerChromosome)
           generator.generateIndividual(toRun).getChromosome();
        int ratio = newChromo.geneCount()/intChromo.geneCount();

        for(int i=0,max=intChromo.geneCount();i<max;i++)
        {
            int value = values[i];

            for(int k=0;k<ratio;k++)
            {
                values[(i*ratio)+k] = value;
            }
        }

        newChromo.setGenes(values);

        return newChromo;
    }

    public double calculateRawScore(Individual ind
                      , Run run, String testName)
    {
        double retVal = -1000.0;
```

```
try
{
    int[] data =
       ((IntegerChromosome)ind.getChromosome()).getGenes();
    data = adjustData(data);//add the first and last value

    int size = data.length;//should be odd, so we can split better

    double scale = 1.0/(size-1);
    double sum = 0.0;

    for(int i=0,max=size-1;i<max;i++)
    {
        double x1 = scale * (double)i;
        double y1 = scale * (double) data[i];
        double x2 = scale * (double)(i+1);
        double y2 = scale * (double) data[i+1];

        sum += Math.sqrt((x2-x1)*(x2-x1) + (y2-y1)*(y2-y1));
    }

    retVal = 1-(sum);

    ind.setUserData("Length: "+sum);
}
catch(Exception exp)
```

```
        {
            exp.printStackTrace();
        }

        return retVal;
    }
}
```

Like Genetik 1.0, the 2.0 version of the library includes code to run on the University of Michigan cluster as well as from the command line.

APPENDIX B

Sting

B.1 An Introduction to Sting

Sting programs consist of a serious of operations that manipulate the data stack or one of the built in data dictionaries. Internally, the Sting interpreter uses two stacks. The data stack which is manipulated by the operations and the execution stack which is manipulated by the interpreter to execute a program.

Because GP can create “bad” programs, all operations that cannot complete do to an inappropriate stack are treated as a no-op. All operations that access indexed memory will be floor’ed and modulo’ed to fit the available choices.

B.2 Executing a Sting Program

Before execution a program is compiled or created as an array of integers. Each integer encodes two pieces of information, an operation index and a depth. The operation indexes are created during compile time by assigning a unique index for each operation in the program. Terminals - or constants - are implemented as a simple push operation, so they two are indexed in this way.

Procedures are compiled in-line but have a depth setting 1 greater than the level they are defined in. So,

```
1 1 add { 1 1 minus } 1 1 times
```

is compiled to 3 operations, two that push the value of 1 onto the stack and one that subtracts. These all have a depth of 1. The other operations, 6 of them, have a depth of 0.

This intermediate format is designed to make it easy to perform genetic programming on a Sting program.

When asked to interpret a compiled program, the interpreter pushes the array of integers onto the execution stack. Then the interpreter begins taking a single element from the stack and executing it. The interpreter performs this operation at a specified depth, 0 for the main program. When integers at a "deeper" depth are encountered, they are collecting into an array, converted to a Procedure object and pushed on the data stack. When a procedure is executed, the interpreter is set to its depth so procedures can contain other procedures.

Sting uses white space to separate operations and values, but does not care about the white space specifically.

Procedures in Sting are distinguished by { and } as in Postscript and other languages. Arrays are indicated by [and].

B.3 Sting Data Types

Sting provides the following built in data types:

- Number - a single precision floating point number
- String - a string of characters

- Array - an array of arrays, strings or floating point numbers, to be used as a vector or matrix

- Procedure - a collection of statements used in a loop or conditional

- IndexedMemory - number slots that can contain the other data types, predefined memory maps are provided for the programs input and output

B.4 Sting Operations

Sting provides the following extensible set of operations:

- dup - duplicate the top item on the stack

- swap - swap the top two items on the stack

- pop - pop the top item off the stack

- roll - (... n i roll) - rolls the previous n items on the stack i times, so (a b c 3 1 roll) becomes (c a b)

- copy - (... n copy) - copies the last N items on the stack, (a b c 2 copy) becomes (a b c b c)

- mark - creates a mark for the current stack size

- cleartomark - clears the stack up to the last mark

- plus - (a b plus) - adds two numbers, a+b

- minus - (a b minus) - subtracts two numbers, a-b

- times - (a b times) - multiplies two numbers, a*b

- divide - (a b divide) - divides two numbers, a/b

- modulo - (a b modulo) - takes the modulo of two numbers, a

- floor - (a floor) - takes one number and finds the closest integer smaller than it

- ceil - (a ceil) - takes one number and finds the closest integer bigger than it

- abs - (a abs) - takes the absolute value of a number

- neg - (a neg) - pops a number and pushes the negative of it

- and - (a b and) - takes two numbers and returns 1 if they are both greater than 0 and -1 if not (optimized)

- or - (a b or) - takes two numbers and returns 1 if they either or both are greater than 0 and -1 if not

- xor - (a b xor) - takes two numbers and returns 1 if they either but not both is greater than 0 and -1 if not

- not - (a not) - takes one number and returns 1 if it is less than or equal to 0 and -1 if not

- input - puts the input indexed memory on the stack

- output - puts the output indexed memory on the stack

- working - puts the working indexed memory on the stack

- read - (i mem read) - reads the i'th element in indexed memory or array instance mem and puts it on the stack

- write - (b i mem read) - buts b in the i'th slot in an indexed memory or array

- add - (b mem read) - adds b to the a new slot at the end of memory or array

- clear - (i mem clear) - clear the i'th slot in memory or an array

- size - (mem size) - pushes the number of slots in mem onto the stack
- lock - (mem lock) - locks mem- fixing the size
- unlock - (mem unlock) - unlocks mem
- null - (null) - places a null value on the stack, generally for adding to indexed memory
- ifeq - (a proc1 proc2 ifeq) - if a is equal to zero then proc1 is executed, otherwise proc2 is executed
- ifgt - (a proc1 proc2 ifgt) - if a is greater than zero then proc1 is executed, otherwise proc2 is executed
- loop - (a b proc loop) - loops over an index starting at a and ending at b (inclusive), executing proc for each loop
- forall - (array proc forall) - loops over array pushing each element in turn onto the stack and executing proc, if proc is a noop, elements accumulate on the stack, for index memory the key and value are pushed onto the stack
- index - push the current index for a loop on the stack, pushes 0 if not in a loop
- noop - places a noop procedure on the stack
- exec - (proc exec) - executes a procedure

B.5 Sting and Binary Chromosomes

While Sting supports a wide range of features, I have primarily used it just to create a stack of numbers, often zero and one. Sting is very fast to compile and interpret programs of this form.

```
1 0 1 0 0 0 1
```

However, programmatically it is important to keep one thing in mind. Sting is stack based, so depending when you see the string of 1s and 0s it may be reversed from the intended value.

BIBLIOGRAPHY

BIBLIOGRAPHY

2011. *PBS User Guide*. http://www.doesciencegrid.org/public/pbs/.

Aickelin, Uwe. 2002. Partnering strategies for fitness evaluation in a pyramidal evolutionary algorithm. *Pages 263–270 of: Proc. Genetic and Evolutionary Comput. Conf. GECCO02.*

Alpay, Bulent, & Holloway, James Paul. 2005. Segmenting Space Shields. *Pages 563–567 of: Proceedings of the Space Nuclear Conference.* American Nuclear Society.

Asbury, Stephen, & Holloway, James Paul. 2009a. Multi-Grid Genetic Algorithms for Space Shield Design. *In: International Conference on Mathematics, Computational Methods & Reactor Physics (M&C 2009).* American Nuclear Society.

Asbury, Stephen, & Holloway, James Paul. 2009b. Optimization of Gamma Radiation Shielding by Genetic Algorithms. *In: Checmical and Biological Defense Science and Technology Conference.* Defense Threat Reduction Agency.

Asbury, Stephen, & Holloway, James Paul. 2011. Designing Shields for KeV Photons with Genetic Algorithms. *In: International Conference on Mathematics, Computational Methods & Reactor Physics (M&C 2011).* American Nuclear Society.

Babbar, Meghna, & Minsker, Barbara. 2003. Multiscale Strategies for Solving Water Resources Management Problems with Genetic Algorithms. *In: Environmental Water Resources Institute (EWRI) World Water Environmental Resources Congress 2003 Related Symposia.*

Banzhal, Wolfgang, Nordin, Peter, Keller, Robert E., & Francone, Frank D. 1998. *Genetic Programming - An Introduction.* Morgan Kauffman.

Bell, J., Lail, D., Martin, C., & Nguyen, P. 2010. *Radiation Shield for a Lunar Base.* http://cmie.lsu.edu/NASA/Teams/Radiation

Berntsson, J., & Tang, Maolin. 2005. Adaptive Sizing of Populations and Number of Islands in Distributed Genetic Algorithms. *Pages 1575–1576 of: GECCO.* American Computing Society.

Cant-paz, Erick. 1998. A survey of parallel Genetic Algorithms. *Calculateurs Paralleles*, **10**.

Cember, Herman, & Johnson, Thomas E. 2009. *Introduction to Health Physics, Fourth Edition*. McGraw-Hill Companies, Inc.

Chilton, Arthur B., Shultis, J. K., & Faw, Richard E. 1984. *Principles of radiation shielding / Arthur B. Chilton, J. Kenneth Shultis, and Richard E. Faw*. Prentice-Hall, Englewood Cliffs, NJ :.

Cowall, Alan. 2006. Radiation Poisoning Killed Ex-Russian Spy. *New York Times*. http://www.nytimes.com/2006/11/24/world/europe/25spycnd.html.

De Jong, E. 2011. *Hierarchical Genetic Algorithms*. http://citeseer.ist.psu.edu/705095.html.

Eby, David, Averill, R. C., Punch, III, William F., & Goodman, Erik D. 1999. Optimal design of flywheels using an injection island Genetic Algorithm. *Artif. Intell. Eng. Des. Anal. Manuf.*, **13**(5), 327–340.

Eiben, A.E., & Smith, J.E. 2003. *An Introduction to Evolutionary Computing*. Springer-Verlag.

Ferguson, Charles D., Kazi, Tahseen, & Perera, Judith. 2003. Commercial Radioactive Sources: Surveying the Security Risks. *Occasional Paper No. 11*.

Fishman, George S. 2006. *A First Course in Monte Carlo*. Thomson Brooks/Cole.

Goldberg, David E. 1989. *Genetic Algorithms in Search, Optimization and Machine Learning*. Boston, MA, USA: Addison-Wesley Longman Publishing Co., Inc.

Goldberg, David E., & Deb, Kalyanmoy. 1991. A comparative analysis of selection schemes used in Genetic Algorithms. *Pages 69–93 of: Foundations of Genetic Algorithms*. Morgan Kaufmann.

Goldberg, David E., Deb, Kalyanmoy, & Clark, James H. 1991. Genetic Algorithms, Noise, and the Sizing of Populations. *COMPLEX SYSTEMS*, **6**, 333–362.

Goldberg, David E., Deb, Kalyanmoy, Kargupta, Hillol, & Harik, Georges. 1993. Rapid, Accurate Optimization of Difficult Problems Using Fast Messy Genetic Algorithms. *Pages 56–64 of: Proceedings of the Fifth International Conference on Genetic Algorithms*. Morgan Kaufmann.

Harik, George, Goldberg, David E., Cantu-Paz, Erick, & Miller, Brad L. 1997. The Gambler's Ruin Problem, Genetic Algorithms, and the Sizing of Populations. *Pages 7–12 of: Evolutionary Computation*. IEEE Press.

Haupt, Randy L., & Haupt, Sue Ellen. 1998. *Practical Genetic Algorithms*. John Wiley and Sons.

Heath, D., & Heath, C. 2007. *Get Back In the Box*. Fast Company (December 2007 / January 2008) p. 74.

Holland, John H. 1992,1975. *Adaptation in Natural and Artifical Systems.* MIT Press.

IAEA. 2002. *Inadequate Control of Worlds Radioactive Sources.* http://www.iaea.org/NewsCenter/PressReleases/2002/prn0209.shtml.

International Commission on Radiation Units and Measurements. 2011. Fundamental Quantities and Units for Ionizing Radiation. **11**(1).

Jong, Kenneth A. De. 2006. *Evolutionary Computation.* MIT Press.

Kanamori, H., Nakamori, N., Inoue, K., & Takenaka, E. 1985. Effects of scattered x-rays on CT images. *Physics in Medicine and Biology*, **3**.

Kwan, A., Boone, J., & Shah, N. 2005. Evaluation of x-ray scatter properties in a dedicated cone-beam breast CT scanner. *Medical Physics*, **32**.

Langon, William B., & Poli, Riccardo. 2002. *Foundations of Genetic Programming.* Springer-Verlag.

Lee, L.W. 1987. *Shielding Analysis of a Compact Space Nuclear Reactor.*

Los Alamos National Lab. 2011. *LANL Cross Section Data.* http://t2.lanl.gov/.

M Babbar, B Minsker, D E Goldberg. 2002. A multiscale island injection genetic algorithm for optimal groundwater remediation design. *In: Proceedings of the Conference on Water Resources Planning and Management, (CWRPM02).* American Society of Civil Engineers (ASCE) Environmental and Water Resources Institute (EWRI.

Mail, N., Moseley, D.J., Slewerdsen, J.H., & Jaffray, D.A. 2009. The influence of bowtie filtration on cone-beam CT image quality. *Medical Physics*, **36**.

McCaffrey, J. P., Mainegra-Hing, E., & Shen, H. 2009. Optimizing non-Pb radiation shielding materials using bilayers. *Medical Physics*, **36**.

Merkle, Laurence D., Gates Jr., George H., & Lamont, Gary B. 1998. Scalability of an MPI-based fast messy Genetic Algorithm. *Pages 386–393 of: SAC '98: Proceedings of the 1998 ACM symposium on Applied Computing.* New York, NY, USA: ACM.

Mitchel, Melanie. 1998. *An Introduction to Genetic Algorithms.* MIT Press.

Monte Carlo Codes Group - Los Alamos National Laboratory. 2011. *MCNP - A General Monte Carlo N-Particle Transport Code.* http://mcnp-green.lanl.gov/.

National Institute of Standards and Technology. 2011. *Lead Cross Section Data.* http://physics.nist.gov/PhysRefData/XrayMassCoef/ElemTab/z82.html.

Oak Ridge National Laboratory. 2011. *ORNL Phantom.* http://mcnp-green.lanl.gov/resources.html.

Pheil, EC. 2006. *Space Reactor Radiation Shield Design Summary.* Lockheed Martin Letter SPP-67210-0011.

Radiobiological Advisory Panel. 1970. *Radiation Protection Guides and Constraints for Space-Mission and Vehicle-Design Involving Nuclear Systems.* National Academy of Sciences.

R.K., Tripathi, J.W., Wilson, F.A., Cucinotta, J.E., Nealy, M.S., Clowdsley, & M.H.Y., Kim. 2001. Deep Space Mession Radiation Shielding Optimization. *Society of Automotive Engineers*, **01ICES-2326**.

Robotics, Berkeley. 2011. *Berkeley Lower Extremity Exoskeleton.* http://bleex.me.berkeley.edu/bleex.htm.

Schuster, Patricia. 2009. *Synopsis: Dirty Bombs.* Undergraduate Research Project.

Shultis, J. Kenneth, & Faw, Richard E. 2000. *Radiation Shielding.* American Nuclear Society Inc.

Skolicki, Zbigniew. 2005. An analysis of island models in evolutionary computation. *Pages 386–389 of: GECCO '05: Proceedings of the 2005 workshops on Genetic and evolutionary computation.* New York, NY, USA: ACM.

Space X. 2011. *Falcon 9 Users Guide.* http://www.spacex.com/falcon9.php.

SQLite. 2011. *Limits in SQLite.* http://www.sqlite.org/limits.html.

Sullivan, Keith, Luke, Sean, Larock, Curt, Cier, Sean, & Armentrout, Steven. 2008. Opportunistic evolution: efficient evolutionary computation on large-scale computational grids. *Pages 2227–2232 of: GECCO '08: Proceedings of the 2008 GECCO conference companion on Genetic and evolutionary computation.* New York, NY, USA: ACM.

Tomassini, Marco. 2005. *Spatially Structured Evolutionary Algorithms.* Springer-Verlag.

US Nuclear Regulatory Commission. 2011. *US-NRC Deep Dose Equivalent.* http://www.nrc.gov/reading-rm/basic-ref/glossary/deep-dose-equivalent-dde.html.

webelements.com. 2011. *Web Elements Data.* http://www.webelements.com/.